Evaluation of bisphenol E cyanate ester for the resin-injection repair of advanced composites

by

Wilber Yaote Lio

A thesis submitted to the graduate faculty

in partial fulfillment of the requirements for the degree of

MASTER OF SCIENCE

Major: Materials Science and Engineering

Program of Study Committee:
Michael Kessler, Co-major Professor
Mufit Akinc, Co-major Professor
Vinay Dayal

Iowa State University

Ames, Iowa

2009

Copyright © Wilber Lio, 2009. All rights reserved.

TABLE OF CONTENTS

ACKNOWLEDGEMENTS iii

CHAPTER 1. INTRODUCTION 1
Thesis Organization 1
Literature Review 1
Composite Repair 1
Adhesives and Lap Shear Tests 10
Nanoparticles 14
Cyanate Esters 17
References 20

CHAPTER 2. LAP SHEAR TESTING OF BISPHENOL E CYANATE ESTER: EFFECTS OF SUBSTRATE, TEMPERATURE, ALUMINA NANOPARTICLES, AND MOISTURE 26
Introduction 26
Materials and Methods 30
Results and Discussion 33
Conclusions 48
Acknowledgments 49
References 50

CHAPTER 3. INJECTION REPAIR OF ADVANCED COMPOSITES USING A LOW-VISCOSITY, HIGH TEMPERATURE CYANATE ESTER RESIN 54
Introduction 54
Materials and Methods 57
Results and Discussion 60
Conclusions 66
Acknowledgements 67
References 67

CHAPTER 4. GENERAL CONCLUSIONS 69

APPENDIX A. HIGH-TEMPERATURE CYANATE ESTER ADHESIVES REINFORCED WITH NANO-ALUMINA 71

APPENDIX B. EFFECT OF ALUMINA NANOPARTICLES ON THE PROPERTIES OF LOW-VISCOSITY CYANATE ESTER ADHESIVES FOR COMPOSITE REPAIR 89

APPENDIX C. TOXICITY OF CYANATE ESTER/NANOCOMPOSITE RESINS FOR COMPOSITE REPAIR 100

ACKNOWLEDGEMENTS

I would like thank my major professors, Dr. Michael Kessler and Dr. Mufit Akinc, for their dedicated support and guidance throughout my studies. I would also like to thank Dr. Vinay Dayal, my other committee member, and Dan Barnard for their guidance and access to their laboratory facilities. Special thanks to the members of Dr. Kessler's Polymer Composites Research Group, all past, present, graduate, undergraduate, post-doc, permanent, and visiting members who I have had the pleasure of meeting and working with, as well as other colleagues, including Katherine Ament, Zhihong Tang, Craig Ament, and Jun Wang for their help with lab work and discussion. Last, but not least, I thank my parents, sister, and close friends for their love and support throughout the years.

This work was supported by a grant from the Strategic Environmental Research and Development Program (SERDP), under the "Environmentally Benign Repair of Composites Using High Temperature Cyanate Ester Nanocomposites" project (Project Number WP-1580). This document has been authored, in whole or in part, under Contract No. DE-AC02-07CH11358 with the U.S. Department of Energy and has been assigned the document number IS-T 2903.

CHAPTER 1. INTRODUCTION

Thesis Organization

This thesis is a compilation of a general introduction and literature review that ties together the subsequent chapters which consist of two journal articles that have yet to be submitted for publication. The overall topic relates to the evaluation and application of a new class of cyanate ester resin with unique properties that lend it applicable to use as a resin for injection repair of high glass transition temperature polymer matrix composites. The first article (Chapter 2) details the evaluation and optimization of adhesive properties of this cyanate ester and alumina nanocomposites under different conditions. The second article (Chapter 3) describes the development and evaluation of an injection repair system for repairing delaminations in polymer matrix composites.

Literature Review

Composite Repair

Background

Composite Materials

Polymer composites are used in a wide range of applications, from airplanes to bicycle frames and as the desire for stronger and lighter materials continues to grow, composites will be in ever-increasing demand. This trend is especially noticeable in the aerospace industry, as composites are gradually replacing metal components as both primary and secondary structures in today's aircraft [1-4] (Figure 1). The Boeing 787, for example, is made up of about 50% composites by weight or nearly 80% by volume [5, 6]. The increased use of composite materials is due to the many superior properties they exhibit compared to metals such as higher specific strength and stiffness, better fatigue and corrosion resistance, and lighter weight [1, 2, 7, 8].

Composite materials however, are susceptible to defects and damage that can greatly compromise their mechanical properties. Depending on their applications, this can yield disastrous effects. Therefore, in order to decrease the likelihood of catastrophe, it is necessary to have a good understanding of the sources of defects and damage, as well as how to detect them, and most importantly, how to repair them.

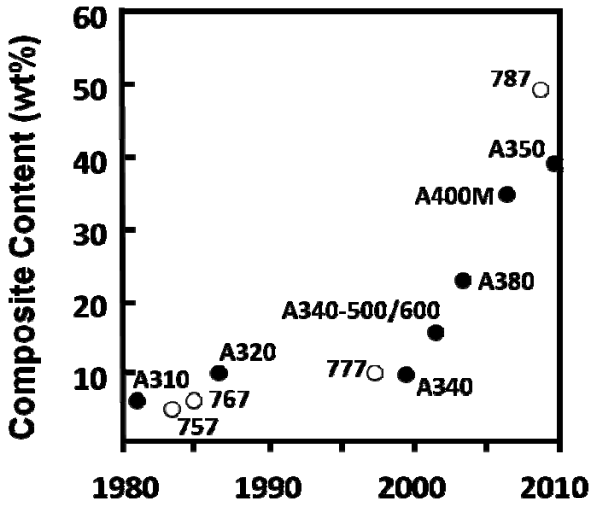

Figure 1. Composite content of Boeing and Airbus aircraft over time [6].

Defects and Damage

Defects in composites can be caused by various events that occur throughout a structure's lifetime. They may arise as a result of poor manufacturing techniques, or they may be introduced when a part is damaged while in service [7, 9, 10]. Defects introduced during the manufacture of composites can include: resin-rich zones, voids, inclusions, and broken and distorted fibers [10].

In-service damage can result from a variety of thermal, environmental, and mechanical stresses. However, the majority of in-service damage results from some form of impact [1, 8, 11]. While some forms of damage may be beneficial to re-distribute stress in high-stress areas [10], the vast majority have deleterious effects. Cracks, dents, and most commonly, delaminations [7] caused

by anything from hail and runway debris to a tool drop or over-torquing a fastener during maintenance [1, 7, 12] can lead to a dramatic decrease in mechanical properties. Low-velocity impacts can be especially troublesome because the presence and amount of damage is often difficult to detect, yet can be greatly detrimental to the integrity of the part [1, 2, 9]—a 70% reduction in compressive strength has been reported in specimens that showed no visible damage [13]. For this reason, it is imperative that the repair of composites be well-understood and innovative practices developed to ensure that the integrity of composites can be properly maintained as the use of composites moves from not only secondary structures, but to primary load-bearing structures as well [3, 4, 14].

Inspection

The most basic methods of inspection are manual techniques that include visually inspecting parts [10] or tapping on areas and listening for differences in the sound, as damaged areas will produce a duller tone [11]. These techniques, however effective, are more prone to oversight than more advanced techniques.

Some of the more advanced non-destructive evaluation (NDE) techniques include ultrasonics, radiography, thermography, and holography. One of the most commonly used NDE methods is ultrasonics [10], and will be discussed in more detail below.

In ultrasonic testing, a transducer transmits high frequency sound waves through a specimen and the signal that is received is used to reveal defects hidden within the specimen. Different methods of ultrasonic testing can be categorized based on: 1) how the sound waves are sent and received (pulse-echo vs. through-transmission), 2) how the transducers are set up (contact vs. immersion), and 3) how the results are presented (A, B, or C-scans) [10, 15].

In pulse-echo systems, one transducer functions as both transmitter and receiver. This method relies on the reflected energy received to determine any discontinuities within the specimen.

In through-transmission systems, two transducers are used: one to transmit and another to receive the sound waves. The through-transmission method does not use reflected energy like the pulse-echo system. Instead, it utilizes variations in the energy received [10, 15].

Contact testing involves either direct contact or contact via some couplant (e.g. air, liquid, or paste) between the transducers and the specimen. Couplants are used to limit attenuation to that caused by discontinuities within the specimen by reducing attenuation at the interface between the transducer and the specimen. An ideal couplant would have the same acoustic impedance as the specimen. The acoustic impedance is the product of the density of the material and the velocity at which sound passes through the material. The more similar the acoustic impedances are between the transducer and specimen, the better the sound transfer [15].

Immersion testing is essentially a liquid-couplant technique in which the specimen as well as the transducers is fully immersed, typically in water. This technique of course has its limitations (e.g. moisture could be detrimental to some samples) [9, 16].

In addition to the items discussed above, there are many other things that are taken into consideration in ultrasonic testing, such as the frequency, size, shape, and position of the transducer; surface and shape of the specimen; and the shape and direction of the flaw.

In ultrasonic testing, there are three main ways of representing the data gathered from a scan: A, B, and C-scan presentations (Figure 2). An A-scan is basically a graph of amplitude versus time, from which the relative location of discontinuities from the surfaces can be determined. B-scans yield cross-sectional views, and C-scans give plan views of the specimen under investigation. Different applications will benefit from different scans, but the C-scan is the most common presentation, as it gives a good, clear overview of the damage within a material. Although C-scans are limited by the fact that only the lateral extent of the delamination damage can be presented and that the presence of underlying defects can be overshadowed by defects nearer the surface, combining

the information from various scans (A, B, and C-scans) has been shown to overcome this drawback [12].

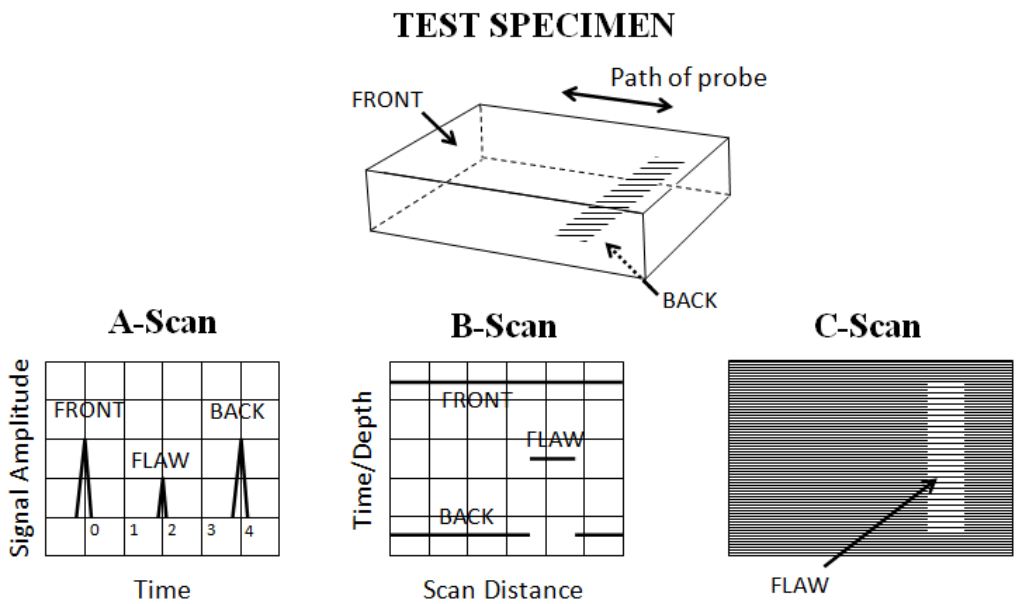

Figure 2. Different methods of presenting data from ultrasonic inspection [17, 18].

Evaluation

Once a part has been inspected, the next step is to assess the need for and feasibility of repair. The need for repair is largely based on the extent of damage a part has experienced.

When damage is either negligible or extensive, there is no need for repair. Insignificant damage that will not affect a part's performance or appearance is not worth repairing. Extensive damage can either be too costly to repair, or simply cannot be repaired. For this reason, extensively damaged parts are often simply replaced. When damage is sufficient to diminish the structural integrity of a part below a designated allowable limit, a structural repair is deemed necessary [9, 11, 16].

When determining the feasibility of repair, numerous factors are considered, including the extent of damage to the part and how well a repair could restore its integrity, the cost of repairing

versus replacing, the amount of time available, and the ease with which a repair can be conducted, including the accessibility of the part and the availability of the proper facilities [7, 11, 14, 16].

Repairs

The ultimate goal of any repair involves the restoration of some property to what it was prior to damage. These properties may include mechanical properties such as strength and stiffness [3, 7, 14] as well as things such as aerodynamic smoothness, which is especially important in certain parts of aircraft [7].

Different types and degrees of damage are repaired in different manners. Damage that is not detrimental to the integrity of a part can be fixed with *cosmetic repairs* that return aesthetic value to the damaged areas. *Structural repairs* are conducted when the damage is to an extent that it decreases a part's performance. *Temporary repairs* are conducted when damage is not yet to the point of diminishing a part's performance, but if left untreated, could worsen to that degree, or when damage occurs out in the field where the proper facilities are not available to conduct a proper repair [11, 16]. The repair techniques that will be discussed further will fall under structural and temporary repairs.

Techniques

Techniques used for composite repair must take into account issues relating to applicability in the field. Factors such as weight restrictions, part accessibility, environmental compatibility, as well as material, equipment, and personnel limitations, must all be considered when selecting or designing a repair technique [4, 7, 19].

Current techniques available for composite repair can be categorized into two main groups: bolted and bonded repairs [7]. Bolted repairs are relatively easy to apply in the field since there are no adhesives to cure. This method is also used when adhesives cannot provide the necessary strength for the application [9]. However, some of the drawbacks to bolted repairs include the added weight

and stress concentrations imparted by the bolts, as well as the delamination and further damage that can be introduced by drilling [1, 7]. Bonded repairs, on the other hand, add much less additional weight and can provide a good distribution of load, but can be a little more difficult to apply. Because of this, bonded repairs more often than not are done in the shop [7].

Bonded repairs can be further classified into two main categories: patch repairs and non-patch repairs [9, 16]. Patch repairs include external patches and bonded scarf patches. These repairs are generally more difficult and time consuming than non-patch repairs, and are also difficult to apply to repairing complex shapes and curved surfaces [19, 20]. However, less complex shapes and surfaces can be relatively easy repair in the field with this method, and can recover 70 to 100% of the original strength [9]. Patch repairs work better for honeycomb or other substructure-type composites, because the substructure helps alleviate bending forces that cause patches to buckle [9].

External patch repairs do not require the removal of large amounts of the original composite material, and so are relatively simpler than scarf repairs; however the use of external patches often results in a loss of aerodynamic smoothness. Scarf patch repairs (Figure 3) require the removal of not only the damaged area, but a portion of the undamaged area as well. Because a great deal of care must be taken during the removal of material, scarf repairs are usually more difficult and time consuming, and require proper facilities and equipment, and are thus not well suited for field repairs. Scarf repairs are, however, good for maintaining a flush surface and distributing shear stress in the adhesive [9].

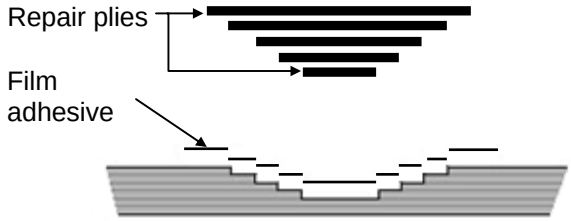

Figure 3. Scarf repair of composite materials [21].

Non-patch repairs are typically conducted on parts that have experienced smaller, generally more minor damage, in the sense that the overall structure has not been compromised. These types of repairs include potting/filler and injection repairs.

In potting or filler repairs, a resin compound is used to fill a defective region, and then is subsequently cured in place. Potting repairs are often used to fill dents or repair sandwich structures. However, because it may be necessary to remove areas around the damaged region before applying the resin compound, this method, similar to scarf repairs, can be a little intrusive [7, 9, 16].

The resin-injection method is a less-intrusive technique that can be used to repair disbonds and stabilize delaminations to restore the compressive and shear strengths and overall damage tolerance of a part [14]. This is done by injecting a compatible resin into the specimen to fill the delamination zone and heating the specimen to cure the resin in place (Figure 4).

As simple as that sounds, there are many things that must be taken into account. Resin viscosity is one of the biggest issues faced when designing an injection repair system. If a resin is able to fully fill the disbonded areas, repair efficacies of up to 98% can be obtained [7]. However, many resins lack the necessary flow requirements for infiltrating delaminations [14], and typical resins for temperatures upward of 200 °C such as bismaleimides (BMI) are very viscous at room temperature [19, 20] and difficult to process. For this reason, resin-injection repairs are often limited to low temperature composites.

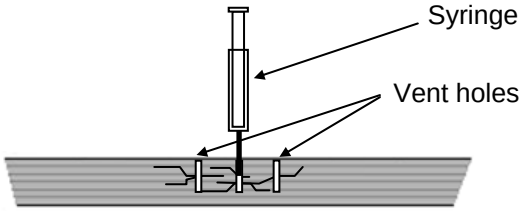

Figure 4. Resin-injection repair of composites [21].

Some other causes for concern with resin-injection include its general inability to be applied in the field, the potential for injection to cause delaminations to grow, as well as the inability and necessity to clean contaminated surfaces before bonding [1, 3, 8, 22, 23]. Despite these drawbacks, many studies have found this technique to work well [3, 8, 14, 23, 24] contrary to other findings [25]. In addition, the non-invasive nature and ability to maintain aerodynamic smoothness certainly make this technique worthy of further investigation.

Evaluation of Repair

After being repaired, composites are then re-evaluated before going back into service to ensure that the structure has been repaired properly. Many of the non-destructive techniques used during the initial inspection for damage are again utilized to evaluate the effectiveness of the repair. Ultrasonic testing is again, very common. Careful attention must be paid to the interface between the original and repaired areas in addition to the overall repaired area [11].

In the laboratory, compression-after-impact tests may be conducted to evaluate the effects of impact damage and subsequent repairs conducted on impacted specimens. This is because composites are generally weaker in compression than tension [7]. These tests have been found to be affected by many different factors including temperature, stacking sequence, as well as specimen dimensions [2], and so proper care must be taken to ensure that conditions are suitable to compare different samples.

The Future of Repairs

New repair materials and methods are constantly being investigated and developed to help minimize the invasiveness and expand the applicability of repair procedures. A current problem being addressed lies in the repair of high-temperature composites, which require the use of high T_g resins, because high T_g's are usually accompanied by high prepolymer viscosities which make these

resins difficult to process [19, 20]. This issue is being addressed by the development and application of new repair resins and techniques [14, 19, 20, 22, 23].

Adhesives and Lap Shear Tests

When joining composite parts, adhesive bonding is often preferred over mechanical fastening because the latter can impart stress concentrations that can decrease the strength of the composite [26, 27]. In addition, adhesives impart a lower weight addition than mechanical fasteners [27, 28] and can be less costly as well [28].

Because of the advantages of adhesive bonding over mechanical fastening in composites, it is important to characterize the bond strengths of adhesives and to understand the various factors that can influence these bond strengths. Because many adhesive joints are subjected to shear stresses [29], it makes sense to evaluate them via lap shear because it is a quick and inexpensive method to assess shear strengths. In fact, lap shear strength is the most commonly reported adhesive property [30, 31].

Various parameters can be varied with lap shear samples including geometric factors such as substrate dimensions and overlap area. Typically, higher bond strengths are observed with larger overlap areas [29, 31]. Additionally, tapering the edges of the bonded surfaces has been shown to decrease peel stresses in the composite and shift the failure to the adhesive [32]. Many of these geometric factors are controlled through standards such as ASTM D 5868-01.

Because the results obtained from lap shear tests can be dependent on so many factors, some find it to be a poor method to test adhesive strengths [30, 31]. Next, additional factors that influence adhesive bonding, specifically regarding lap shear tests, will be discussed.

Effects of Adhesive

One way of changing adhesive properties is by altering the adhesive resin. There have been various studies that have utilized nanoparticles to improve adhesion. One study [33] found bond

strength to increase with uniform dispersion of nano-fillers such as alumina or carbon nanotubes. This increase in bond strength was mainly attributed to the ability of the nanoparticles to fill gaps and porosities. The high surface area of the particles was also postulated to create an almost mechanical interlocking via the many contact points between the filler and adhesive. However, the increase in strength was not seen above certain nanoparticle loadings, above which a decrease in strength was observed. This was explained as being due to the inability of excessive particles to interact effectively, as well as the possibility of agglomerations that act as failure sites.

The method via which adhesive is applied as well as the amount applied (the bondline thickness) also can have an effect on lap shear properties. As one study found [29], the application of adhesive to both adherends in a lap shear sample showed higher adhesive strengths compared to samples in which adhesive was applied to only one adherend. Bondline thickness can be controlled by using glass beads, a scrim, or other materials, which is sometimes designated in specific standards.

Effects of Substrate

The other main component of the lap shear sample is the substrates. There are many factors related to the substrate that can greatly affect lap shear strength. Aside from substrate geometry [30, 31], one of the biggest factors involves proper preparation of the substrate surface [26, 34].

There are various treatments that can be used to alter the roughness and/or the chemical composition at the surfaces [28]. It has been found that completely untreated surfaces are often contaminated with fluorine residue from the release agents used during manufacture [26, 28]. This contamination has even been shown to withstand solvent wiping treatments [27]. While fluorine residue has been shown to be detrimental to bond strengths, one study has shown that untreated surfaces were superior to peel ply surfaces [26].

Peel plies are often incorporated onto composite surfaces during manufacture, and after curing, are peeled off the surface to reveal a clean, textured surface ready for bonding. Many studies

have found peel ply surfaces to give high bond strengths compared to other surface preparations [27, 28]; however, there have also been contradictory studies that suggest peel ply surfaces are detrimental to bond strength [26, 30]. Peel plies can impart a high level of surface roughness. While a small level of roughness is desirable for better adhesion [27], extensive roughness can prove detrimental by trapping air [26, 27] or preventing the escape of moisture [30]. Another case has been made that the surface created by a peel ply is actually microscopically mirror-smooth, rendering the surface inert, as opposed to "active" for better adhesion [30]. Some other limitations of peel plies include their impracticality on highly contoured surfaces [26] and repair applications [30].

Similar treatments to help clean the surface and impart roughness include grit blasting, sanding, and laser ablation. With grit blasting, there have been conflicting findings that report inferior [27] and superior bond strengths [26, 30]. It seems that in general, sanding is not the best technique due to non-uniformity of the treatment and the possibility of introducing excessive damage [26].

Laser ablation of a composite surface can do as little as clean the surface or as much as remove the outer matrix layer to reveal the fibers within, depending on the intensity and exposure time of the laser. One study found that slight protrusion of fiber at the surface led to an increase in bond strengths [28].

Plasma treatment of the substrate surface can not only clean and roughen the surface, but can also alter the surface chemistry to affect properties such as surface energy. Oxygen plasma treatment, for example, has been shown to increase the surface energy and wettability by increasing the surface oxygen concentration and creating a highly polar surface [27]. Unfortunately, while a higher surface energy means better wetting, better wetting does not always yield higher strengths [26].

Effects of Environment

Environmental conditions to which a lap shear sample is exposed, whether prior to or during a test, can also have significant effects on lap shear strength. Moisture can be a real problem in adhesive bonding, as it is well known that composites will absorb some water—even when sealed and stored in a freezer [34]. Moisture, whether present in the composite prior to cure (pre-bond) or absorbed by the joint/adhesive after cure, has been shown to drastically reduce bond strengths [34, 35]. In fact, as little as 0.2% pre-bond moisture has been reported to reduce lap shear strength by as much as 80% [30]. The detrimental effects of pre-bond moisture can be enhanced by excessive surface roughness. The effect of moisture on the failure mode (e.g. interfacial, cohesive, etc.) largely depends on the adhesive and substrate in the system [35]. While moisture can significantly lower adhesive strength by introducing voids, interfering with the cure process, or plasticizing the adhesive [34], it is possible to avoid this merely by careful drying of the substrates prior to bonding, and testing them soon after preparation [34].

Another environmental factor that can significantly affect adhesive strength is test or service temperature [34]. Depending on the temperature and the type of adhesive, temperature may not have a huge affect. However, it has been shown in numerous studies that an increase in temperature leads to a decrease in joint strength [27, 35].

Conclusion

Lap shear tests provide a quick and inexpensive method for evaluating adhesive strengths. However, as discussed throughout this thesis, many different factors either related to the adhesive, substrate, or the environment, may play significant roles in determining adhesive properties. Different surface treatments, for example, are often used to enhance adhesion. To complicate things further, different studies have reported contradictory results on how surface treatments affect adhesion. For example, some state that peel ply surfaces improve strength while others report the

exact opposite. One thing is certain, and that is that adhesive properties are very sensitive to many different parameters, and the effect of these parameters are in turn highly dependent on the adhesive and substrate in the system.

Nanoparticles

Property Enhancements via Fillers and Nanoparticles

Filler materials are often incorporated into polymers to improve mechanical, thermal, and rheological properties for a variety of applications [36-38]. Property improvements, however, often come at the cost of another. Filler materials used to improve strength, for example, in turn decrease toughness [39-41].

The types of filler that are used span a wide range of materials, morphologies, and sizes. In more recent times, nanoparticles have been studied rather extensively due to their abilities to drastically improve properties beyond those which can be obtained by their microparticle counterparts and beyond that which was predicted by conventional models [42-45]. This may be due to the fact that nanoparticles have such a high specific surface area compared to other morphologies. Because atoms at the surface behave quite differently than in the bulk, and because there are so many surface atoms in nanoparticles, even a small loading of nanoparticles can drastically change material properties [46] such as strength and toughness by as much as 50% [40].

Nanocomposites sometimes also exhibit enhanced properties with fewer drawbacks compared to conventional filler composites. Combinations of properties not possible with conventional fillers are also obtainable [39, 41, 43, 47]. For example, nanoparticles have been shown to simultaneously enhance both strength and toughness—properties that are typically inversely related [39].

Problems Associated with Nanocomposites

Despite the possibilities of creating nanocomposites with properties that far exceed those of current materials, there are certain limitations that currently constrain their potential. Many studies on fillers have shown there to be a limit to the property enhancement abilities of fillers such as nanoparticles. Properties will increase up to a certain filler loading level, beyond which those properties begin to deteriorate [43, 44, 48]. It has been suggested that the decline of properties beyond an optimal loading level is due to dispersion issues [36, 43, 48, 49].

One of the biggest problems with nanoparticles is their affinity to agglomerate [40, 42, 43, 49]. Agglomerations are cause for inhomogeneity and poor particle dispersion within the matrix, which as noted above, can have detrimental effects on composite properties. Having good particle-matrix adhesion can help reduce agglomerations. The stronger the bond is between the particles and matrix, the less affinity for particles to bond with each other. This link between particle-matrix adhesion and improved properties is well-established [40, 42].

While some studies have shown the ability to obtain good dispersions via simple mechanical mixing [44], many have found the need to modify particles via surface functionalization [40, 46, 49]. Studies have shown surface modified particles to be better dispersed within the matrix, and the resulting nanocomposites to exhibit greater property enhancements, which further supports the importance of good dispersions for improved properties [42, 46-48]. Other processing procedures may need to be optimized for nanocomposites, as nanoparticles have also been shown to catalyze cure reactions [45, 50, 51].

Effect of Nanoparticles on Rheology

Nanoparticles are often used to adjust rheological properties. Fumed oxides, for example, have been used to impart shear thinning properties in suspensions [38, 40, 47, 51, 52]. Because nanoparticles have greater surface area and shorter interparticle distances, there are greater and

stronger interactions between particles that make it easier to form agglomerations thus causing the increase in viscosity and resulting pseudoplastic behavior [37, 41, 52]. The shear thinning behavior occurs because as the shear rate is increased, the weak network of particles is broken to release "entrapped" fluid [51]. The extent of these effects is not only influenced by the size of the particles, but also by their amount, distribution, and shape [37, 52].

Effect of Nanoparticles on Adhesion

Many studies have reported the incorporation of nanoparticles to adhesives such as epoxies to improve adhesive properties by as much as 50% [33, 40, 41, 44, 53]. Most studies have found that there is a limit to the improvement, and that at higher loadings, these properties begin to decline [40, 41]. In addition, properties that are typically inversely related, such as peel strength and lap shear strength have been simultaneously increased with the addition of nanofillers [41].

Improvements to adhesion have been attributed to both chemical and mechanical interactions between the filler and matrix [33, 40, 43, 44, 49]. Nanoparticles can fill in any microscopic "gaps" in the resin and create many contact points within the adhesive as well as at the adhesive-substrate interface [43, 48]. The particles also serve to blunt the crack tip and force cracks to follow a more tortuous path to improve toughness [41, 42]. In addition, particle-substrate interactions such as the formation of bonds between the hydroxyl groups of alumina or silica particles and aluminum substrates have also been reported [43, 49]. The decrease in properties beyond a certain particle loading is largely attributed to poor dispersion.

To help prevent agglomeration, particle loadings can be kept to a minimum or particles can be functionalized [40]. Surface chemistries can be altered to improve particle-matrix adhesion thereby enabling the maintenance of good particle dispersion and enhanced adhesive properties.

Conclusion

It is clear that fillers are able to affect a variety of properties and that the use of nano-sized fillers can give rise to unique properties from conventional fillers. And while the application of nanotechnologies comes with its own set of problems, such even particle distribution, there are strategies for overcoming such problems such as surface functionalization. With these approaches, it is likely that nanocomposites will continue to draw appeal for expanding today's technology into the future.

Cyanate Esters

Cyanate esters (CEs) are a category of thermoset resins that exhibit excellent thermal, mechanical, dielectric, and processing properties. These properties are well-known to be correlated with the monomer structure, and as such, the wide varieties of monomers that exist have found applications in industries that span from aerospace to electronics. Formulations of these monomers and other additives are a main focus of research today [54], and as new formulations and processing methods are developed CEs will continue to replace more common resins such as epoxies.

Epoxies are a very common class of resins by and large due to their versatility. Not only do epoxies exhibit good mechanical, adhesive, processing properties, they are also relatively cheap. In addition, their properties can be tuned and tailored by incorporating a variety of additives and fillers. Despite these qualities, they are rather brittle and lack good hot/wet performance. Compared to epoxies, CEs have much improved hydro/thermal stability [55-61]. With T_g's in the 200 – 300 °C range, not even the highest temperature epoxy formulation can compare [54].

A common replacement for epoxies due to their high temperature stability, are polyimides, such as bismaleimide (BMI). Though they may outmatch CEs in temperature stability, they also have a poor shelf-life and are more difficult to process. Phenolics, another common class of resins, also

have similar disadvantages despite their widespread use due to good heat and fire resistance and low cost [54].

In addition to their excellent hydro/thermal performance, CEs also outmatch the aforementioned resins in their processability [50, 54, 62], shelf-life [54], and compatibility with a variety of reinforcements [54, 58]. CEs also have a low water absorptivity [50, 55, 61, 63] and good adhesion to a variety of substrates [54, 55, 58, 61].

CEs have slowly replaced epoxies in today's electronics industry in wiring boards and circuitry [54, 61, 62], and are steadily expanding into both structural and non-structural aerospace applications such as aircraft composites, radomes, and satellites [54, 62]. However, the biggest drawback of CEs is their high cost [54]. This cost currently limits the use of CEs to areas in which cost is only of secondary concern, such as in electronics and aerospace applications. However, with continued research and development, CEs will likely replace many of the aforementioned resins, and as such, are one of the most important engineering thermoset resins to date [63].

Property Enhancement via Nanofillers

As discussed earlier, fillers are often added to polymer systems to enhance a variety of properties (e.g. thermal, mechanical, rheological, etc.). This is no different in CE systems. A variety of additives have been studied in CE systems from rubbers and thermoplastics to inorganic fillers such as oxide nanoparticles, clays, and carbon nanotubes. Nanofillers in particular can give rise to combinations of properties not possible with conventional fillers. The incorporation of clays for example, has been reported to increase modulus and toughness as well as strength and T_g [45, 50, 63].

Because it is suggested that CEs may form covalent bonds with hydroxyl groups, and since oxide nanoparticles are known to contain hydroxyl groups on their surfaces, it follows that the incorporation of such particles would likely be highly compatible within a cyanate ester matrix. Fumed silica is a very common additive for tailoring the processing characteristics of thermosets, and

in CEs, has been shown to impart shear thinning behavior [64] via interparticle hydrogen bonds that form under low shear rates and are broken apart at high shear strain rates. The same effect was shown in CE/alumina suspensions, although the effect was much less apparent at low loadings [51].

As discussed in a previous section, particles are often functionalized to enhance particle-matrix interfacial adhesion. In one study, functionalizing agents used to treat silica particles were found to slightly enhance properties compared to non-functionalized particles [65].

Bisphenol E Cyanate Ester Nanocomposite Properties and Applications

A new class of cyanate esters, bisphenol E cyanate ester (BECy) has a peculiarly low viscosity at room temperature, 0.09–0.12 Pa s [64], for its high T_g, 274 °C [66], that makes it a reasonable candidate for the resin-injection repair of high T_g composites. The incorporation of nanoparticles is used to optimize rheological properties and enhance mechanical properties for the repair process. Alumina was chosen as it was low cost, readily available, and has been shown to effect rheological and mechanical properties in other studies [41, 44, 51].

In the latter chapters, studies to evaluate the applicability of BECy as an injection repair resin will be discussed, beginning with adhesive testing in Chapter 1, where issues regarding processing conditions will be emphasized. In Chapter 2, the resin will be evaluated in a laboratory-scale injection repair process.

References

[1] Li, H.C.H., P.J. Callus, and I. Herszberg. "Through-thickness Reinforcement Repair of Delaminated Carbon-epoxy Panels." Composite Structures 75.1-75.4 (2006): 539-44.

[2] Aktas, Mehmet, Ramazan Karakuzu, and Yusuf Arman. "Compression-after Impact Behavior of Laminated Composite Plates Subjected to Low Velocity Impact in High Temperatures." Composite Structures 89 (2009): 77-82.

[3] Dehm, S., and D. Wurzel. "Fast, In-situ Repair of Aircraft Panel Components." Journal of Aircraft 26.5 (1989): 476-81.

[4] Sherwin, Glen R. "Non-autoclave Processing of Advanced Composite Repairs." International Journal of Adhesion & Adhesives 19.2-19.3 (1999): 155-59.

[5] Teresko, John. "Boeing 787: A Matter of Materials -- Special Report: Anatomy of a Supply Chain." IndustryWeek 1 Dec. 2007.

[6] Cookson, Ian. "Grant Thornton on US Aerospace Component M&A, 2008." Defense Industry Daily - Military Purchasing News for Defense Procurement Managers and Contractors. 15 Mar. 2009. 17 July 2009 <http://www.defenseindustrydaily.com/>.

[7] Wu, Kuo-Wei, Chang-Lun Lee, Yuan-Chang Chang, and Ching-Long Ong. "Compressive Strength of Delaminated and Repaired Composite Plates." Materials Chemistry and Physics 43 (1996): 173-77.

[8] Russell, A. J., and J. S. Ferguson. Composite Repair Issues on the CF-18 Aircraft. Rep. no. AGARD-CP-550-PAP-14. Victoria, BC (CAN): Defence Research Establishment Pacific, 1995. 30 June 2009 <http://pubs.drdc-rddc.gc.ca/>.

[9] Baker, A. A. Composites Materials in Aircraft Structures. Ed. D. H. Middleton. New York, England: Addison-Wesley Longman, Limited, 1990. 207-27.

[10] Cantwell, W. J., and J. Morton. "The Significance of Damage and Defects and their Detection in Composite Materials: A Review." Journal of Strain Analysis 27 (1992): 29-42.

[11] Hexcel Composites. Composite Repair. Brochure. 1999.

[12] McRae, Kenneth I., Allan G. McCray, Allan J. Russell, and Christopher P. Bowers. "Ultrasonic Imaging of Delamination Damage around Fastener Holes in a Graphite/Epoxy Composite." ASTM special technical publication 1128 (1992): 163-79.

[13] Bartus, S. D. "A Review: Impact Damage of Composite Materials." Journal of Advanced Materials 39.3 (2008): 3-21.

[14] Russell, A. J., C. P. Bowers, and A. J. Moss. "Repair of Delaminations and Impact Damage in Composite Aircraft Structures." Proceedings of the 6th International Conference on Composite Structures, Paisley, Scotl. Barking, Engl: Elsevier Science Publ Ltd, 1991. 145-59.

[15] Smilie, Robert W. Nondestructive Testing: Ultrasonics: Basic Principles. Ed. George Pherigo. 2nd ed. Vol. 1. Harrisburg, NC: PH Diversified, Incorporated, 1999.

[16] Baker, Alan, Stuart Dutton, and Donald Kelly, eds. Composite Materials for Aircraft Structures. Second ed. Reston, VA: American Institute of Aeronautics and Astronautics, Inc., 2004.

[17] "Data Presentation." Ed. Brian F. Larson. Iowa State University. 14 July 2009 < http://www.ndt-ed.org/index_flash.htm >.

[18] "Ultrasonic Non-Destructive Inspection Method (NDI) - Engineers Edge." Engineers Edge - Design, Engineering and Manufacturing Solutions. 3 July 2008 <http://www.engineersedge.com/inspection/ultrasonic.htm>.

[19] Mehrkam, Paul, and Roland Cochran. "Wet Lay-up Patch Repair for Elevated Temperature Composite Structures." Proceedings of the 26th International SAMPE Technical Conference. Atlanta, Georgia. Vol. 26. Covina, CA: SAMPE, 1994. 215-24.

[20] Mehrkam, P., and R. Cochran. "Liquid Dicyanate Ester Monomer Resin for Elevated Temperature Composite Repair Applications." Proceedings of the 7th Technical Conference of the American Society for Composites. Lancaster, PA: Technomic Publ Co Inc., 1992. 12-21.

[21] "Types of Repair - NetComposites." NetComposites - Composites and Reinforced Plastics. 11 July 2008 <http://www.netcomposites.com/EducationIntro.asp>.

[22] Rider, A. N., and D. Parslow. Progress Report on Activities in Support of Composite Repair Engineering Development Program Tasks AF, AH and AI. Rep. no. DSTO-TR-1932. Nov. 2006. Defence Science and Technology Organisation Air Vehicles Div. 10 June 2008 < http://www.dtic.mil/dtic/ >.

[23] Russell, A. J., and C. P. Bowers. Repairing Delaminations with Low Viscosity Epoxy Resins. Rep. no. AGARD-CP-530-PAP-25. Victoria BC (CAN): Defence Research Establishment Pacific, 1992. 30 June 2009 <http://pubs.rddc-drdc.gc.ca/>.

[24] Russell, A. J., and C. P. Bowers. "Resin Requirements for Successful Repair of Delaminations." Proceedings of the 36th International SAMPE Symposium. San Diego, CA. Vol. 36. Covina, CA: SAMPE, 1991. 2279-290.

[25] Bhatia, N. M., and J. D. Labor. Depot Level Repairs for Composite Structures, Development and Validation. Rep.No. 79172-60. Naval Air Development Center. 1985. 24-27.

[26] Pocius, Alphonsus V. and Robert P. Wenz. "Mechanical Surface Preparation of Graphite-epoxy Composite for Adhesive Bonding." SAMPE Journal 21.5 (1985): 50-58.

[27] Chin, Joannie W., and James P. Wightman. "Surface Characterization and Adhesive Bonding of Toughened Bismaleimide Composites." Composites: Part A 27.6 (1996): 419-28.

[28] Benard, Q., M. Fois, M. Grisel, P. Laurens, and F. Joubert. "Influence of the Polymer Surface Layer on the Adhesion of Polymer Matrix Composites." Journal of Thermoplastic Composite Materials 22.1 (2009): 51-61.

[29] Balkova, R., S. Holcnerova, and V. Cech. "Testing of Adhesives for Bonding of Polymer Composites." International Journal of Adhesion & Adhesives 22.4 (2002): 291-95.

[30] Hart-Smith, L.J. "Adhesive Bonding of Composite Structures—Progress to Date and Some Remaining Challenges." Journal of Composites Technology & Research 24.3 (2002): 133-51.

[31] Minford, J. Dean. Handbook of Aluminum Bonding Technology and Data. New York: M. Dekker, 1993.

[32] L.F.M. da Silva and R. D. Adams. "Effect of Temperature on the Mechanical and Bonding Properties of Carbon-reinforced Bismaleimide." Proceedings of the Institution of Mechanical Engineers, Part L: Journal of Materials: Design and Applications 222.1 (2008): 45-52.

[33] Meguid, S.A. and Y. Sun. "On the Tensile and Shear Strength of Nano-reinforced Composite Interfaces." Materials and Design 25.4 (2004): 289-96.

[34] Ashcroft, I.A., D.J. Hughes, and S.J. Shaw. "Adhesive Bonding of Fibre Reinforced Polymer Composite Materials." Assembly Automation 20.2 (2000): 150-61.

[35] Parker , B.M. "Some Effects of Moisture on Adhesive-bonded CFRP-CFRP Joints." Composite Structures 6.1-6.3 (1986): 123-39.

[36] Hussain, M., Y. Oku, A. Nakahira, and K. Niihara. "Effects of Wet Ball-milling on Particle Dispersion and Mechanical Properties of Particulate Epoxy Composites." Materials Letters 26.3 (1996): 177-84.

[37] Li, Joshua Q., and Ronald Salovey. "Model Filled Polymers: The Effect of Particle Size on Rheology of Filled Poly(methyl methacrylate) Composites." Polymer Engineering and Science 44.3 (2004): 452-62.

[38] Hanemann, T. "Influence of Particle Properties on the Viscosity of Polymer-alumina Composites." Ceramics International 34.8 (2008): 2099-105.

[39] Kim, Byung C., Sang W. Park, and Dai G. Lee. "Fracture Toughness of the Nano-particle Reinforced Epoxy Composite." Composite Structures 86.1-86.3 (2008): 69-77.

[40] Hartwig, Andreas, Andreas Luhring, and Jasmin Trautmann. "Spheroidal Nanoparticles in Epoxide-based Adhesives." Macromolecular Materials and Engineering 294.6-294.7 (2009): 363-379.

[41] Gilbert, Eric N., Brian S. Hayes, and James C. Seferis. "Nano-alumina Modified Epoxy Based Film Adhesives." Polymer Engineering and Science 43.5 (2003): 1096-104.

[42] Zunjarrao, Suraj C., and Raman P. Singh. "Characterization of the Fracture Behavior of Epoxy Reinforced with Nanometer and Micrometer Sized Aluminum Particles." Composites Science and Technology 66.13 (2006): 2296-305.

[43] Zheng, Yaping, and Rongchang Ning. "Study of SiO_2 Nanoparticles on the Improved Performance of Epoxy and Fiber Composites." Journal of Reinforced Plastics and Composites 24.3 (2005): 223-33.

[44] Zhai, Lanlan, Guoping Ling, Jian Li, and Youwen Wang. "The Effect of Nanoparticles on the Adhesion of Epoxy Adhesive." Materials Letters 60.25-60.26 (2006): 3031-033.

[45] Dean, Derrick, M. Abdalla, and S. Ganguli. "Big Things in Small Packages – Opportunities and Challenges Await Nano-engineered Adhesives, Sealants, and Coatings." Adhesives Age 46.3 (2003): 12-19.

[46] Dodiuk, H., S. Kenig, I. Blinsky, A. Dotan, and A. Buchman. "Nanotailoring of Epoxy Adhesives by Polyhedral-oligomeric-sil-sesquioxanes (POSS)." International Journal of Adhesives & Adhesives 25.3 (2005): 211-18.

[47] Hartwig, Andreas, Monika Sebald, Dirk Putz, and Lisa Aberle. "Preparation, Characterisation and Properties of Nanocomposites Based on Epoxy Resins – An Overview." Macromolecular Symposia 221 (2005): 127-35.

[48] Zheng, Yaping, Ying Zheng, and Rongchang Ning. "Effects of Nanoparticles SiO_2 on the Performance of Nanocomposites." Materials Letters 57.19 (2003): 2940-944.

[49] Yuan, Junjie, Shuxue Zhou, Guangxin Gu, and Limin Wu. "Effect of the Particle Size of Nanosilica on the Performance of Epoxy/silica Composite Coatings." Journal of Materials Science 40.15 (2005): 3927-932.

[50] Dean, Derrick, Mohamed O. Abdalla, Sabyasachi Ganguli, Moncy Jose, Sandi Campbell, Jeffrey Gillman, Walid H. Awad, and Richard Vaia. "High Temperature Thermoset Nanocomposites." International SAMPE Symposium and Exhibition. Long Beach, CA. Vol. 48. 2003. 2572-584.

[51] Lawler, Katherine A. "Viscosity of Aqueous and Cyanate Ester Suspensions Containing Alumina Nanoparticles." Thesis. Iowa State University, 2009.

[52] Zhou, Yabin, Shifeng Wang, Yong Zhang, Yinxi Zhang, Xuhua Jiang, and Dengfeng Yi. "Rheological Properties of PDMS filled with $CaCO_3$: The Effect of Filler Particle Size and Concentration." Journal of Applied Polymer Science 101.5 (2006): 3395-401.

[53] Hsiao, Kuang-Ting, Justin Alms, and Suresh G. Advani. "Use of Epoxy/multiwalled Carbon Nanotubes as Adhesives to Join Graphite Fibre Reinforced Polymer composites." Nanotechnology 14.7 (2003): 791-93.

[54] Reghunadhan Nair, C. P., Dona Mathew, and K. N. Ninan. "Cyanate Ester Resins, Recent Developments." Advances in Polymer Science 155 (2001): 1-99.

[55] Koh, Henry C.Y., Jie Dai, and Eileen Tan. "Curing Behavior and Thermal Mechanical Properties of Cyanate Ester Blends." Journal of Applied Polymer Science 102.5 (2006): 4284-290.

[56] Wang, Jinhe, Guozheng Liang, Hongxia Yan, and Shaobo He. "Mechanical and Thermal Properties of Functionalized Multiwalled Carbon Nanotubes/cyanate Ester Composite." Polymer Engineering and Science 49.4 (2009): 680-84.

[57] Chao, Fen, Nicola Bowler, Xiaoli Tan, Guozheng Liang, and Michael R. Kessler. "Influence of Adsorbed Moisture on the Properties of Cyanate Ester/$BaTiO_3$ Composites." Composites Part A: Applied Science and Manufacturing 40.8 (2009): 1266-271.

[58] Kasehagen, Leo J., Idelette Haury, Christopher W. Macosko, and David A. Shimp. "Hydrolysis and Blistering of Cyanate Ester Networks." Journal of Applied Polymer Science 64.1 (1997): 107-13.

[59] Ramirez, Michael L., Richard Walters, Richard E. Lyon, and Edward P. Savitski. "Thermal Decomposition of Cyanate Ester Resins." Polymer Degradation and Stability 78.1 (2002): 73-82.

[60] Possart, Wulff, and Stefan Dieckhoff. "Adhesion Mechanisms in a Cyanurate Prepolymer on Silicon and on Aluminium." International Journal of Adhesion & Adhesives 19.6 (1999): 425-34.

[61] Wooster, Tim J., Simmi Abrol, and Douglas R. MacFarlane. "Polymeric Toughening of Particle Filled Cyanate Ester Composites." Macromolecular Materials and Engineering 290.10 (2005): 961-69.

[62] Fang, Treliant, and David A. Shimp. "Polycyanate Esters: Science and Applications." Progress in Polymer Science 20.1 (1995): 61-118.

[63] Ganguli, Sabyasachi, Derrick Dean, Kelvin Jordan, Gary Price, and Richard Vaia. "Mechanical Properties of Intercalated Cyanate Ester-layered Silicate Nanocomposites." Polymer 44.4 (2003): 1315-319.

[64] Goertzen, William K., Xia Sheng, Mufit Akinc, and M. R. Kessler. "Rheology and Curing Kinetics of Fumed Silica/cyanate Ester Nanocomposites." Polymer Engineering and Science 48.5 (2008): 875-83.

[65] Wooster, Tim J., Simmi Abrol, Jeffrey M. Hey, and Douglas R. MacFarlane. "The Effect of Particle Matrix Adhesion on the Mechanical Properties of Silica Filled Cyanate Ester Composites." Macromolecular Materials and Engineering 289.10 (2004): 872-79.

[66] Sheng, X., M. Akinc, and M. R. Kessler. "Cure Kinetics of Thermosetting Bisphenol E Cyanate Ester." Journal of Thermal Analysis and Calorimetry 93.1 (2008): 77-85.

CHAPTER 2. LAP SHEAR TESTING OF BISPHENOL E CYANATE ESTER: EFFECTS OF SUBSTRATE, TEMPERATURE, ALUMINA NANOPARTICLES, AND MOISTURE

A paper to be submitted to a peer reviewed journal

Wilber Lio, Mufit Akinc, Michael R. Kessler

Introduction

Polymer matrix composites (PMCs) are becoming the material of choice in a wide array of applications as advancing technologies require stronger and lighter materials. This trend is most prominent in the aircraft industry; however other civilian and military sectors are also seeing an increase in the use of PMCs in recent years. The choice of using composites is often made due to their superior strength, stiffness, and fatigue and corrosion resistance compared to metals in addition to the drastic weight savings that can be achieved [1-4].

One of the greatest drawbacks of PMCs, in aircraft applications especially, is their susceptibility to impact damage, such as from a bird strike or a tool drop. Though sometimes invisible to the naked eye (Figure 1), delaminations and microcracks caused by impact damage can be highly detrimental to mechanical properties [5].

Resin-injection is a non-patch repair technique that has advantages over other techniques such as the ability to create a smooth repair surface with minimal invasion into the composite (Figure 1). Resins that are used for this technique must have low viscosities for injection purposes, and must also exhibit adequate temperature stability and adhesive strength for the intended application.

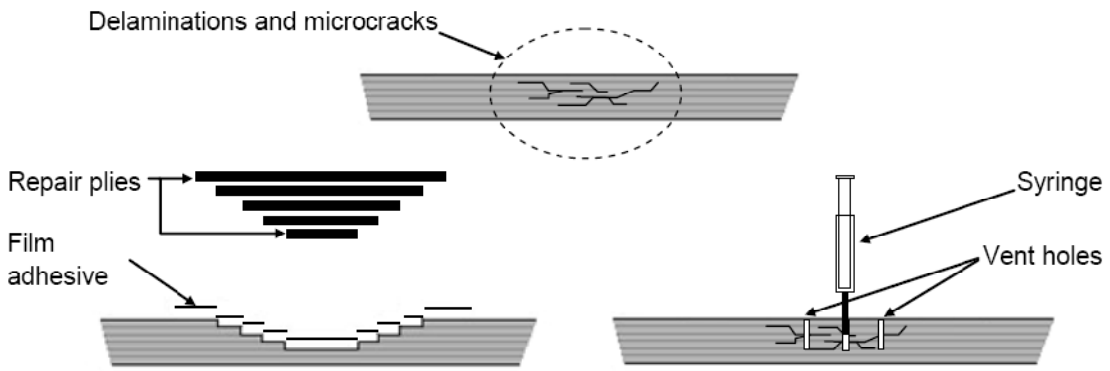

Figure 1. Impact damage (top), scarf repair (bottom left), and resin-injection (bottom right) [6].

The low viscosity requirement becomes a problem in the resin-injection repair of high glass transition temperature (T_g) composites because of the typical trend for resin viscosity to increase with cured T_g (Figure 2). High temperature resins tend to have higher viscosities, and are therefore less processible and difficult to inject. However, a new class of cyanate esters defies this trend. Bisphenol E cyanate ester (BECy) has a peculiarly low viscosity for its high T_g that makes it a reasonable candidate for the resin-injection repair of high T_g composites.

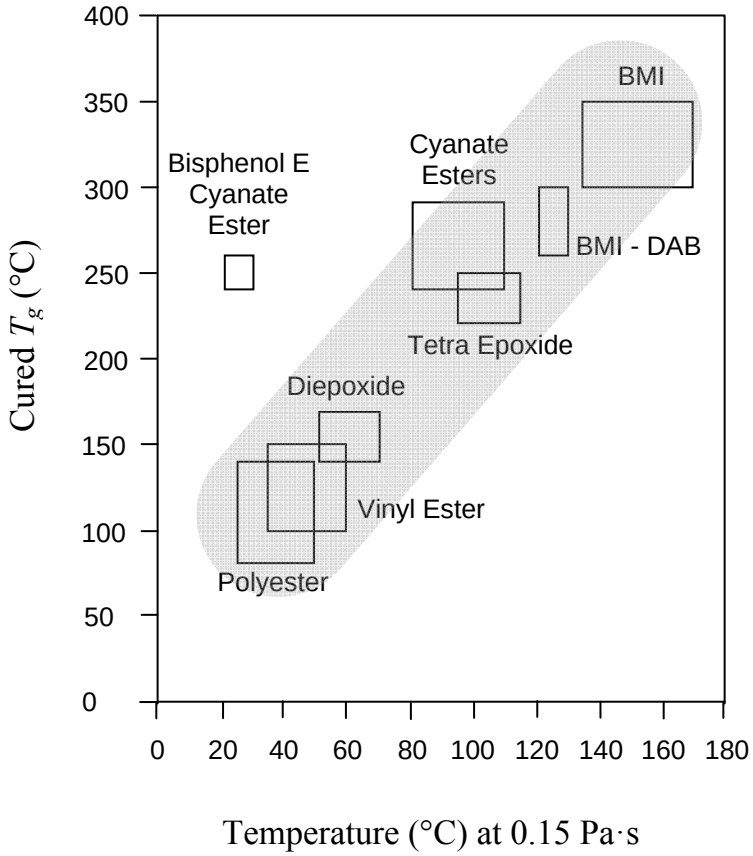

Figure 2. High T_g resins typically have high viscosities; bisphenol E cyanate ester is an exception [7].

The creation of nanocomposites is becoming quite commonplace for the improvement of material properties. The types of filler that are used span a wide range of materials, morphologies, and sizes. Nanoparticles have been studied rather extensively due to their ability to drastically improve properties beyond those which can be obtained by their microparticle counterparts and beyond that which has been predicted by conventional models [8-11]. This may be due to the fact that nanoparticles have such a high specific surface area compared to other morphologies, and because atoms at the surface behave quite differently than in the bulk. Even small loadings of nanoparticles are able to drastically change material properties [12] such as strength and toughness by as much as 50% [13]. Additionally, combinations of properties not possible with conventional fillers

are sometimes obtainable through nanocomposites [9, 14-16], such as the simultaneous improvement of strength and toughness—properties that is typically inversely related [13-15].

Numerous studies have shown rheological properties to be tunable with nanoparticle loading. Fumed oxides are one of the most common fillers, and have been shown to impart shear thinning properties in suspensions [13, 16-19]. The extent of these effects is not only influenced by the size of the particles, but also by their amount, distribution, and shape [19, 20].

The incorporation of nanoparticles to adhesives such as epoxies has also been quite extensively studied. Nanoparticles have been shown to improve adhesive properties by as much as 50% [10, 13, 15, 21, 22]. Studies typically find a limit to this improvement, where at higher loadings, these properties begin to decline [13, 15].

Because of the importance of adhesive bonding in the injection repair application of BECy, it is imperative to characterize the adhesive strength and to understand the various factors that can influence these bond strengths. Because many adhesive joints are subjected to shear stresses [23], it is logical to examine shear strengths. Lap shear tests are a quick and inexpensive method to assess shear strengths, and in fact, lap shear strength is the most commonly reported adhesive property [24, 25].

In this study, lap shear tests were conducted on BECy and BECy/alumina nanocomposites. Alumina was chosen as it was low cost, readily available, and has been shown to effect rheological and mechanical properties in other studies [10, 15, 18] that may prove beneficial for the resin injection repair application of BECy. The effects of nanoparticle loading, preparation, test temperatures, as well as substrate and surface preparation are investigated.

Materials and Methods

Resins

The bisphenol E cyanate ester (BECy) monomer (EX1510 resin), purchased from Bryte Technologies, Inc. (Morgan Hill, CA), was used as received without further purification. The liquid phase organometallic-based catalyst, EX1510-B, was supplied with the resin.

Spherical alumina nanoparticles (ANP) were supplied by Nanophase Technologies, Inc. (Romeoville, IL) as NanoTek aluminum oxide, which is γ-phase alumina with an average particle diameter of 48 nm. Before use, the nanoparticles were dried at 110 °C for 2 h.

BECy-ANP suspensions containing 2.5, 5, and 10 volume percent (v%) alumina were prepared by first weighing the BECy monomer in a glass vial. Then the dried ANP were weighed and added. The vial was sealed and suspended in an ultrasonic water bath for 50 min. The suspensions were re-sonicated in the water bath for 15 min prior to use.

An epoxy resin, EPON 828, was used as a benchmark comparison to the cyanate ester being investigated. The epoxy along with its curing agent, Epikure™ 3223, was purchased from Miller-Stephenson Chemical Company, Inc. (Morton Grove, IL). Butyl glycidyl ether (BGE) was used as a reactive diluent to lower the viscosity of the benchmark resin, and was purchased from Sigma-Aldrich (Milwaukee, WI).

Substrates

Aluminum and bismaleimide-carbon fiber (BMI-cf) coupons for lap shear tests were machined roughly to ASTM standard (D 1002-05 and 5868-01, respectively). Aluminum coupons were bead blasted, and cleaned with acetone prior to bonding. BMI-cf prepreg was supplied as HTM 512 prepreg by Advanced Composites Group, Inc. (Tulsa, OK). The lay-up of prepreg plies were cured in a hot press at 190 °C and 0.6 MPa (90 psi) compaction pressure for 6 hours followed by a

free-standing post-cure for 8 h at 240 °C based on a schedule suggested by the supplier. Coupons were then cut from the panel and cleaned by sonicating in acetone.

A polyester peel ply, Release ply Super F, was supplied by Airtech International (Huntington Beach, CA). This ply was added to the prepreg lay-up and cured onto the composite surfaces. Upon curing, the peel ply was removed to reveal a clean and textured surface ready for bonding. Sandpaper (100 and 180 grit) was also used to prepare surfaces of several BMI-cf samples for bonding. Unless otherwise stated, all BMI-cf lap shear samples discussed used peel ply surfaces.

Lap Shear Sample Preparation

Lap shear specimens were prepared by first applying resin onto one coupon. The second coupon was then placed accordingly to obtain the desired overlap length and excess resin was wiped from the edges. Small metal binder clips were used to clamp the specimens together during curing.

For both BECy and BECy-ANP suspensions, catalyst was added in a 100:3 (resin:catalyst) weight ratio. The benchmark epoxy and curing agent were mixed in a 10:1 weight ratio. In addition, the diluent BGE was added to the epoxy (25 weight percent BGE) in order to decrease its viscosity to the same level as that of BECy.

The standard cure schedules for BECy and the epoxy are listed below:

A. BECy: 180 °C for 2 h, 250 °C for 2 h (1 °C/min) in convection oven

B. Epoxy: 80 °C for 1 h (1 °C/min) in convection oven

Aluminum lap shear and all epoxy samples were cured following their standard cure schedules. However, for BMI-cf lap shear samples, several other cure schedules were tested:

C. 180 °C for 2 h, 250 °C for 2 h (0.3 °C/min) in convection oven

D. 100 °C for 4 h (1 °C/min) in convection oven, followed by (A)

E. 100 °C for 4 h (1 °C/min) in vacuum, followed by (A)

F. 100 °C for 8 h (0.3 °C/min) in convection oven, followed by (A)

G. 100 °C for 8 h (0.3 °C/min) in vacuum, followed by (A)

H. 100 °C for 8 h (0.3 °C/min) in convection oven, followed by (C)

I. 100 °C for 4 h (0.3 °C/min) in convection oven, followed by

   a. 150 °C for 2 h (1 °C/min)

   b. then 160 °C for 2 h (1 °C/min)

   c. then 170 °C for 2 h (1 °C/min)

   d. then 180 °C for 2 h (1 °C/min)

   e. then 250 °C for 2 h (1 °C/min)

Some samples were subjected to thermal cycling prior to room temperature lap shear tests. This was done using a vertical tube furnace setup, in which samples were mechanically raised and lowered into and out of the furnace chamber. Samples were cycled 100 times between room temperature (10 min) and 200 °C (30 min).

Lap Shear Testing

An Instron 5569 tensile testing machine (Norwood, MA) was used to perform lap shear tests. Spacers were attached to opposite sides of the ends of the lap shear specimens during tests to compensate for the inherent offset of the coupons. Aluminum and BMI-cf substrate samples were pulled at extension rates of 1.3 and 0.5 mm/min, respectively, until failure. High-temperature tests (conducted at 200 °C) were performed using an Instron SFL Heatwave temperature controlled chamber. Samples were allowed to equilibrate for 5 minutes at 200 °C prior to starting the test.

Thermogravimetric Analysis

Thermogravimetric analysis (TGA) on the BMI-cf composite as well as neat BMI resin was conducted with a TA Instruments Q50 thermogravimetric analyzer (New Castle, DE). Specimens that were tested included cubes (0.1 in × 0.1 in × 0.1 in) of post-cured BMI-cf as well as small pieces of

post-cured BMI obtained from the flash produced during laminate manufacture. Samples were heated from room temperature (RT) to 400 °C at 10 °C/min in air.

Differential Scanning Calorimetry

Differential scanning calorimetry (DSC) was conducted using a TA Instruments Q2000 differential scanning calorimeter (New Castle, DE). Two samples were tested:

1. BECy + catalyst
2. BECy + catalyst + BMI-cf powder (15 weight percent)

The components were sealed in an aluminum sample pan and initially ramped to 350 °C at 6 °C/min to obtain a dynamic cure scan, after which, the specimen was cooled to 30 °C and re-heated to 350 °C at 10 °C/min.

Results and Discussion

Due to the small sample sizes, box-and-whisker plots were chosen to represent a majority of the data. In these plots, the main "box" is split into upper and lower halves (quartiles), by a line that represents the median data value. The whiskers extend from the top and bottom of the box to the maximum and minimum data values that are not considered outliers. Outliers are represented as dots beyond the whiskers, and are typically considered any values beyond 1.5 times the upper or lower quartile.

BECy and BECy-ANP outperformed the benchmark epoxy in lap shear tests on aluminum substrates, especially at high temperatures (Figure 3). This is expected as the T_g of the epoxy is below 200 °C [26, 27]. The high adhesion on aluminum may be due to covalent interaction with surface hydroxyl groups [28, 29], however other adhesion mechanisms have been described as well [30]. Although it may be inferred that the addition of 5 v% ANP may slightly increase the lap shear strength, because of the large amount of scatter within each sample, this conclusion is not well-

supported. It can be more confidently stated that the addition of ANP does not drastically improve the lap shear strength and that no more than 10 v% ANP should be used to avoid a decrease in lap shear strength. Similar trends are seen at 200 °C.

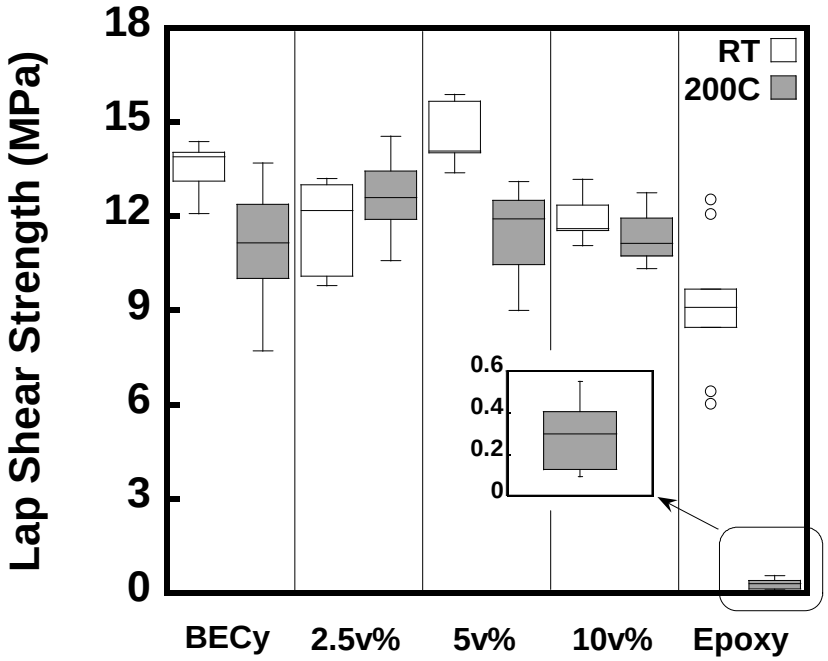

Figure 3. Effect of ANP loading and temperature on lap shear strength on aluminum substrates with 0.5 in^2 overlap areas (3 to 10 samples were tested for each condition).

The lap shear strengths of BECy and BECy-ANP on BMI-cf were found to be inferior to that of the epoxy—even at high temperatures for BECy-ANP (Figure 4). More testing may be necessary to confirm this observation, but due to time and material constraints, further testing down this avenue was not pursued.

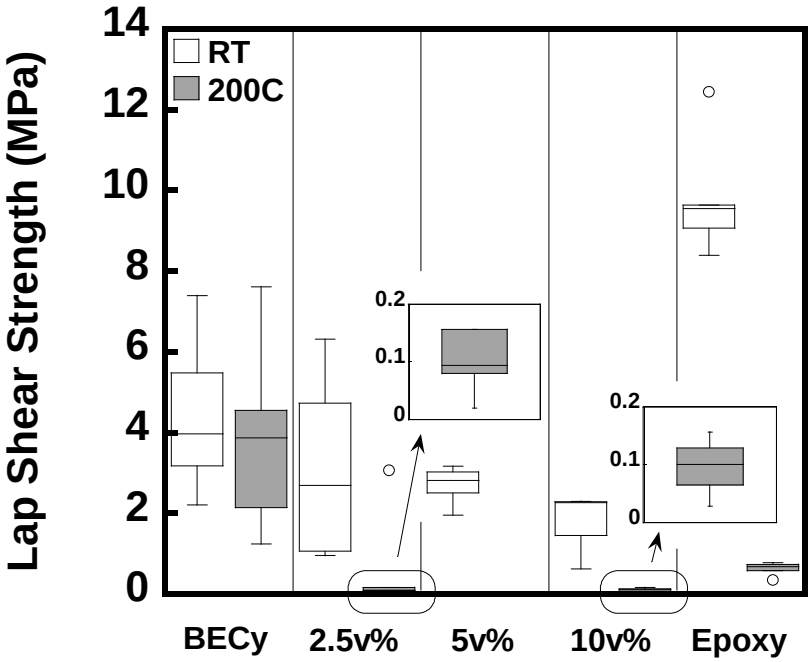

Figure 4. Effect of ANP and temperature on lap shear strength on BMI-cf substrates with 1 in^2 overlap areas (3 to 23 samples were tested for each condition).

Note: Data used to create this figure encompass all curing conditions to represent the range of lap shear strengths that have been obtained. No samples of 5 v% ANP were tested at 200 °C.

The lap shear strengths in Figure 4 are also inferior to the strength of samples on aluminum substrates in Figure 3. However, because overlap area can have a significant effect on lap shear strength [23, 25], those strengths cannot be directly compared. The reason for the different overlap areas was merely a matter of conforming to standards. ASTM standard D 1002-05, which governs the lap shear testing of adhesives on metal substrates, calls for a 1 in × 0.5 in overlap area and ASTM standard D 5868-01, which governs lap shear testing with fiber-reinforced plastic substrates, calls for an overlap area of 1 in × 1 in.

In order to compare the lap shear strengths on aluminum and BMI-cf, BMI-cf lap shear samples were next prepared with 1 in × 0.5 in overlap areas (Figure 5). Although more comparable in

strength to aluminum samples, the lap shear strengths are still inferior. ANP also seem to have a more pronounced detrimental effect beginning from as low as 2.5 v% loadings.

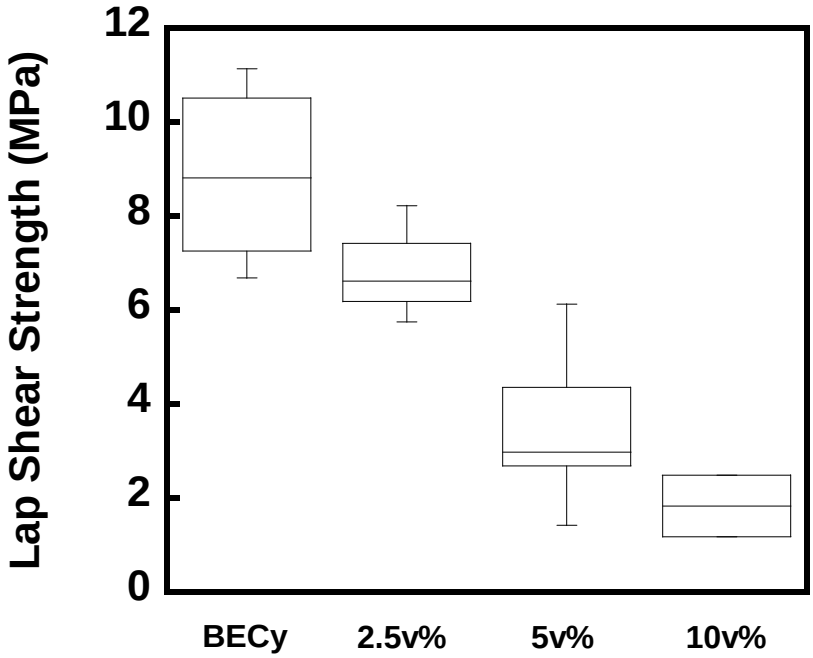

Figure 5. Effect of ANP on lap shear strength on BMI-cf substrates with 0.5 in^2 overlap areas (2 to 16 samples were tested for each condition).

As seen in Figure 4 and Figure 5, decreasing the overlap area leads to a decrease in lap shear strength on BMI-cf substrates. This is contrary to some findings [23, 25] as well as what would be intuitively expected; however, it may be the result of thinner adhesive thicknesses attributed to the increased clamping pressure on the decreased overlap area due to the utilization of the same clamping force to hold coupons together during curing [31]. All lap shear samples reported were prepared using binder clips, so the exact pressure was unknown. The effect of overlap area can be seen more clearly in Figure 6.

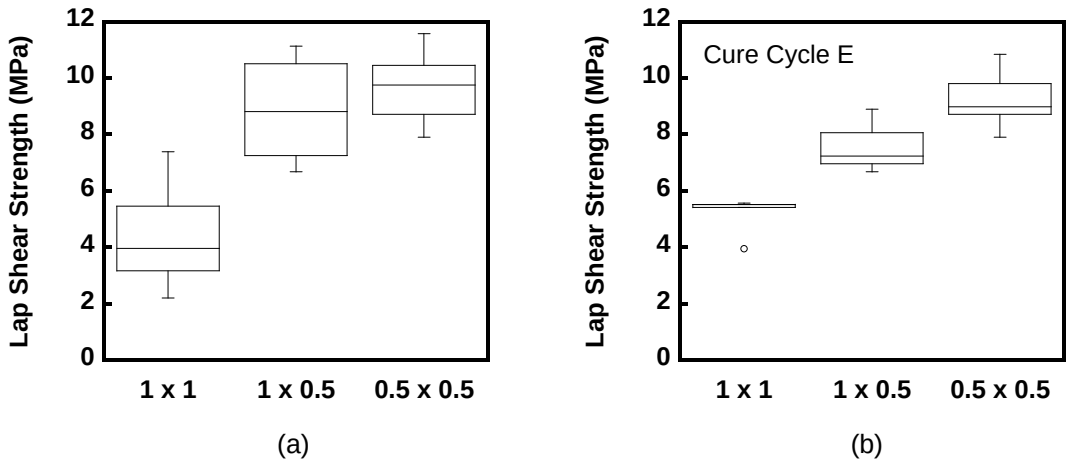

Figure 6. Effect of overlap area on lap shear strength on BMI-cf substrates. (a) All cure schedules, (b) Cure schedule E only (11 to 23 and 3 to 7 samples were tested for each overlap area, respectively).

The effects of thermal cycling (Figure 7) on neat BECy as well as on the epoxy benchmark are minimal. For the neat BECy, this is expected, as BECy has a T_g greater than 200 °C. However, the effect on the epoxy is not as intuitive. It would be expected that the epoxy would degrade at temperatures above its T_g, and thus, cycling to temperatures such as 200 °C would be detrimental to its later performance at room temperature. However this was not the case, and in fact, a possible increase in lap shear strength was seen. One explanation for this is that the epoxy had not been fully cured prior to conditioning, and that the thermal cycling schedule further cured the resin, leading to enhanced performance. The effect of a 200 °C test temperature, however, was especially detrimental to the epoxy as well as to BECy-ANP, as seen before on samples of different overlap areas. The reason for the 0.25 sq in overlap areas in the thermally cycled samples is due to the size constraints of the furnace used for thermal cycling.

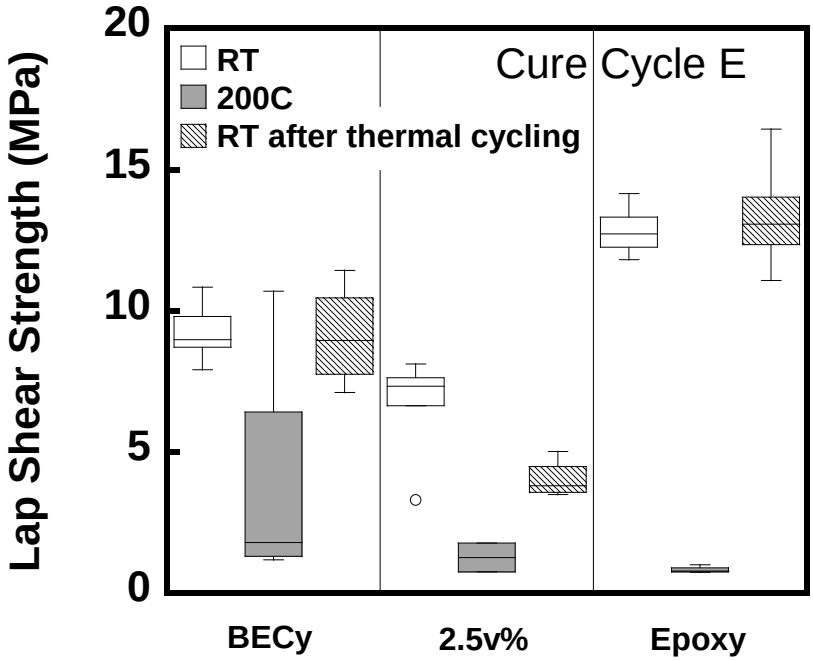

Figure 7. Temperature and thermal cycling effects on lap shear strength on BMI-cf substrates with 0.25 in^2 overlap areas (2 to 7 samples were tested for each condition).

It is clear that the addition of alumina nanoparticles does not greatly enhance the lap shear strength of BECy. At its worst, the ANP may even be detrimental to lap shear strength and high temperature stability of the resin. Kinloch and Taylor [32] found a variety of oxide particles including aluminum oxide to have little to no effect on toughening in bisphenol A cyanate esters. Their study further reported that nano-sized particulates actually reduced the fracture energy of the resin. These findings may be related to those in this study, as toughness is related to strength.

Nanoparticles have also been shown to catalyze cure reactions in cyanate ester systems [11, 18, 28, 33-36]. Dynamic DSC scans have revealed exothermic peak temperatures to decrease with ANP nanoparticle loading [18, 36]. Two exothermal peaks have also been observed at low particle loadings (0 to 4 v%) which indicate the introduction of a different curing environment and

mechanism. These effects were attributed to hydroxyl functionalities on the surfaces of the nanoparticles reacting with the matrix as well as the presence of adsorbed moisture.

These findings imply that the cure schedule for neat BECy may not be suitable for BECy-ANP resins, and that the cure schedule of BECy-ANP nanocomposites needs to be optimized in order to positively evaluate and conclude the effects of ANP additions. The same can be said to explain the inferiority in both magnitude and consistency of lap shear strengths on BMI-cf substrates to those on aluminum substrates. This may also be merely a result of less-than-optimal processing conditions for the particular resin/substrate system, as opposed to adhesive properties of the resins themselves.

An unusual artifact appeared in lap shear samples made with BECy and BECy-ANP on BMI-cf substrates. These samples exhibit bubbles on the edges of the overlap areas that are not apparent on aluminum substrates (Figure 8). It is believed that the bubbles are related to the poor and inconsistent adhesion observed on BMI-cf substrates.

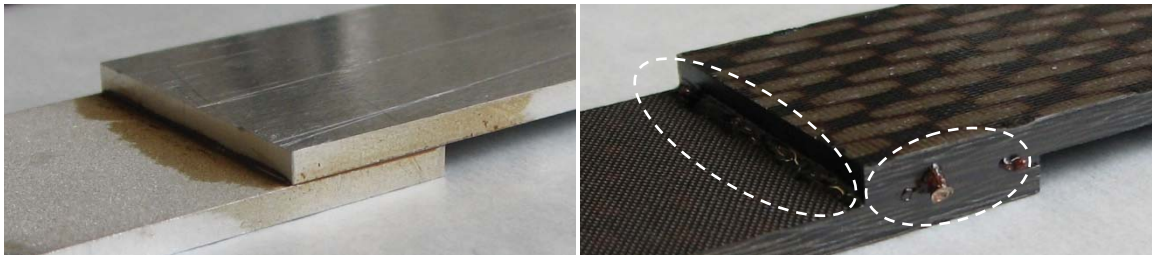

Figure 8. Aluminum (left) and BMI-cf (right) lap shear samples that show the pristine edges on aluminum and bubbles on BMI-cf.

Several hypotheses to explain the cause of these bubbles and in turn the poor lap shear strengths were examined. Experiments were conducted to investigate the effects of surface preparation, cure schedule, and moisture.

It is well known that surface preparation plays an important role in adhesive bonding. Untreated composite surfaces are typically contaminated with release agents used during the

manufacturing process. Typical surface treatments include sanding, blasting, and the use of a peel ply; less common include laser and plasma treatments.

Trials with sanded BMI-cf surfaces (using 100 and 180 grit sandpapers) resulted in poor adhesion compared to peel ply surfaces, as well as the continued bubbling (Figure 9). The problem with sanded samples was partly related to the smooth surface obtained even with medium-grit sandpaper. As a result, very little resin remained in the overlap area after sandwiching the lap shear coupons together.

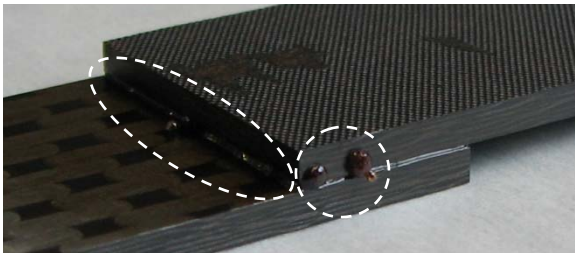

Figure 9. Sanded BMI-cf substrates continue to exhibit bubbles. This indicates the rough peel ply surfaces are not the culprit.

Sand-blasted surfaces gave higher strengths that were more comparable to that of aluminum substrate samples, but the strength values may have been affected by more than just the surface preparation. Sand blasting the composite surface left peaks and valleys on the length-scale of millimeters as depicted in Figure 10.

The result is a rather large adhesive thickness that may be responsible for the increased lap shear strength. Though bubbling was less apparent in these samples, it is possible that the gas causing the bubbles were better able to dissipate into the atmosphere due to the increased resin surface area open to the atmosphere.

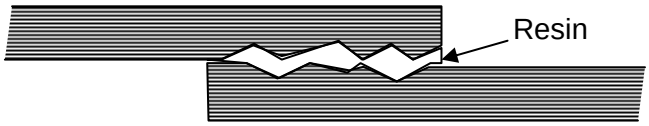

Figure 10. Depiction of the uneven surface produced from sand-blasted BMI-cf lap shear samples and its effect on the amount of resin within the overlap area.

Samples using peel ply surfaces were further examined in a continued attempt to reduce bubbles and improve lap shear strength. Because peel ply surfaces have been reported to trap air and moisture between substrates due to the surface roughness [24, 37, 38], samples were initially heated for a period of time (4 to 8 h) at a lower temperature (100 °C) in vacuum [31], similar to a degassing process (cure schedules E and G). Though several samples were bubble free and exhibited greater strength, the results were inconsistent and varied from batch to batch. The vacuum technique was therefore not pursued further.

The pre-cure step described above was performed due to limitations of the vacuum oven. However, it was noted that an initial pre-cure at lower temperatures for longer times seemed beneficial to lap shear strength (Figure 11). It is possible that due to the thermal properties of the composite substrate, that the exothermic heat from the curing of BECy is not readily dissipated, leading to localized temperatures that exceed the temperature limits of the resin. To that same effect, lower heating rates were also found to be beneficial to lap shear strength (Figure 12).

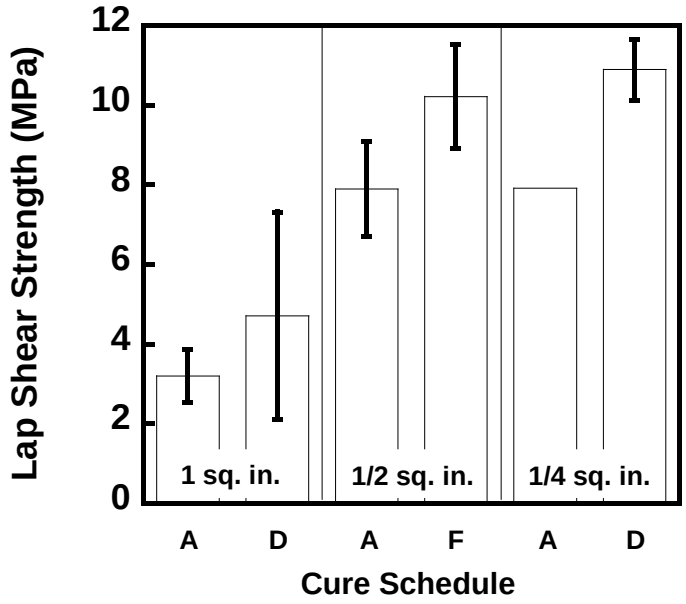

Figure 11. The effect of adding a pre-cure step on RT lap shear strength of BECy on BMI-cf (1 to 9 samples were tested for each condition). See the Materials and Methods section for cure cycle details.

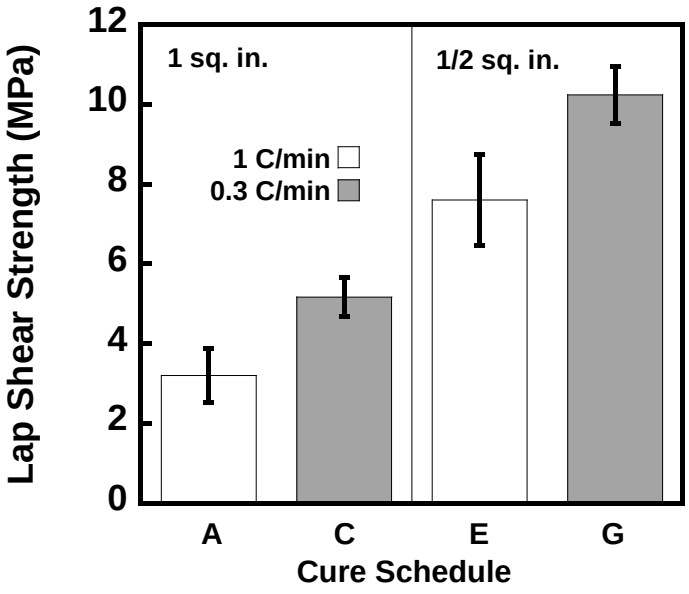

Figure 12. The effect of heating rate on RT lap shear strength of BECy on BMI-cf (3 to 9 samples were tested for each condition). See the Materials and Methods section for cure cycle details.

Because of this, a cure schedule that combined both a pre-cure step and a slower heating rate was tested (cure schedule H). The results, however, were not as expected; the lap shear strengths were actually lower than obtained via other cure schedules (average: 7.6 MPa, standard deviation: 0.77). It is possible that the slower heating rate at high temperatures was detrimental because the highest temperature during the cure schedule (250 °C) was too high for the particular resin/substrate system.

The findings described above then led to an investigation of the effect of cure temperature on lap shear strength (cure schedules I.a. through I.e.). The results are summarized in Table 1.

Table 1. The effect of curing temperature on RT lap shear strength of BECy on BMI-cf.

Sample[†,‡]	Cure Schedule	Lap Shear Strength[††] (MPa)
1	150 °C for 2 h (1°C/min)	10.4
2	+160 °C for 2 h (1 °C/min)	10.6
3	+170 °C for 2 h (1 °C/min)	8.3
4	+180 °C for 2 h (1 °C/min)	9.0
5	+250 °C for 2 h (1 °C/min)	6.7

† All samples were subjected to a 100 °C for 4 h pre-cure (0.3 °C/min).
‡ All samples had bubbles.
†† A 0.5 sq in overlap area was used.

The lap shear strength decreased with increasing cure temperature which supports the hypothesis that the cure temperature affects the strength of the adhesive. The failure surface of sample 5 was also notably different than the other four samples (Figure 13). It was also noted that bubbles appeared in all samples, and developed at temperatures as low as 150 °C.

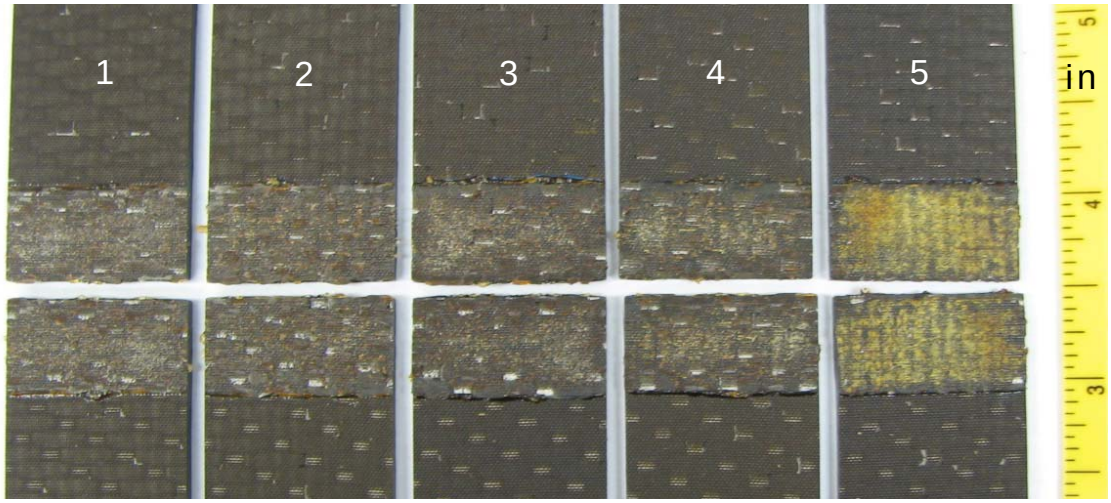

Figure 13. Failure surfaces of BECy lap shear samples on BMI-cf prepared via cure schedule I.

Another possible explanation for the bubbles and decreased lap shear strengths on BMI-cf is hydrolysis of cyanate groups in the presence of moisture. Moisture can lead to the formation of unstable carbamates that can lead to the evolution of CO_2 [39-41]. In fact, blistering is a commonly reported problem in cyanate ester laminates as a result of as little as 2% moisture content [42-44]. Kasehagen et al. [40] proposed that blisters form due to hydrolysis in local regions that decrease the local T_g. When the temperature of the resin exceeds the local T_g, the built up pressure from hydrolysis reactions then expand to form a blister. Though CO_2 formation is usually reported as occurring at temperatures greater than 170 °C , thin films of carbamate-containing polymers have been reported to decompose after 1 hour at as low as 150 °C [43]. The thin film of BECy between the lap shear coupons may therefore, be more susceptible to degradation from moisture than in bulk samples.

Though cyanate esters are known for low moisture absorption, thermosets in general have a tendency to absorb large amounts of water in humid environments [45, 46]. Thermogravimetric analysis of BMI and BMI-cf specimens was used to determine the amount of moisture, if any, absorbed by the composite substrates that may have been causing the bubbling in lap shear samples (Figure 14). Both cubes of BMI-cf and pieces of neat BMI resin that had undergone the same

processing conditions were tested. Normalized weight losses for the samples are summarized in Table 2 to account for the fact that BMI-cf samples were roughly 36% resin. The percent weight loss observed up to 250 °C (the maximum temperature for all BECy cure schedules) was relatively consistent. Deviations can be attributed to differences in sample shape and surface area. For example, the BMI-cf sample that had been prepared with a peel ply (peel ply removed) exhibited the greatest weight loss because of the large amount of surface area that was exposed due to the rough peel-ply texture.

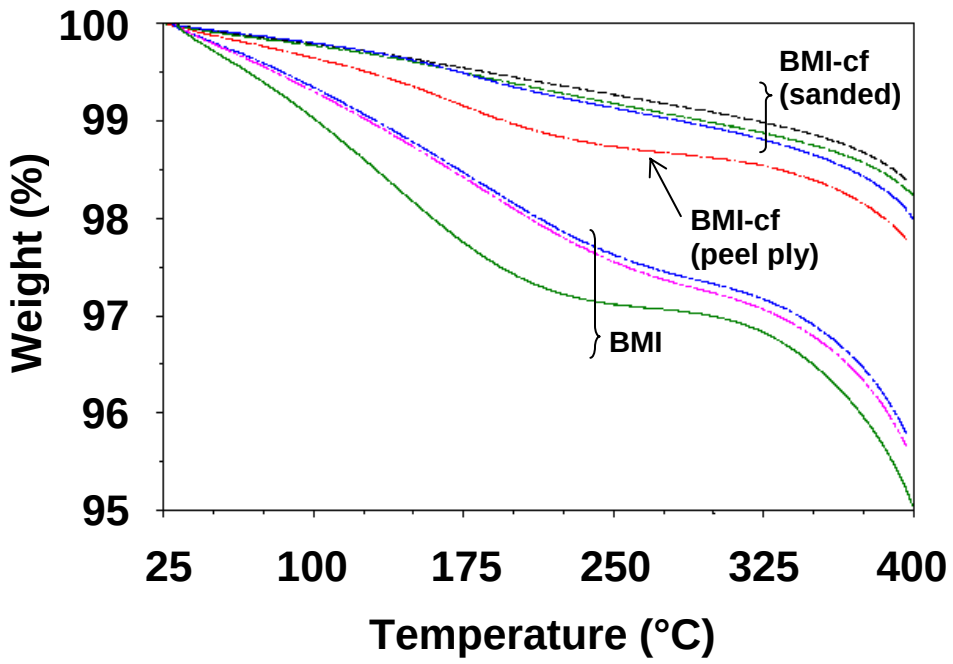

Figure 14. TGA curves of BMI and BMI-cf samples.

Table 2. Average cumulative weight loss of BMI and BMI-cf samples at different temperatures, normalized with respect to BMI content.

Sample	Weight (%) lost by 100 °C	Weight (%) lost by 180 °C	Weight (%) lost by 250 °C
BMI-cf (sanded)	0.60	1.4	2.3
BMI-cf (peel ply)†	1.0	2.5	3.5
Post-cured BMI	0.78	1.8	2.6

† Only one sample was tested.

Similar TGA curves to those obtained in this study were reported by Simpson et al. [47], who attributed the weight loss at temperatures below 250 °C to desorption of water. In their study, it was also noted that dried samples that were left in air overnight regained moisture as seen in subsequent TGA scans. Other studies have also reported weight loss due to moisture in BMI composites [48]. This strongly supports the hypothesis that absorbed moisture from the composite diffuses out of the BMI substrate during the curing of BECy lap shear samples to react with the cyanate groups by some mechanism as shown in Figure 15.

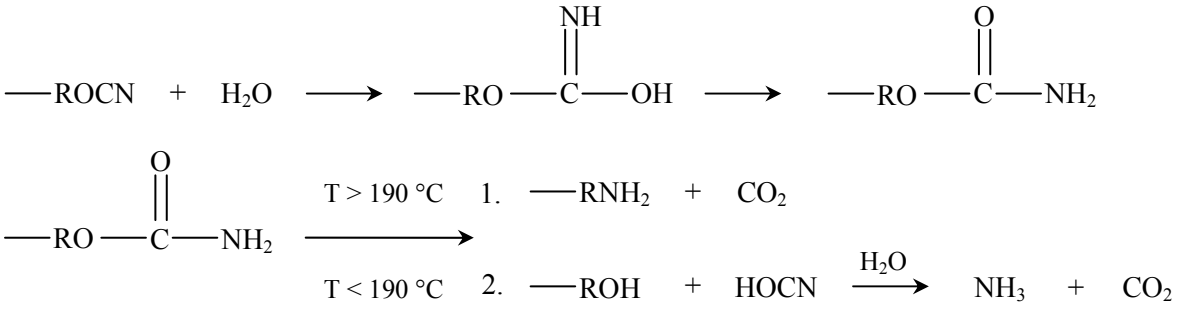

Figure 15. Hydrolysis of cyanate groups that can lead to the evolution of CO_2 [44].

As a quick confirmation of the effect of water on the curing of BECy, two gelled pieces of BECy (cured at 100 °C for 4 h) were placed in separate glass vials. A couple drops of water were

then added to one of the vials and covered. The result after the typical cure schedule (A) resulted in bubbles in the specimen cured in the presence of water (Figure 16).

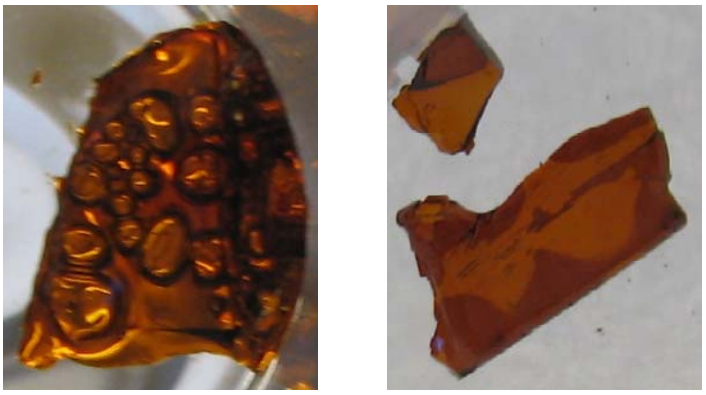

Figure 16. BECy resin cured in the presence of water (left) developed bubbles. Regularly cured sample (right) exhibited no such bubbling.

Dynamic DSC scans revealed a significant decrease in the T_g of BECy due to the presence of BMI-cf as summarized in Table 3. This decrease could be due to the effect of moisture in the BMI-cf powder. Water could hydrolyze the cyanate groups in the BECy monomer leaving fewer groups to participate in the cyclotrimerization reaction, rendering the resultant network with fewer cross-links and a lower T_g.

Table 3. Dynamic DSC scans reveal a decrease in the T_g of BECy in the presence of BMI-cf.

Sample	T_g (°C)
BECy + catalyst	281.5
BECy + catalyst + BMI-cf powder	272.4

For the samples containing BMI-cf, post-cured BMI-cf composite was ground into a powder which was added to a BECy and catalyst solution at 15 wt% BMI-cf. This was done to create a more homogenous DSC sample although not perfectly mimicking the effects of BMI-cf on BECy in lap

shear samples. However, because only a thin layer of resin is used in lap shear samples, most of the resin would be interacting with the BMI-cf and so the effects of BMI-cf in lap shear tests, though maybe not as pronounced as from DSC tests in which the resin was mixed with BMI-cf, are likely to still be profound enough to drastically affect lap shear strengths.

In another study by Karad et al. [49], cure schedules were found to affect the moisture uptake in a cyanate ester-modified epoxy. The increase in moisture absorption with post-cure temperature was attributed to the increase of free volume with cross-link density as post-cure temperatures were raised due to the fact that cross-link sites are not very conducive to close-packing of network chains. This, along with the fact that there may still be residual (unreacted) cyanate groups even after post-curing [49] helps relate the beneficial effects of a pre-cure at lower temperatures and slower heating rate (described earlier) with the detrimental effects of moisture reported in this study.

In general, high curing temperatures (> 150 °C) were detrimental to BECy sandwiched between BMI-cf substrates. At these temperatures, both the increased moisture diffusion out of the BMI and moisture uptake by the BECy increased the chance of hydrolysis of residual cyanate groups that led to bubbles in the resin, a decrease in T_g, and the lower lap shear strengths observed. At low temperatures (100-150 °C), not only is the hydrolysis reaction less likely to occur, but there is also less water diffusing out of the BMI and slower uptake of water by the BECy. This helps to explain why a pre-cure as well as a slow heating rate at low temperatures proved beneficial while a post-cure as well as a slow heating rate at high temperatures, detrimental.

Conclusions

Adhesive properties of BECy and BECy-ANP nanocomposites were evaluated through lap shear tests on different substrates and at different temperatures. On aluminum substrates, BECy outperformed the benchmark epoxy in lap shear at both room and elevated temperature, a result possibly due to interactions with hydroxyl groups on aluminum surface.

BECy exhibited much lower lap shear strengths on BMI-cf substrates than on aluminum, and on BMI-cf was much weaker than the benchmark epoxy. This is believed to have been mostly a result of less-than-optimal processing conditions for the particular resin/substrate system, as opposed to adhesive properties of the resins themselves. It was found that moisture in the BMI is likely to have diffused out during the BECy cure cycle that led to hydrolysis of unreacted cyanate groups and the bubbling, decrease in T_g, and poor lap shear strengths observed.

Alumina nanoparticles were not observed to increase lap shear strength significantly, considering the amount of scatter in lap shear strengths. On aluminum, little to no improvement was seen with the addition of ANP; on BMI-cf the addition of ANP decreased strength, especially at elevated temperature tests. It is believed that less-than-optimal processing conditions, again, are responsible for these observations, as previous studies have shown alumina to have a catalytic effect on curing which could mean the cure schedule for neat BECy may not be well-suited for BECy-ANP.

Further study is required to determine optimal conditions for both adhesion on BMI-cf and incorporation of ANP.

Acknowledgments

The research described in this article was supported by a grant from the Strategic Environmental Research and Development Program (SERDP), under the “Environmentally Benign Repair of Composites Using High Temperature Cyanate Ester Nanocomposites” project (Project Number WP-1580).

Special thanks to Brian Richard and Jonathan Henson for their help with sample preparation, as well as Zhihong Tang for his assistance with the thermal cycling of samples. Thanks also to the members of the Polymer Composites Research Group and Katherine Ament for their helpful discussion.

References

[1] Li, H.C.H., P.J. Callus, and I. Herszberg. "Through-thickness Reinforcement Repair of Delaminated Carbon-epoxy Panels." Composite Structures 75.1-75.4 (2006): 539-44.

[2] Aktas, Mehmet, Ramazan Karakuzu, and Yusuf Arman. "Compression-after Impact Behavior of Laminated Composite Plates Subjected to Low Velocity Impact in High Temperatures." Composite Structures 89.1 (2009): 77-82.

[3] Wu, Kuo-Wei, Chang-Lun Lee, Yuan-Chang Chang, and Ching-Long Ong. "Compressive Strength of Delaminated and Repaired Composite Plates." Materials Chemistry and Physics 43.2 (1996): 173-77.

[4] Russell, A. J., and J. S. Ferguson. Composite Repair Issues on the CF-18 Aircraft. Rep. no. AGARD-CP-550-PAP-14. Victoria, BC (CAN): Defence Research Establishment Pacific, 1995. 30 June 2009 <http://pubs.drdc-rddc.gc.ca/>.

[5] Bartus, S. D. "A Review: Impact Damage of Composite Materials." Journal of Advanced Materials 39.3 (2008): 3-21.

[6] "Types of Repair - NetComposites." NetComposites - Composites and Reinforced Plastics. 11 July 2008 <http://www.netcomposites.com/EducationIntro.asp>.

[7] Goertzen, W. K., and M. R. Kessler. "Thermal and Mechanical Evaluation of Cyanate Ester Composites with Low-temperature Processability." Composites: Part A 38.3 (2007): 779-84.

[8] Zunjarrao, Suraj C., and Raman P. Singh. "Characterization of the Fracture Behavior of Epoxy Reinforced with Nanometer and Micrometer Sized Aluminum Particles." Composites Science and Technology 66.13 (2006): 2296-305.

[9] Zheng, Yaping, and Rongchang Ning. "Study of SiO_2 Nanoparticles on the Improved Performance of Epoxy and Fiber Composites." Journal of Reinforced Plastics and Composites 24.3 (2005): 223-33.

[10] Zhai, Lanlan, Guoping Ling, Jian Li, and Youwen Wang. "The Effect of Nanoparticles on the Adhesion of Epoxy Adhesive." Materials Letters 60.25-60.26 (2006): 3031-033.

[11] Dean, Derrick, M. Abdalla, and S. Ganguli. "Big Things in Small Packages – Opportunities and Challenges Await Nano-engineered Adhesives, Sealants, and Coatings." Adhesives Age 46.3 (2003): 12-19.

[12] Dodiuk, H., S. Kenig, I. Blinsky, A. Dotan, and A. Buchman. "Nanotailoring of Epoxy Adhesives by Polyhedral-oligomeric-sil-sesquioxanes (POSS)." International Journal of Adhesives & Adhesives 25.3 (2005): 211-18.

[13] Hartwig, Andreas, Andreas Luhring, and Jasmin Trautmann. "Spheroidal Nanoparticles in Epoxide-based Adhesives." Macromolecular Materials and Engineering 294.6-294.7 (2009): 363-379.

[14] Kim, Byung C., Sang W. Park, and Dai G. Lee. "Fracture Toughness of the Nano-particle Reinforced Epoxy Composite." Composite Structures 86.1-86.3 (2008): 69-77.

[15] Gilbert, Eric N., Brian S. Hayes, and James C. Seferis. "Nano-alumina Modified Epoxy Based Film Adhesives." Polymer Engineering and Science 43.5 (2003): 1096-104.

[16] Hartwig, Andreas, Monika Sebald, Dirk Putz, and Lisa Aberle. "Preparation, Characterisation and Properties of Nanocomposites Based on Epoxy Resins – An Overview." Macromolecular Symposia 221 (2005): 127-35.

[17] Hanemann, T. "Influence of Particle Properties on the Viscosity of Polymer-alumina Composites." Ceramics International 34.8 (2008): 2099-105.

[18] Lawler, Katherine A. "Viscosity of Aqueous and Cyanate Ester Suspensions Containing Alumina Nanoparticles." Thesis. Iowa State University, 2009.

[19] Zhou, Yabin, Shifeng Wang, Yong Zhang, Yinxi Zhang, Xuhua Jiang, and Dengfeng Yi. "Rheological Properties of PDMS filled with $CaCO_3$: The Effect of Filler Particle Size and Concentration." Journal of Applied Polymer Science 101.5 (2006): 3395-401.

[20] Li, Joshua Q., and Ronald Salovey. "Model Filled Polymers: The Effect of Particle Size on Rheology of Filled Poly(methyl methacrylate) Composites." Polymer Engineering and Science 44.3 (2004): 452-62.

[21] Meguid, S.A. and Y. Sun. "On the Tensile and Shear Strength of Nano-reinforced Composite Interfaces." Materials and Design 25.4 (2004): 289-96.

[22] Hsiao, Kuang-Ting, Justin Alms, and Suresh G. Advani. "Use of Epoxy/multiwalled Carbon Nanotubes as Adhesives to Join Graphite Fibre Reinforced Polymer Composites." Nanotechnology 14.7 (2003): 791-93.

[23] Balkova, R., S. Holcnerova, and V. Cech. "Testing of Adhesives for Bonding of Polymer Composites." International Journal of Adhesion & Adhesives. 22.4 (2002): 291-95.

[24] Hart-Smith, L.J. "Adhesive Bonding of Composite Structures—Progress to Date and Some Remaining Challenges." Journal of Composites Technology & Research. 24.3 (2002): 133-51.

[25] Minford, J. Dean. Handbook of Aluminum Bonding Technology and Data. New York: M. Dekker, 1993.

[26] Sottos, N. R. "The Influence of the Fiber/Matrix Interface on Local Glass Transition Temperature." Polymer Solutions, Blends, and Interfaces 11 (1992): 339-58.

[27] Erdogan, Fazil. Fracture Mechanics (ASTM Special Technical Publication// Stp). New York: American Society for Testing & Materials, 1995.

[28] Goertzen, William K., Xia Sheng, Mufit Akinc, and M. R. Kessler. "Rheology and Curing Kinetics of Fumed Silica/cyanate Ester Nanocomposites." Polymer Engineering and Science 48.5 (2008): 875-83.

[29] D.A. Shimp, ‘‘Technologically Driven Applications for Cyanate Ester Resins,’’ in Chemistry and Technology of Cyanate Ester Resins, I. Hamerton, Ed., Chapman and Hall, London, 282 (1994).

[30] Possart, Wulff, and Stefan Dieckhoff. "Adhesion Mechanisms in a Cyanurate Prepolymer on Silicon and on Aluminium." International Journal of Adhesion & Adhesives 19.6 (1999): 425-34.

[31] Da Silva, Lucas F. M., R. D. Adams, and M. Gibbs. "Manufacture of Adhesive Joints and Bulk Specimens with High-temperature Adhesives." International Journal of Adhesion & Adhesives 24.1 (2004): 69-83.

[32] Kinloch, A. J., and A. C. Taylor. "The Toughening of Cyanate-ester Polymers - Part I - Physical Modification using Particles, Fibres and Woven-mats." Journal of Materials Science 37.3 (2002): 433-60.

[33] Dean, Derrick, Mohamed O. Abdalla, Sabyasachi Ganguli, Moncy Jose, Sandi Campbell, Jeffrey Gillman, Walid H. Awad, and Richard Vaia. "High Temperature Thermoset Nanocomposites." International SAMPE Symposium and Exhibition. Long Beach, CA. Vol. 48. 2003. 2572-584.

[34] Chao, Fen, Nicola Bowler, Xiaoli Tan, Guozheng Liang, and Michael R. Kessler. "Influence of Adsorbed Moisture on the Properties of Cyanate Ester/$BaTiO_3$ Composites." Composites Part A: Applied Science and Manufacturing 40.8 (2009): 1266-271.

[35] Ganguli, Sabyasachi, Derrick Dean, Kelvin Jordan, Gary Price, and Richard Vaia. "Mechanical Properties of Intercalated Cyanate Ester-layered Silicate Nanocomposites." Polymer 44.4 (2003): 1315-319.

[36] Sheng, Xia, Mufit Akinc, and Michael Kessler. "The Effects of Alumina Nanoparticles on the Cure Kinetics of Bisphenol E Cyanate Ester." Polymer Engineering & Science. Submitted for peer review.

[37] Pocius, Alphonsus V. and Robert P. Wenz. “Mechanical Surface Preparation of Graphite-epoxy Composite for Adhesive Bonding.” SAMPE Journal 21.5 (1985): 50-58.

[38] Chin, Joannie W., and James P. Wightman. “Surface Characterization and Adhesive Bonding of Toughened Bismaleimide Composites.” Composites: Part A. 27.6 (1996): 419-28.

[39] Reghunadhan Nair, C. P., Dona Mathew, and K. N. Ninan. "Cyanate Ester Resins, Recent Developments." Advances in Polymer Science 155 (2001): 1-99.

[40] Kasehagen, Leo J., Idelette Haury, Christopher W. Macosko, and David A. Shimp. "Hydrolysis and Blistering of Cyanate Ester Networks." Journal of Applied Polymer Science 64.1 (1997): 107-13.

[41] Ramirez, Michael L., Richard Walters, Richard E. Lyon, and Edward P. Savitski. "Thermal Decomposition of Cyanate Ester Resins." Polymer Degradation and Stability 78.1 (2002): 73-82.

[42] Fang, Treliant, and David A. Shimp. "Polycyanate Esters: Science and Applications." Progress in Polymer Science 20.1 (1995): 61-118.

[43] Shimp, David, and Mark Southcott. "Controlling Moisture Effects during the Curing of High T_g Cyanate Ester/aramid Composites." 38th International SAMPE Symposium. Anaheim, CA. Vol. 38. 1993. 370-79.

[44] Kasehagen, Leo J., and Christopher W. Macosko. "Structure Development in Cyanate Ester Polymerization." Polymer International 44.3 (1997): 237-47.

[45] Bao, Li-Rong, and Albert F. Yee. "Moisture Diffusion and Hygrothermal Aging in Bismaleimide Matrix Carbon Fiber Composites: Part I—Uni-weave Composites." Composites Science and Technology 62.16 (2002): 2099-110.

[46] Bao, Li-Rong, and Albert F. Yee. "Effect of Temperature on Moisture Absorption in a Bismaleimide Resin and its Carbon Fiber Composites." Polymer 43.14 (2002): 3987-997.

[47] Simpson, M., P. M. Jacobs, and F. R. Jones. "Generation of Thermal Strains in Carbon Fibre-reinforced Bismaleimide (PMR-15) Composites Part 3: A Simultaneous Thermogravimetric Mass Spectral Study of Residual Volatiles and Thermal Microcracking." Composites 22.2 (1991): 105-12.

[48] Chatterjee, Amit. "Thermal Degradation Analysis of Thermoset Resins." Journal of Applied Polymer Science 114.3 (2009): 1417-425.

[49] Karad, Sunil K., David Attwood, and Frank R. Jones. "Moisture Absorption by Cyanate Ester Modified Epoxy Resin Matrices. Part IV: Effect of Curing Schedules." Polymer Composites 24.4 (2003): 567-76.

CHAPTER 3. INJECTION REPAIR OF ADVANCED COMPOSITES USING A LOW-VISCOSITY, HIGH TEMPERATURE CYANATE ESTER RESIN

A paper to be submitted to a peer reviewed journal

Wilber Lio, Mufit Akinc, Michael R. Kessler

Introduction

As the need for stronger and lighter materials continues to grow, polymer matrix composites will be in ever-increasing demand. This trend is most prominent in the aircraft industry, as today's aircraft are becoming predominantly composed of composites (Figure 1). Composites are often the material of choice due to their superior specific strength and stiffness as well as fatigue and corrosion resistance compared to metals [1-4]. Drastic weight savings are also attainable through the use of composites as shown in Table 1.

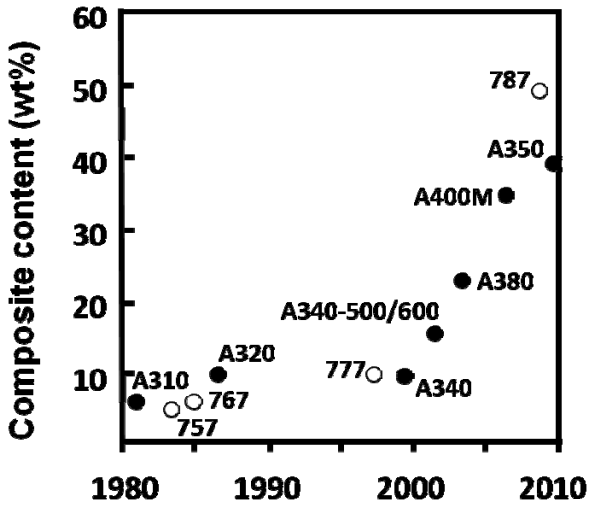

Figure 1. Composite content of Boeing and Airbus aircraft over time [5].

Table 1. Potential weight savings from the use of composites in a variety of structures [6].

	USD/lb	USD/kg
Fighter	200	440
Commercial Aircraft	400	880
Satellites	10000	22000
Space Shuttle	15000	33000

Composites however, are especially susceptible to impact damage that may result from anything from striking a bird in-flight to being struck by a stray rock on the runway. Impact damage can often lead to delaminations and microcracks that, although may not be invisible to the naked eye, can be highly detrimental to mechanical properties [7]. Current methods of repair include a variety of patch and non-patch techniques (Figure 2).

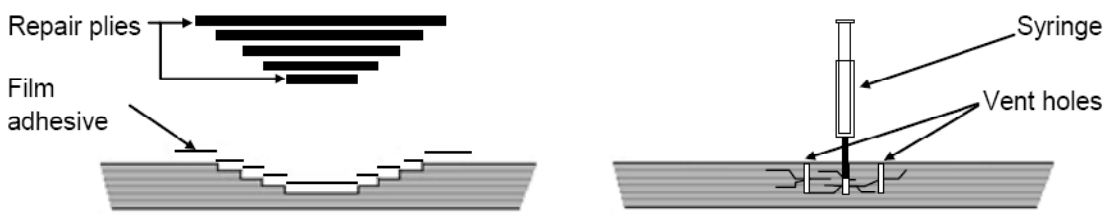

Figure 2. Examples of composite repair techniques: scarf repair (left) and injection repair (right) [8].

In aerospace applications especially, the ability to maintain a smooth and continuous surface after repair with the surrounding area is very important and is one of the major drawbacks to external patch repairs. With other patch techniques such as a scarf repairs, although a smooth surface is more easily obtained, a great deal of care must be taken to ensure that removal of material does not further damage the composite.

Resin-injection is a much less invasive non-patch repair technique that can be used to repair delaminations [9]. Resins that are used for this technique must not only have low viscosities for

injection, but must also exhibit adequate temperature stability and adhesive strength for the intended application. The low viscosity requirement is a problem for the resin-injection repair of high glass transition temperature (T_g) composites because of the typical trend for high temperature resins to have higher resin viscosities (Figure 3), making them less processible and not injectable. However, an outlier to this trend is a new class of cyanate esters. Bisphenol E cyanate ester (BECy) has a peculiarly low viscosity for its high T_g that makes it a reasonable candidate for the resin-injection repair of high T_g composites.

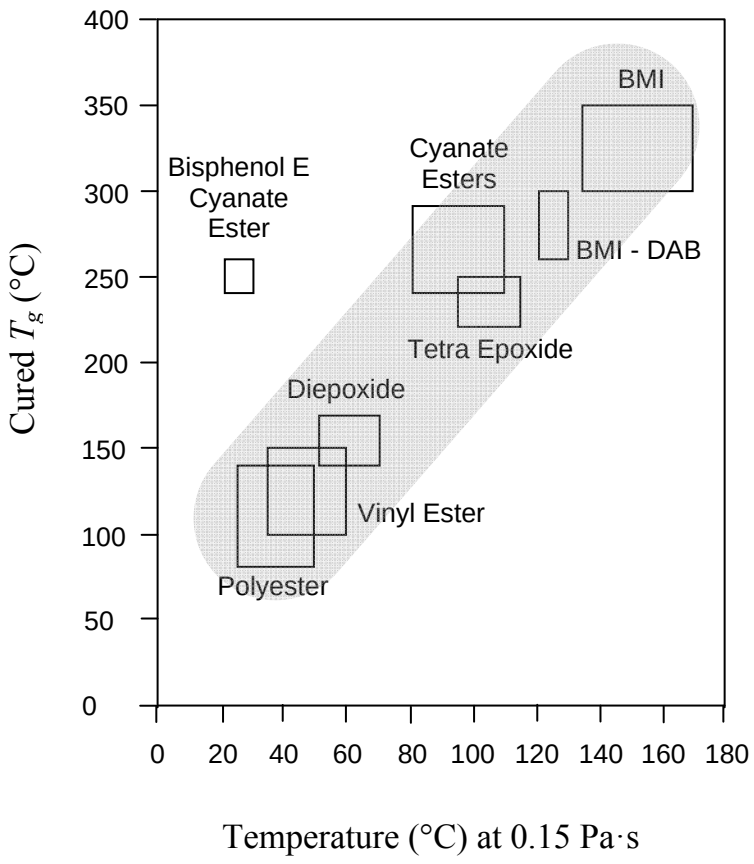

Figure 3. High T_g resins typically have high viscosities minus one exception that is bisphenol E cyanate ester [10].

In a previous work [11], the adhesive properties of BECy and BECy-ANP were investigated. In this study, a resin-injection repair apparatus was designed, and the ability and efficiency of the BECy resin to infiltrate delaminations and successfully repair delamination damage was evaluated through ultrasonic testing and compression-after-impact tests.

Materials and Methods

The BECy monomer (EX1510 resin) and liquid phase organometallic-based catalyst (EX1510-B) were purchased from Bryte Technologies, Inc. (Morgan Hill, CA), and used as received without further purification.

Bismaleimide-carbon fiber (BMI-cf) prepreg was supplied as HTM 512 prepreg by Advanced Composites Group, Inc. (Tulsa, OK). The prepreg lay-up was cured in a hot-press at 190 °C and 0.6 MPa (90 psi) compaction pressure for 6 hours followed by a free-standing post-cure for 8 h at 240 °C based on a schedule suggested by the supplier.

Square plates (4 in × 4 in) were machined from the approximately 0.2 in thick laminates and a 0.25 in diameter through hole with a 82 degree countersink about a third of the way through was drilled in each plate.

To introduce delaminations into the composite plates, a holed plate shear (HPS) method was used (Figure 4). The plate was sandwiched between two metal rings and centered under a load cell. A ball bearing was placed in the countersunk hole, and a compressive load was applied on the plate via the load cell and ball bearing. An Instron 5569 tensile testing machine (Norwood, MA) was used to perform these tests. A compressive extension rate of 1 mm/min was used and the specimen was loaded until there was either a drop in the load greater than 30% of the peak load or a compressive extension of 2 mm was reached.

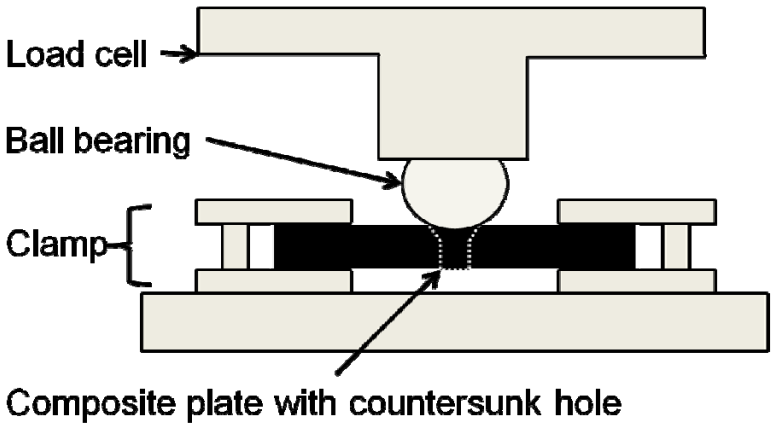

Figure 4. Holed plate shear method by which delaminations were introduced into composite plates.

A resin-injection repair apparatus was designed such that evacuation of air from within the delaminations and injection of repair resin could be done through the same access hole to avoid the need to drill additional vent holes. The apparatus consisted of a clamping fixture and a series of tubing and connectors through which a vacuum was pulled and resin injected. A schematic of the apparatus is shown in Figure 5.

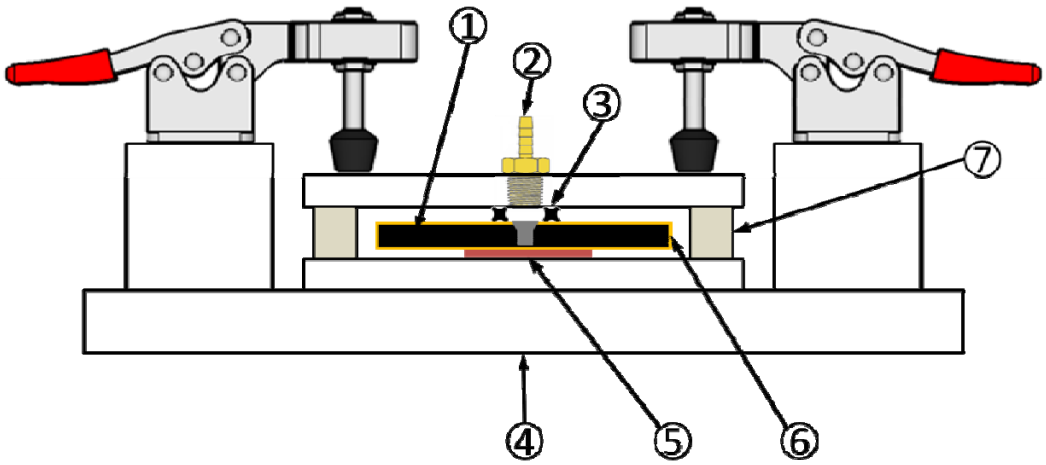

Figure 5. Clamping fixture used for resin injection repairs of composite plates. Component 1) Composite plate, 2) port through which vacuum was pulled and resin injected, 3) quad-ring, 4) polycarbonate base, 5) silicone rubber, 6) Kapton tape, 7) vacuum sealant tape.

To repair the delaminations, the damaged plate was first wrapped on all sides with Kapton® tape (Figure 5, Component 6) except around the countersunk end of the hole, which was left open for the repair resin to enter. The tape served to seal any surface cracks as well as to block the resin from flowing out of the bottom of the center hole in the plate. The plate was then sealed within the clamping fixture (Figure 5) and a vacuum was pulled through an assembly of tubing, connectors, and valves (not depicted) that were attached to the port on the top of the fixture (Figure 5, Component 2). The repair resin was then manually injected via a syringe that attached to a Luer-activated connector that remained sealed to maintain the vacuum until the syringe was attached. After injection, the tubing assembly connected to the port was disconnected, the port re-sealed, and both the fixture and the plate within placed in a convection oven to begin curing the resin. Due to the temperature limits of the clamping fixture, the resin was first cured for a minimum of 4 h at 100 °C to gel the resin, after which, the plate was removed from the fixture and replaced in the oven to fully cure the resin at 180 °C for 2 h, followed by a post-cure at 250 °C for 2 h, at a heating rate of 1 °C/min. Before further testing, resin-filled holes were re-drilled.

An air-coupled, through-transmission system using 120 kHz focused probes was used to create C-scans of undamaged, delaminated, and repaired plates. A small piece of duct tape was placed over both sides of the through-hole in each plate. Each plate was also surrounded by a foam frame. Both these techniques were used to minimize the noise around the edges by preventing an excess amount of sound from leaking through. Despite these precautions, images near the edges were still somewhat unclear. Some plates were also sectioned and examined via optical microscopy to verify infiltration of delaminations with BECy.

To evaluate the repair efficiency, compression-after-impact (CAI) tests were conducted on undamaged, delaminated, and repaired plates. A standard (ASTM Standard D 7137) CAI test fixture was modified to accommodate smaller-than-standard-sized plates. The fixture and specimen were loaded onto a 250 kN MTS load frame at a compressive extension rate of 1 mm/min (0.04 in/min)

until there was a sudden drop in the load with a 0.2 in compressive extension limit to protect the fixture from damage. Data from specimens that did not fail within the bulk (e.g. via end-crushing) were not included in calculations.

Results and Discussion

The load-displacement curves obtained from the HPS method of delamination introduction are shown in Figure 6. As described by Russell et al. [9], this method simulates delamination damage that can occur from over-torquing a fastener or inadequate joint support. The similar-looking curves demonstrate similar composite properties, which is desirable for the comparison purposes of this study. For the most part, all the plates experienced a sudden drop in load followed by a slight increase in load upon subsequent loading up to 2 mm in compressive extension.

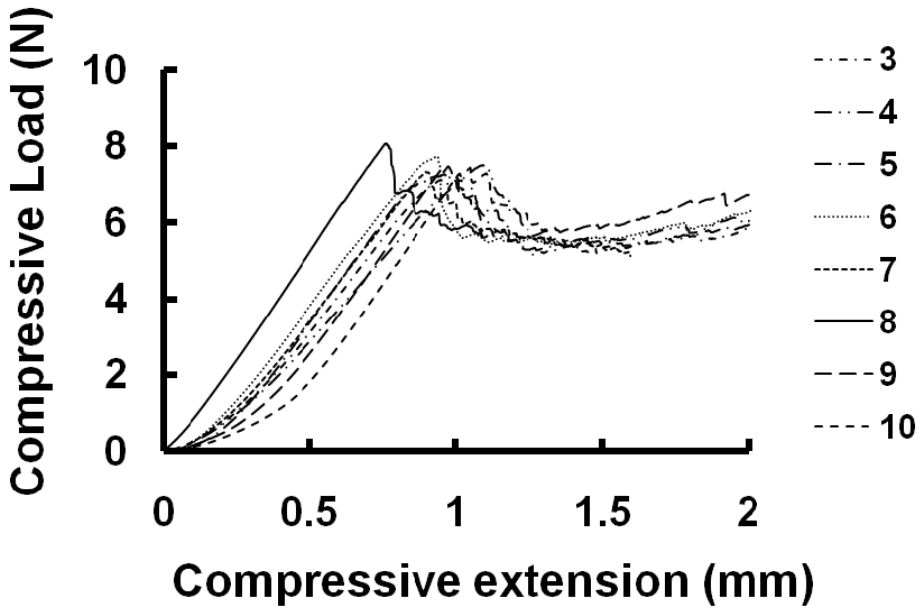

Figure 6. Load-extension curves from HPS tests.

Air-coupled ultrasonic inspection verified the introduction of delaminations into the composite plates as seen in Table 2. As the attenuation of sound in air increases rapidly with frequency, air-coupled scans were possible due to the low frequency transducers used. Delaminations are visible because sound waves are attenuated due to impedance mismatches from layer to layer which, in most cases, cause a reduction in the amplitude of the received signal as the waves pass through numerous interfaces. C-scans confirmed the HPS method to be a successful technique in introducing controlled and reproducible damage that was confined within the diameter of the clamping ring.

Table 2. C-scan images of undamaged, delaminated, and repaired composite plates.†

Plate	Undamaged	Delaminated	Repaired
1	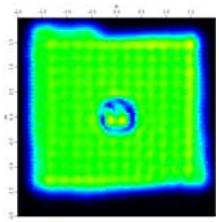	NA	NA
2	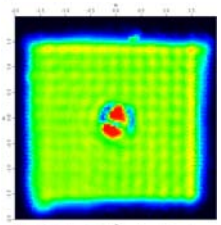	NA	NA
3	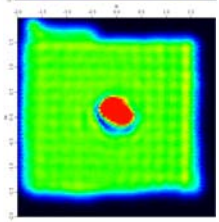	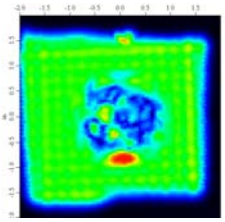	NA
4	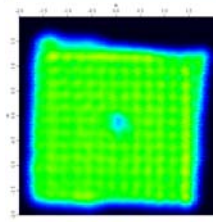	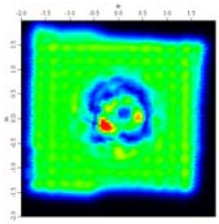	NA

Table 2. (continued).†

Plate	Undamaged	Delaminated	Repaired
5	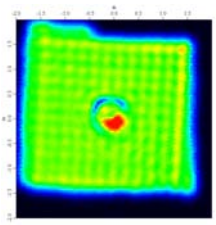	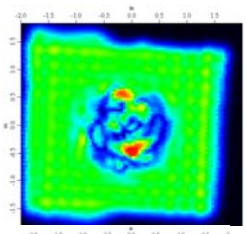	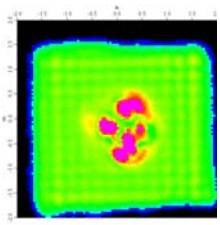
6	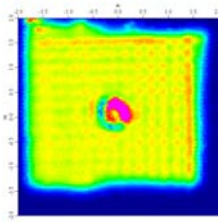	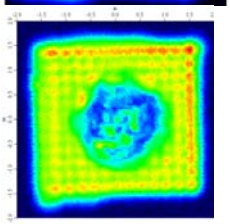	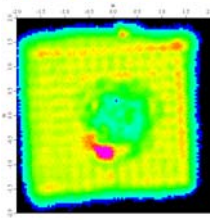
7	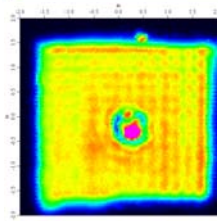	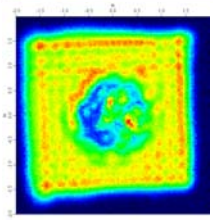	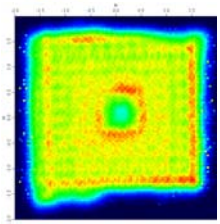
8	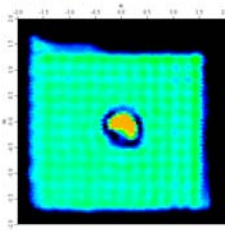	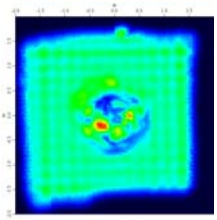	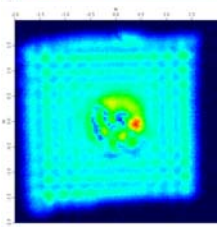
9	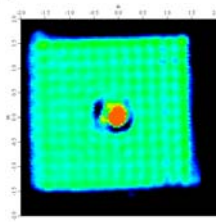	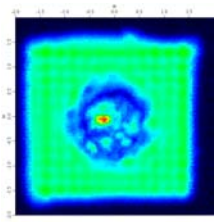	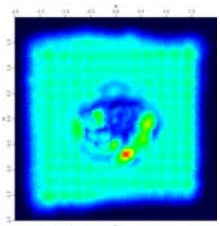
10	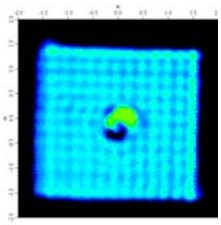	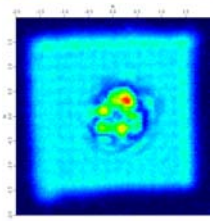	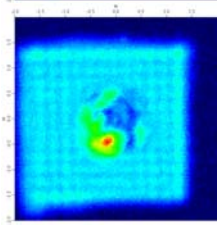

† All plates exhibited a dark center region due to the through-hole drilled in each specimen. A larger region appears in delaminated plates due to delamination damage, and images of repaired plates differ from delaminated ones due to infiltration of repair resin into the delaminations.

Although C-scans are useful in determining the lateral extent of delaminations, they do not give any information on depth of damage, and a shadowing effect can sometimes occur where delaminations near the surface overshadow and hide underlying damage which may be of interest [12]. However, in this study, due to time and material constraints, it sufficed to assume that the extent of delamination was identical as judged by the load-displacement curves and C-scans.

C-scans of the injection repaired plates are shown in Table 2. Some of the images of the repaired plates are almost identical to their images before delamination. This qualitatively demonstrates adequate filling of the delaminations that allow the sound waves to pass through with less attenuation, although some attenuation is inevitable due to impedance mismatches between the repair resin and composite. Other images, though not identical to their undamaged counterparts, differ slightly from their delaminated images, which could mean partial, if not complete filling of the delaminations.

Because non-destructive techniques such as ultrasonics cannot detect the quality of the bond [1], CAI tests were chosen to evaluate the effect of delaminations and repair because the strength in fiber reinforced composites is typically lower in compression than in tension [3]. The ultimate compressive residual strength (σ_{CAI}) was calculated using Equation 1:

$$\boldsymbol{\sigma_{CAI} = \frac{F_{max}}{A}} \qquad \textbf{Equation 1}$$

where F_{max} is the maximum force prior to failure and A is the cross-sectional area. A summary of the average compressive strengths of the undamaged, delaminated, and repaired samples are shown in Table 3.

Table 3. Average ultimate compressive residual strengths of undamaged, delaminated, and repaired composite plates obtained via CAI tests.

	Average σ_{CAI} (MPa)	**Standard Deviation**
Undamaged	210.56	13.84
Delaminated	122.79	6.41
Repaired	154.39	17.38

Repaired plates exhibited a compressive residual strength about 26% greater than delaminated plates. The efficiency of the repair (E_{repair}) was calculated via Equation 2:

$$\boldsymbol{E_{repair}} = \frac{\sigma_{CAI}^{repair} - \sigma_{CAI}^{delam}}{\sigma_{CAI}^{undamaged} - \sigma_{CAI}^{delam}} \qquad \textbf{Equation 2}$$

where σ_{CAI}^{repair}, σ_{CAI}^{delam}, and $\sigma_{CAI}^{undamaged}$ are the compressive residual strengths of the repaired, delaminated, and parent laminates, respectively. An 80% repair efficiency typically satisfies permanent repair requirements [3], and so it can be seen that the repairs conducted in this study have not quite approached this standard at only about 36%.

After CAI tests, some plates were sectioned into quarters and examined with an optical microscope to see the extent of resin-infiltration into the delaminations. These images were captured after CAI tests, and so do not best-represent completely repaired plates. This was done merely to save on the limited amount of material available at the time. These images reveal that BECy successfully infiltrated some, but not all of the cracks and delaminations (Figure 7).

A phenomenon seen in several of the repaired plates was the development of bubbles in the BECy resin, though more apparent in some plates than others. These observations are similar to those described in a previous study [11]. The worst cases of bubbling such as seen in Figure 8 resulted in a giant bubble around the countersunk hole in the plate. This is likely due to carbon dioxide evolved from the hydrolysis of cyanate groups in the presence of moisture diffused from the BMI resin at the

high cure temperatures [13-15]. These results indicate the need to adequately dry the composites prior to injection in future studies.

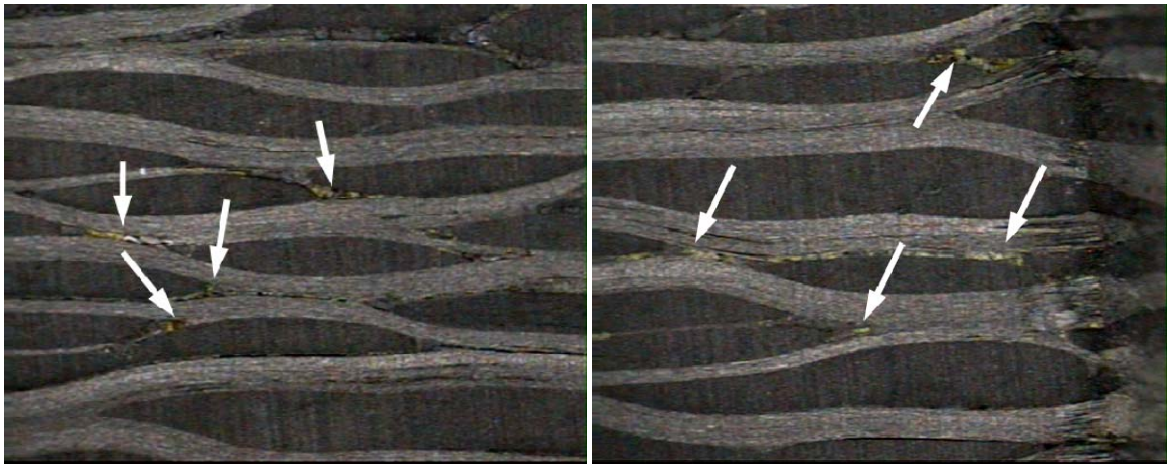

Figure 7. Cross-section of repaired plate showing BECy infiltration into delaminations.

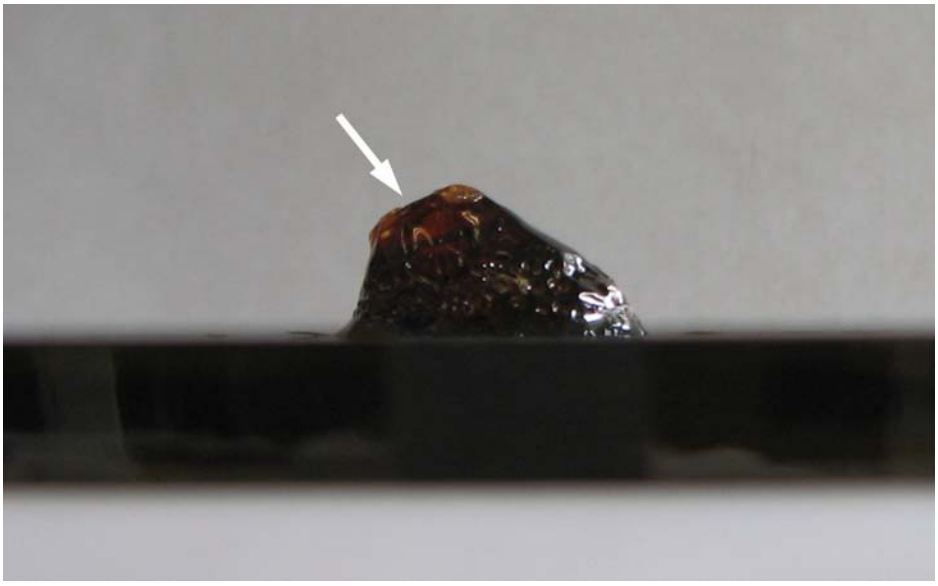

Figure 8. Bubble formation in BECy resin after curing within the composite and in the countersunk hole.

There are several issues that were not specifically addressed regarding the direct applicability of the injection-repair method in this study to actual composite components. These issues can be largely grouped into two areas: accessibility and compatibility. Ideally, a component could be repaired without further complication from disassembly off the main structure. However, procedures that require autoclaves and pressure typically cannot be conducted in situ [16].

Similarly, with resin-injection repair, depending on the extent of damage, access to the back surface may be necessary so that surface cracks can be sealed. This would almost certainly require some amount of disassembly in order to access the back surface and hence rule out in-the-field repairs [17]. In this study, access to and sealing of surface cracks was accomplished by wrapping the composite plate with a tape. This would not be feasible for inaccessible parts as just described.

The ability to evacuate air from within delaminations prior to injection would also rely on accessibility of the part as well as compatibility of the repair apparatus. Some modifications to the device used in this study would have to be made in order to create a vacuum-tight seal around the damaged area as most structures would not exhibit as simple a geometry as a square plate. Determining the extent of damage, and hence where to drill holes and inject resin in a more complex part would also require more extensive non-destructive techniques than those used in this study.

Conclusions

The ability and effectiveness of BECy to repair delamination damage via resin-injection was evaluated. A resin-injection system was developed to eliminate the need for drilling additional holes in the composite. C-scans and optical micrographs indicated infiltration of the resin into delaminations; however, complete infiltration was confirmed in only one specimen via ultrasonic evaluation. Compression-after-impact tests demonstrated a 36% repair efficiency, and repaired plates exhibited a 26% higher compressive strength compared to delaminated plates. Application of the

resin-injection method developed in this study on actual composite components will require slight modifications and further optimization.

Acknowledgements

The research described in this article was supported by a grant from the Strategic Environmental Research and Development Program (SERDP), under the “Environmentally Benign Repair of Composites Using High Temperature Cyanate Ester Nanocomposites” project (Project Number WP-1580).

Special thanks to Jonathan Henson and Mahendra Thunga for their help in the lab and in developing the resin injection system. Thanks also to Dr. Vinay Dayal and Dan Barnard for their guidance and use of their lab facilities.

References

[1] Li, H.C.H., P.J. Callus, and I. Herszberg. "Through-thickness Reinforcement Repair of Delaminated Carbon-epoxy Panels." Composite Structures 75.1-75.4 (2006): 539-44.

[2] Aktas, Mehmet, Ramazan Karakuzu, and Yusuf Arman. "Compression-after Impact Behavior of Laminated Composite Plates Subjected to Low Velocity Impact in High Temperatures." Composite Structures 89 (2009): 77-82.

[3] Wu, Kuo-Wei, Chang-Lun Lee, Yuan-Chang Chang, and Ching-Long Ong. "Compressive Strength of Delaminated and Repaired Composite Plates." Materials Chemistry and Physics 43 (1996): 173-77.

[4] Russell, A. J., and J. S. Ferguson. Composite Repair Issues on the CF-18 Aircraft. Rep. no. AGARD-CP-550-PAP-14. Victoria, BC (CAN): Defence Research Establishment Pacific, 1995. 30 June 2009 <http://pubs.drdc-rddc.gc.ca/>.

[5] Cookson, Ian. "Grant Thornton on US Aerospace Component M&A, 2008." Defense Industry Daily - Military Purchasing News for Defense Procurement Managers and Contractors. 15 Mar. 2009. 17 July 2009 <http://www.defenseindustrydaily.com/>.

[6] M., Jones, Robert. Mechanics of Composite Materials. Philadelphia, PA: Taylor & Francis, 1999.

[7] Bartus, S. D. "A Review: Impact Damage of Composite Materials." Journal of Advanced Materials 39.3 (2008): 3-21.

[8] "Types of Repair - NetComposites." NetComposites - Composites and Reinforced Plastics. 11 July 2008 <http://www.netcomposites.com/EducationIntro.asp>.

[9] Russell, A. J., C. P. Bowers, and A. J. Moss. "Repair of Delaminations and Impact Damage in Composite Aircraft Structures." Proceedings of the 6th International Conference on Composite Structures, Paisley, Scotl. Barking, Engl: Elsevier Science Publ Ltd, 1991. 145-59.

[10] Goertzen, W. K., and M. R. Kessler. "Thermal and Mechanical Evaluation of Cyanate Ester Composites with Low-temperature Processability." Composites: Part A 38.3 (2007): 779-84.

[11] Lio, Wilber, Mufit Akinc, and Michael R. Kessler. "Lap Shear Testing of Bisphenol E Cyanate Ester: Effects of Substrate, Temperature, Alumina Nanoparticles, and Moisture." To be submitted.

[12] McRae, Kenneth I., Allan G. McCray, Allan J. Russell, and Christopher P. Bowers. "Ultrasonic Imaging of Delamination Damage around Fastener Holes in a Graphite/Epoxy Composite." ASTM special technical publication 1128 (1992): 163-79.

[13] Reghunadhan Nair, C. P., Dona Mathew, and K. N. Ninan. "Cyanate Ester Resins, Recent Developments." Advances in Polymer Science 155 (2001): 1-99.

[14] Kasehagen, Leo J., Idelette Haury, Christopher W. Macosko, and David A. Shimp. "Hydrolysis and Blistering of Cyanate Ester Networks." Journal of Applied Polymer Science 64.1 (1997): 107-13.

[15] Ramirez, Michael L., Richard Walters, Richard E. Lyon, and Edward P. Savitski. "Thermal Decomposition of Cyanate Ester Resins." Polymer Degradation and Stability 78.1 (2002): 73-82.

[16] Sherwin, Glen R. "Non-autoclave Processing of Advanced Composite Repairs." International Journal of Adhesion & Adhesives 19.2-19.3 (1999): 155-59.

[17] Dehm, S., and D. Wurzel. "Fast, In-situ Repair of Aircraft Panel Components." Journal of Aircraft 26.5 (1989): 476-81.

CHAPTER 4. GENERAL CONCLUSIONS

A new class of resin that exhibits a low monomer viscosity and high glass transition temperature (T_g), bisphenol E cyanate ester (BECy), was evaluated for the resin-injection repair of advanced composite materials. Adhesive properties and repair efficiencies were examined through lap shear tests, ultrasonic evaluation, and compression-after-impact tests.

Lap shear tests on aluminum substrates revealed excellent strength of neat BECy at room temperature and 200 °C compared to a benchmark epoxy resin, possibly due to interactions with surface hydroxyl groups on the aluminum. On bismaleimide-carbon fiber (BMI-cf) substrates, however, BECy performed inferior to the benchmark epoxy at room temperature, but superior at 200 °C. Thermal cycling did not seem to affect the room temperature lap shear strength of neat BECy nor the benchmark epoxy.

The addition of alumina nanoparticles (ANP) to the BECy resin had little effect on lap shear strength on aluminum substrates. The slight increase in strength up to 5 volume% (v%) loading followed a decrease at 10 v% observed cannot be inferred with the utmost confidence due to the natural scatter from sample to sample. On BMI-cf, the addition of ANP was more clearly detrimental to lap shear strength at both room temperature and 200 °C.

It is likely that the cure schedule used for BECy should in fact be altered for BECy-ANP, as the addition of alumina has been shown to alter the curing kinetics of BECy. However, further optimization of the cure schedule may not prove to be vastly beneficial to the nanocomposite repair resin, as the high nanoparticle loadings (greater than 10 v%) required to impart significant shear thinning behavior is not only detrimental to the T_g of the resin, but also likely detrimental to adhesive strength.

The inferior strength, unusually large scatter, as well as bubbling observed at the edges of BECy and BECy-ANP lap shear specimens on BMI-cf warranted further investigation. These

observations were believed to be largely due to non-optimal processing conditions, partly due to the catalytic nature of ANP described above. Factors that were found to increase lap shear strength included decreasing overlap area and decreasing heating rate (at lower temperatures), and adding a pre-cure step (also at lower temperatures).

The bubbling is believed to be due to hydrolysis of unreacted cyanate groups by moisture in the BMI resin, as both hydrolysis and diffusion of moisture are things that happen around the BECy cure temperatures. Thermogravimetric analysis of the BMI-cf substrate revealed steady weight loss up to around 250 °C which was attributed to the diffusion of moisture out of the composite, as described in other studies. Differential scanning calorimetry confirmed a decrease in the T_g of BECy cured in the presence of BMI-cf by about 10 °C. These findings suggest that the use of BECy to adhere composites must be precluded by adequate drying of composite substrates.

Ultrasonic C-scans and optical micrographs showed BECy to successfully infiltrate delamination damage through a resin-injection method. Though filling was not 100% complete, the amount that was able to infiltrate the damage zone was enough to yield a 36% repair efficiency and an improvement in ultimate compressive residual stress by about 26% compared to delaminated (unrepaired) plates. Bubbling of the repair resin was also observed, which re-confirm the necessity for adequate drying of the composite before repair.

Further optimization of the repair system to accommodate the repair of actual composite components is required. Because of the qualitative nature of ultrasonic inspection and the material-intensive compression-after impact (CAI) tests, different methods may need to be developed for evaluating repairs that would utilize less material, and provide more quantitative data. Such methods that are currently being investigated include fluorescence imaging and short beam shear tests.

APPENDIX A.

HIGH-TEMPERATURE CYANATE ESTER ADHESIVES REINFORCED WITH NANO-ALUMINA

Published in Proceedings of the SAMPE 2008 Fall Technical Conference

Michael R. Kessler, Wilber Lio, Xia Sheng, Mufit Akinc

Department of Materials Science and Engineering, Iowa State University

Abstract

Composite materials are susceptible to delamination damage when subjected to sustained thermo-mechanical loadings or low energy impacts. Once detected, localized delaminations may be repaired using a resin infusion process, whereby a low viscosity resin is injected into the damaged region. However, for high-temperature polymer composites (such as bismaleimide-based composites) repairs are not attempted because of the low glass transition temperature (T_g) of current repair resins after cure. In this study, we evaluate a low viscosity bisphenol-E cyanate ester (BECy) adhesive which has a combination of low pre-polymer viscosity, for resin infusion, and high cured T_g, for high-temperature effectiveness. This resin is reinforced with alumina nanoparticles to tailor the thermo-mechanical properties of the adhesive. The nanoparticles are functionalized with a silane coupling agent to achieve better dispersion and stronger interfacial bonding between the nano-alumina and polymer matrix. The thermo-mechanical properties of the resin system are evaluated as a function of nano-alumina loading and surface functionalization. In addition, the adhesive strength is evaluated against two benchmark resins, a bisphenol-A type epoxy resin (EPON 828) and a cycloaliphatic (CA) epoxy, through lap shear testing at room and elevated temperatures. The BECy-based adhesive performed much better than the benchmark systems at both temperatures.

1. Introduction

Matrix microcracking is a long standing problem in polymer matrix composites (PMCs) subjected to repeated thermo-mechanical loadings. These microcracks lead to other damage modes such as ply delamination [1-5]. Delamination damage can also be caused by low velocity impacts. If the damage is too severe the structural component is replaced entirely. For less extensive damage, repairs are attempted.

One method of repair involves injecting resin into the failed area. When the resin has infiltrated the damage zone, it is then cured (typically at elevated temperatures). This resin-injection method eliminates the need to remove outer, undamaged plies and can result in higher repair strengths than the alternative "scarf" repair method, where material from the damaged area is ground out and filled with repair plies.

Several requirements for an ideal resin system for the resin-injection repair method include:

1. *Low viscosity*. Once injected into the damage zone the repair resin must be drawn into the furthest reaches of the cracks. In some cases, resin must be diluted with volatile organic solvents to achieve the required viscosity for infiltration.
2. *Stability in the damage zone*. Once in the crack plane, the repair system should react to bond the crack surfaces closed. The resin system should not evaporate or diffuse away from the cracks. Thus a shear thinning fluid is ideal, so that it will act as a low viscosity liquid at high shear, and a stable, more viscous liquid at very low shear to remain in the damage zone until polymerization is complete.
3. *Compatible adhesive*. The polymerized repair resin must be a strong adhesive to the matrix and reinforcement. Cure induced shrinkage should also be minimal to avoid debonding during cure.

4. *Long shelf-life*. The repair resin should be stored as a dormant liquid until it is needed for repair applications. If the storage life is not very long, then the unused, expired material will generate unnecessary expense and hazardous waste.
5. *High-temperature stability*. Many composites require stability at elevated temperatures up to 260 °C. In order to repair these composites, the polymerized resin should have a T_g above the maximum service temperature. Low viscosity resins usually have lower T_g's, limiting their application to lower temperatures.
6. *Environmentally benign*. Increasing environmental and safety concerns and regulations dictate that repair processes not generate significant volatile organic compounds (VOCs) or hazardous air pollutants (HAPs).

Currently, repairs are not even attempted for high-temperature composites, such as bismaleimide, (BMI) because of the low T_g of current repair resins after cure. In order for resin infusion to be possible, the monomer should be a liquid with a relatively low viscosity that allows complete infusion of the damage zone; however, most high-temperature pre-polymers are either solids or highly viscous liquids at room temperature. In general, polymers with higher T_g's in the cured state have higher viscosities at room temperature. Figure 1 shows the correlation between the cured state T_g and the temperature at which the uncured thermoset monomer has a viscosity of 0.15 Pa·s [6]. Polyimides are not shown in Figure 1 because their lowest melt viscosities are higher than 0.15 Pa·s [7].

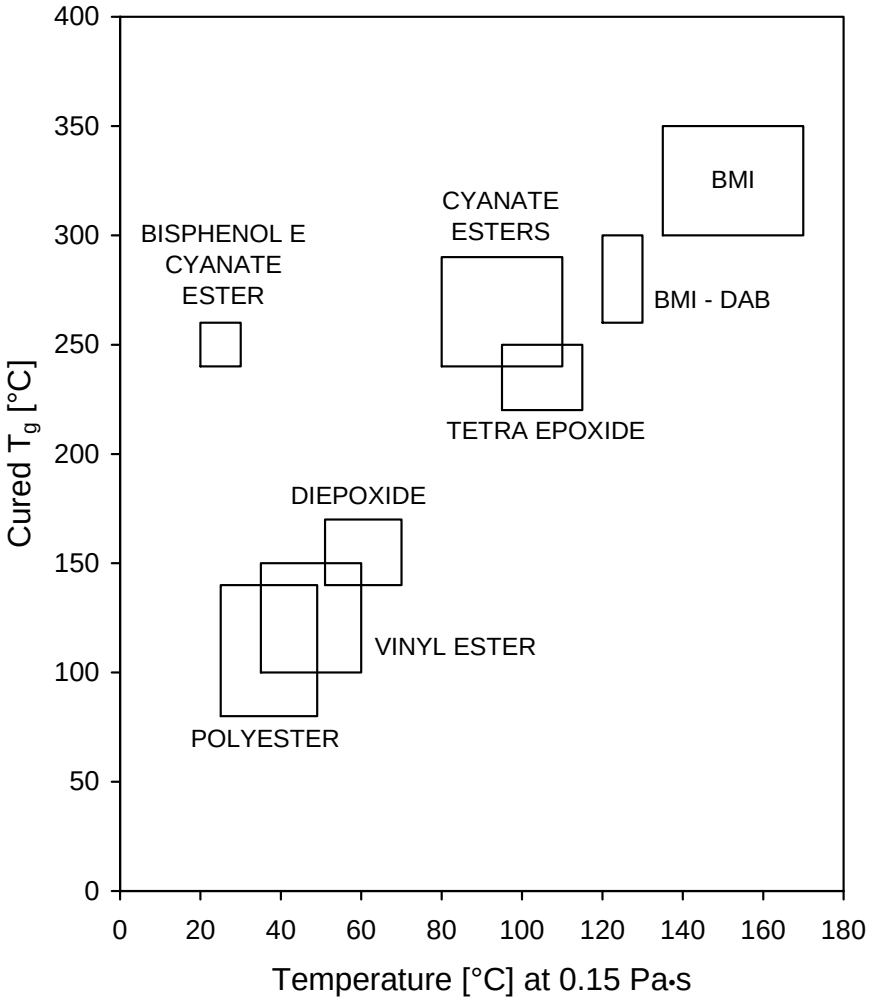

Figure 1. Relationship between processing temperature of the pre-polymer and its cured T_g. The processing temperature is the temperature the resin needs to be heated to in order to obtain a viscosity of 0.15 Pa·s [6, 8].

From Figure 1, the one exception to the trend of a higher viscosity with higher T_g is a unique type of cyanate ester monomer called the bis(4-cyanatophenyl)-1,1-ethane monomer (bisphenol-E cyanate ester, or BECy) [6, 7, 9]. BECy has excellent processing capabilities even at low temperatures with an extremely low viscosity of 0.09 to 0.12 Pa·s at room temperature [6-8]. These processing characteristics make it an excellent candidate for the resin-injection repairs of high-

temperature PMCs. Cyanate esters also possess a good combination of high-temperature stability and excellent mechanical properties [10], and while they are not capable of withstanding as high of temperatures as bismaleimides, they are capable of withstanding extreme temperature variations, which is a significant improvement over epoxies. In addition, cyanate esters have excellent adhesive properties and are more resistant to moisture absorption than other thermosets [11]. They have extremely low toxicity, which makes them much less hazardous than polyimides and bismaleimides [6, 12], and the pre-polymer also has near infinite room temperature stability, which reduces waste due to spoilage compared to traditional thermosets. All in all, BECy meets nearly all of the requirements mentioned earlier for a resin-injection composite repair resin.

The extremely low viscosity and good wetting characteristics of BECy, along with its high degree of adhesion and cross-linking, makes it an excellent candidate for the incorporation of nano-reinforcements. In many systems, nanocomposites have shown increased thermal stability (T_g) and mechanical performance (strength, stiffness, and dimensional stability). Recent results also indicate that the incorporation of nanoparticles into thermosetting adhesives can improve the adhesive strength by as much as five times [13-15]. In addition, numerical simulations using molecular dynamics suggest that the inclusion of nanoparticles into a pre-polymer mixture results in an increased volume fraction of nanoparticles near the crack tip due to depletion attraction effects which results in a significant reduction in the stress concentration at the crack tip, potentially resulting in higher repair effectiveness [16].

Studies have also shown particle suspensions to exhibit shear thinning behavior approaching a constant value at high shear rates [17, 18]. Extrapolation of this model to nanoparticle suspensions implies that the viscosity and yield strength should be higher resulting in a gel at zero shear rate and a low viscosity liquid at high shear rates. This behavior can be extremely attractive for the resin-injection repair applications. Not only does the addition of particles to the monomer allow the

viscosity of the system to be adjusted, but also shear thinning allows easy injection to the damaged region and provides sufficient integrity to the suspension until the monomer cures in the repair area.

Functionalized nanoparticles may provide additional reaction sites during polymerization or react with the polymer matrix to form strong interfacial bonds, and thus enhance compatibility with and dispersion within the monomer. Therefore, polymer composites with functionalized nanoparticles are expected to show improvements in many properties compared to the unfunctionalized alternatives, such as increased tensile strength [19], hardness [20], and T_g [21].

2. Experimental

2.1. Materials

BECy monomer was supplied by BRYTE Technologies, Inc. (Morgan Hill, CA) as EX1510 resin, which was used as received without further purification. The liquid phase organometallic-based catalyst, EX1510-B, was supplied with the resin. Alumina nanoparticles were supplied by Nanophase technologies, Inc. (Romeoville, IL) as NanoTek aluminum oxide, which is γ-phase alumina with an average particle size (diameter) of 40 nm and a specific surface area of 44 m^2/g. Before use, nanoparticles were dried in *vacuo* at 120 °C for 24 hours unless otherwise stated.

EPON 828 was purchased from Miller-Stephenson Chemical Company, Inc.(Morton Grove, IL) along with its curing agent Epikure™ 3223. All other chemicals were purchased from Sigma-Aldrich (Milwaukee, WI). In some cases, 3-Glycidyloxypropyl trimethoxysilane (GPS) was used to functionalize the alumina nanoparticles. A cycloaliphatic epoxy, 3,4-epoxycyclohexylmethyl 3,4-epoxycyclohexanecarboxylate, along with its curing agents and catalysts, hexahydro-4-methylphthalic anhydride (HHMPA), ethylene glycol (EG), and N,N-dimethylbenzylamine (DBA), were used as benchmarks for comparison with the BECy. Butyl glycidyl ether (BGE) was used as a reactive diluent to lower the viscosities of the benchmark resins.

2.2. Specimen preparation

The nanoparticle functionalization reaction scheme is shown in Figure 2. Carefully dried alumina nanoparticles (4 g) were first dispersed in dry THF (100 mL) using water-bath sonication. Then, excess GPS (about 2 mL) was added to the suspension via syringe. After refluxing in THF for 2 days, the functionalized alumina nanoparticles were isolated from the reaction mixture by centrifugation. The nanoparticles were then dispersed into fresh THF by water-bath sonication and centrifuged again. This washing process was repeated three times before the functionalized alumina nanoparticles were dried in a vacuum oven at 120 °C for 24 hr.

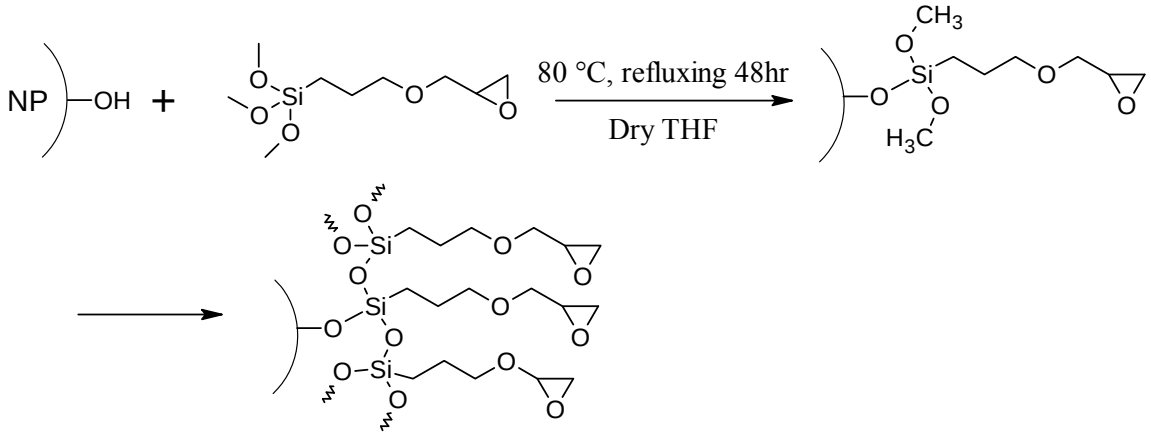

Figure 2. Functionalization of alumina nanoparticles with GPS.

BECy monomer (c.a. 3 g) was added to the dried nanoparticles according to the desired nanoparticle loading. The mixture of BECy and nanoparticles was then subjected to a two hour ultrasonication treatment in a water bath, followed by a high-power tip-ultrasonication at a frequency of 23 kHz for a total of 30 seconds with intervals to allow the suspension to cool down.

The suspensions of BECy/alumina were mixed with catalyst at the manufacturer's suggested loading of 3 parts per hundred resin (phr). The catalyzed BECy/alumina suspensions were poured into

high-temperature silicone molds and degassed under a vacuum at 24 mm-Hg for 1 hr at room temperature. The suspensions were then cured in a convection oven under the following cure schedule: 1) heat from room temperature to 180 °C at a rate of 1 °C/min; 2) isothermally cure at 180 °C for 2 hr; 3) increase temperature to 250 °C at 1 °C/min and isothermally cure for 2 hr; 4) cool down to room temperature in the oven at a cooling rate of 2 °C/min. The samples were then cut from fully cured blocks using a diamond blade cutting saw.

EPON 828 and Epikure 3223 were mixed in a 10:1 weight ratio and cured at 80 °C for 1 hour. The cycloaliphatic epoxy, HHMPA, EG, and DBA were added in a 10:9:0.285:0.285 weight ratio and first cured at 80 °C for 1 hour, followed by 150 °C for 30 minutes. The diluent BGE was added to some samples of EPON and CA (25 and 10 wt% BGE, respectively) in order to decrease the viscosity of the benchmark resins to the same level of that of BECy. Aluminum coupons for lap shear tests were machined to ASTM D 1002-05 standard and bead-blasted on one end to aid in adhesion. Lap shear specimens were prepared by applying the adhesive onto the bead-blasted area of one coupon, laying the second coupon in place, and applying adequate compaction pressure, before heating in an oven for their respective cure cycles.

2.3. Experimental procedure

Thermogravimetric analysis (TG) measurements were performed on a TG model Q50 (TA Instruments, Inc., New Castle, Delaware). A 10 mg sample was placed in a platinum pan and tested at a heating rate of 20 °C/min from 25 °C to 800 °C under dry air purge at 60 mL/min.

The thermo-mechanical properties of cured BECy/alumina nanocomposites were evaluated by a TA Instruments DMA Q800 (dynamic mechanical analysis). All samples were tested in the thin film tension mode at an oscillating strain of 0.025% (amplitude of 5 μm) and single frequency of 1 Hz, using a sample size of 0.4 × 4 × 30 mm ($t \times w \times l$). A temperature scan was applied from 30 to 330 °C at a heating rate of 3 °C/min under nitrogen atmosphere.

Lap shear specimens were tested following ASTM standard D 1002-05. Spacers were implemented by taping coupons to the ends of the specimens in order to compensate for their inherent offset and to ensure that a pure tensile load was applied during testing. An Instron 5569 tensile testing machine (Norwood, MA) was used to test the lap shear samples, which were pulled at an extension rate of 1.3 mm/min until failure. For high-temperature tests (at 200 °C) an Instron SFL Heatwave temperature controlled chamber was used. A thermocouple was attached to the sample, and tests were begun after the sample temperature equilibrated at 200 °C.

3. Results & Discussion

3.1. Characterization of nanoparticles

Dried GPS functionalized alumina nanoparticles (Al-GPS) and bare alumina nanoparticles (Al) were tested with TG to evaluate the amount of silane immobilized on the surface. TG test results are shown in Figure 3. The TG curves of alumina can be separated into four regimes: a) room temperature to 150 °C, desorption gas; b) 100-400 °C, desorption of physically absorbed water; c) 400-800 °C, dehydrolysis of adjacent -OH groups on the surface; and d) >800 °C, diffusion and desorption of isolated -OH groups [22]. The densities of physically absorbed water and hydroxyl groups on the surface of alumina nanoparticles are calculated to be 11 μmol/m^2 (~7 water molecule/nm^2) and 4 μmol/m^2 (~2.5 -OH groups/nm^2), respectively, which are close to the reported values for Al_2O_3 [23, 24]. Similarly, the GPS graft density can be estimated to be 2 molecules/nm^2 from the mass loss between 150 and 800 °C.

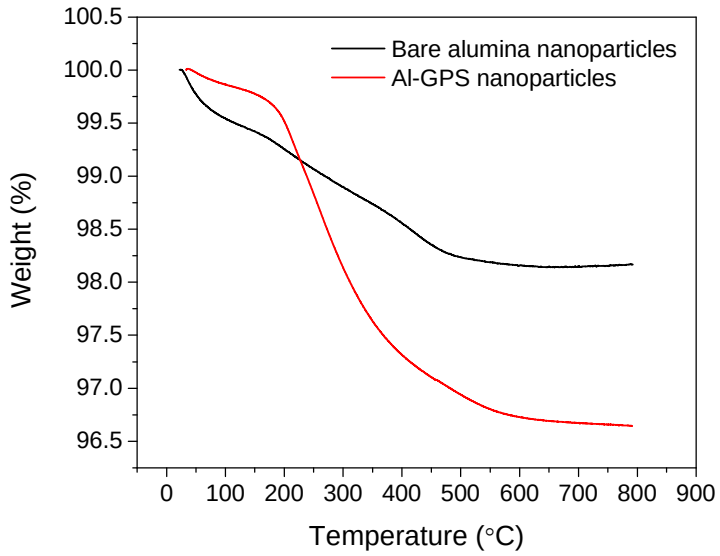

Figure 3. TG test results of bare and GPS functionalized alumina nanoparticles.

Figure 4 gives the FT-IR spectra of bare and GPS functionalized alumina particles. Both samples show an -OH stretching peak at ~3500cm^{-1}. The peak at 1630 cm^{-1} is assigned to hydrogen bonding occurring at inter or intra nanoparticle surfaces [22]. The spectra of Al-GPS shows C-H stretching at 2929 and 2868 cm^{-1}, Si-CH_2 stretching at 1280 cm^{-1}, and Si-O at 1097 cm^{-1} as a shoulder. Since the nanoparticles were washed with fresh THF and free of excess GPS silanes, the FT-IR spectra confirm that the GPS silanes were immobilized on the surface of the alumina nanoparticles.

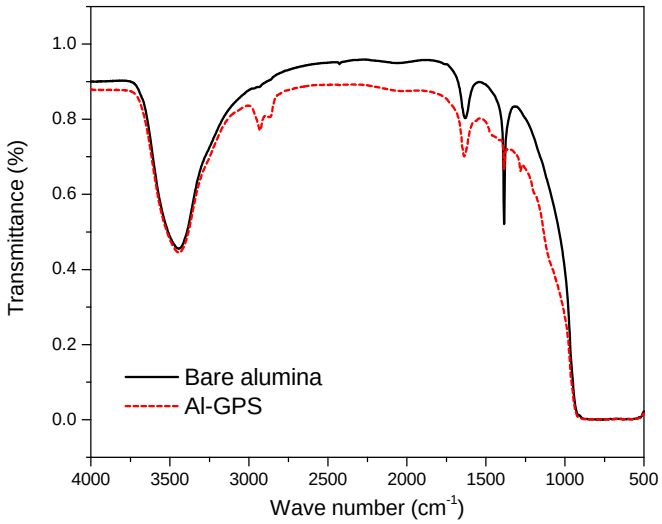

Figure 4. FT-IR spectra of bare and GPS functionalized alumina nanoparticles.

3.2. Thermo-mechanical properties

Cured BECy/alumina nanocomposites were cut into small pieces (0.4 × 4 × 30 mm) and tested with DMA. The actual nanoparticle loadings were determined by TG tests. Figure 5 shows typical DMA curves of BECy/10 wt% Al nanocomposites. The T_g can be determined by the onset of the drop in storage modulus, *E'*; the peak in loss modulus, *E";* or the peak in tanδ. In this study, the peak in *E"* was used as the indication of T_g.

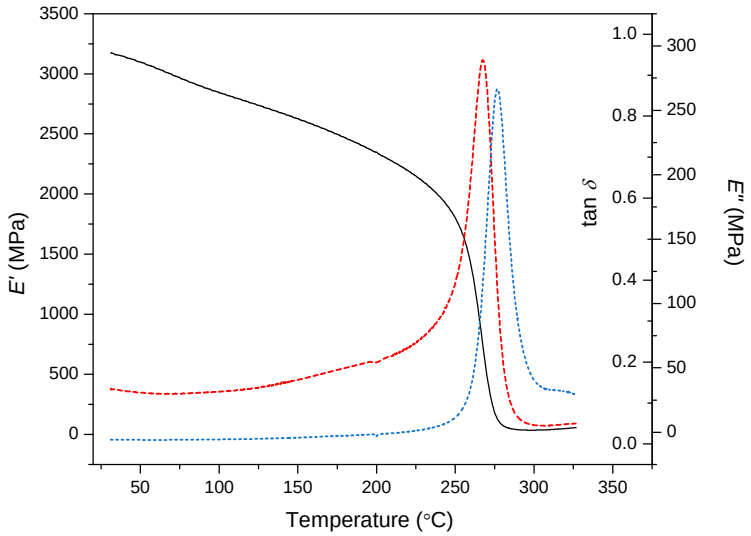

Figure 5. DMA curves of BECy/10 wt% Al nanocomposite.

An increase in nanoparticle loading corresponded with an increase in the storage modulus below the T_g in both samples with Al and with Al-GPS; however, there is not a clear difference between the storage modulus of nanocomposites with Al and nanocomposites with Al-GPS (Figure 6).

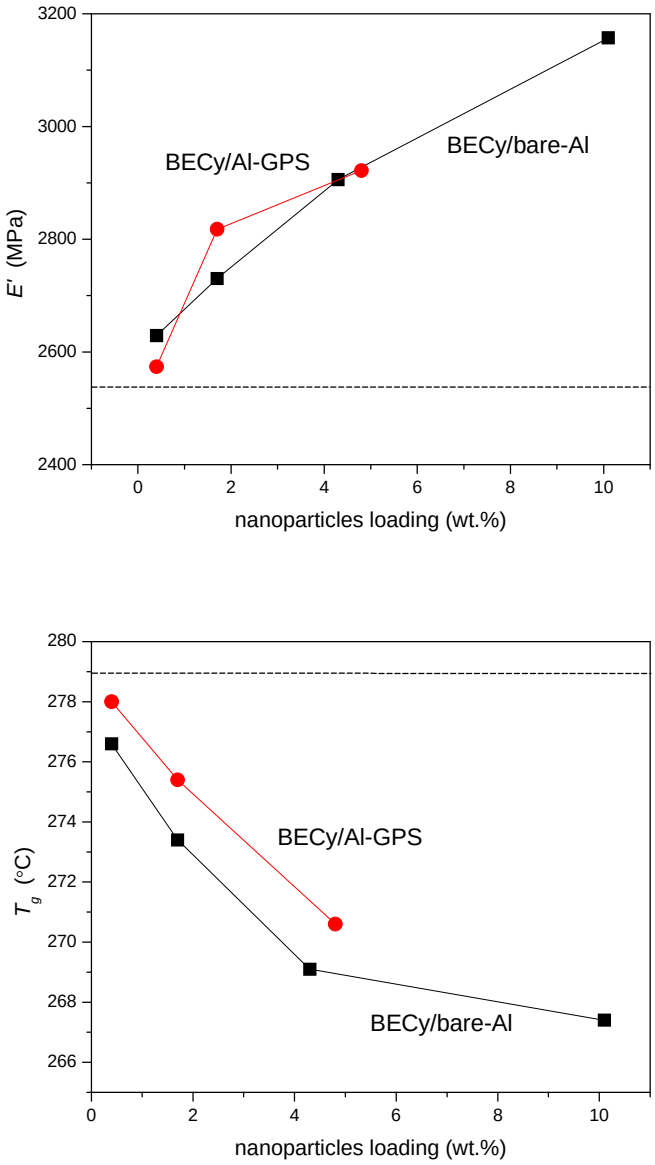

Figure 6. Summary of DMA test results. Effect of nanoparticle loading on (upper) storage modulus E' (at 35 °C) and (lower) T_g. The dashed line indicates the corresponding values for neat BECy resin.

The addition of alumina nanoparticles decreased the T_g of the BECy nanocomposites. This thermal behavior was also reported in a study of poly(methyl methacrylate)/alumina nanoparticles composites [21]. The nanoparticles actually increase the polymer mobility in the nanocomposites.

Nanoparticles that are not wet by the polymer act similar to voids in the polymer matrix; therefore, a decrease in T_g is often observed. Alumina nanoparticles contain a significant amount of physically adsorbed water on the surface even after drying at high temperatures. The water on the surface of alumina nanoparticles plays a role as a plasticizer or diluent, and can be attributed to the decrease in T_g. As a comparison, fumed silica nanoparticles contain much less physically adsorbed water on their surface, and the T_g of BECy/silica nanocomposites remains constant with increased loadings of silica nanoparticles [25]. An increased loading of Al-GPS also decreases the T_g of BECy nanocomposites (Figure 6). The T_g of BECy/Al-GPS nanocomposites was slightly higher than that of the BECy/Al nanocomposites at similar nanoparticle loading levels. The surface GPS groups make alumina nanoparticles more compatible with the BECy matrix. The epoxy groups on the surface of the Al-GPS nanoparticles may also react with BECy during cure. Strong interfacial bonding between nanoparticles and the BECy matrix is formed. As a result, the mobility of the polymer is more limited and a smaller decrease in T_g observed.

3.3. Adhesive strength

Metal-on-metal lap shear tests following ASTM standard D 1002-05 revealed the superior adhesive strength of the BECy. Its adhesive strength far surpassed that of the benchmark systems at both room temperature and at 200 °C (Figure 7). Adhesive strength diminished for all systems at elevated temperatures, as expected; however, the strength of the BECy decreased far less than that of the benchmark systems.

The reactive diluent BGE was added to the benchmark systems to give the benchmarks similar viscosities to that of BECy. The amount of BGE necessary to obtain the desired viscosity was determined via viscometer measurements on solutions with different weight percents of BGE. It was found that adding 25 wt% and 10 wt% BGE to EPON 828 and CA resins, respectively, yielded approximately the same viscosity as neat BECy resin. The incorporation of BGE to the benchmark

systems actually increased their adhesive strengths at room temperature. As mentioned earlier, BGE is a reactive diluent, and so it acts as an internal plasticizer. The resin cross-links with monomer as well as diluent, which decreases the network density of the cured adhesive, and potentially increases the strain-to-failure, energy absorption, and in turn, adhesive strength. In essence, the adhesive becomes less brittle and more ductile, and therefore can withstand greater stresses before failure. This phenomena, however, was not observed in tests conducted at 200 °C. This is likely due to the fact that the T_g's of the benchmark resins with BGE decreased due to their lower cross-link densities, and hence the difference between the testing temperature and the T_g is greater for the diluted benchmark resins.

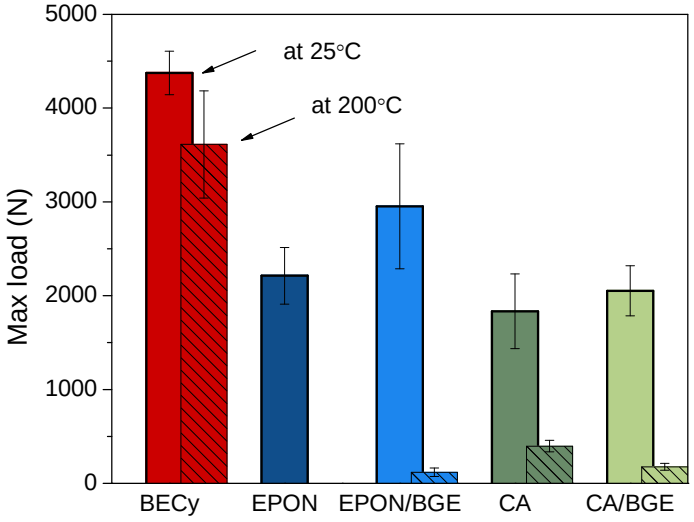

Figure 7. Maximum load of lap shear specimens at room temperature and 200 °C.

Further tests on fiber-reinforced plastic substrates, as well as tests with the nanoparticle-reinforced adhesives have yet to be conducted.

4. Conclusions

BECy has a combination of low pre-polymer viscosity and a high cured T_g that make it a desirable candidate for resin-injection composite repair techniques. Alumina nanoparticles were functionalized and used to reinforce the resin to help improve its thermal stability and mechanical performance as well as processing characteristics. Successful functionalization of the alumina nanoparticles with GPS silanes was confirmed through TG and FT-IR.

An increase in nanoparticle loading corresponded with a decrease in the T_g in both samples with bare and with functionalized nanoparticles. This decrease is partially attributed to water on the surface of alumina nanoparticles that acts as a plasticizer or diluent. The surface GPS groups make alumina nanoparticles more compatible and possibly more reactive with the BECy matrix, and therefore the T_g of BECy/Al-GPS nanocomposites was slightly higher than that of the BECy/Al nanocomposites at similar nanoparticle loading levels. Strong interfacial bonds between nanoparticles and the BECy matrix are formed resulting in decreased polymer mobility and a smaller decrease in T_g.

The adhesive strength of BECy was evaluated against two benchmark resins, EPON 828 and a cycloaliphatic epoxy, through lap shear testing at room and elevated temperatures. The BECy performed much better than the benchmark systems at both temperatures.

5. Acknowledgement

The research described in this article was supported by a grant from the Strategic Environmental Research and Development Program (SERDP), under the “Environmentally Benign Repair of Composites Using High Temperature Cyanate Ester Nanocomposites” project (Project Number WP-1580). Special thanks are extended to Katherine Lawler and Dr. Will Goertzen for their assistance and technical support.

6. References

[1] R. Talreja. Damage Development in Composites: Mechanisms and Modeling. Journal of Strain Analysis for Engineering Design, 1989. 24: p. 215-222.

[2] S. Bandyopadhyay, E.P. Gellert, V.M. Silva, and J.H. Underwood. Microscopic Aspects of Failure and Fracture in Cross-Ply Fibre Reinforced Composite Laminates. Journal of Composite Materials, 1989. 23: p. 1216-1231.

[3] R. Talreja (ed.). Damage Mechanics of Composite Materials. New York: Elsevier Press, 1994.

[4] W.D. Bascom, J.L. Bitner, R.J. Moulton, and A.R. Siebert. The Interlaminar Fracture of Organic-Matrix, Woven Reinforcement Composites. Composites, 1980. 11(1): p. 9-18.

[5] E.K. Gamstedt, and R. Talrega. Fatigue Damage Mechanisms in Unidirectional Carbon-Fibre-Reinforced Plastics. Journal of Material Science, 1999. 34: p. 2535-2546.

[6] D.A. Shimp, and W.M. Craig, Jr. New Liquid Dicyanate Monomer for Rapid Impregnation of Reinforcing Fibers. Proceedings of the 34th Annual International SAMPE Symposium, May 1989. p. 1336-1346.

[7] M.A. Meador. Recent Advances in the Development of High-Temperature Polymers. Annual Review of Materials Science, 1998. 28: p. 599-630.

[8] W.K. Goertzen, and M.R. Kessler. Thermal and Mechanical Evaluation of Cyanate Ester Composites with Low-Temperature Processability. Composites: Part A, 2007. 38: p. 779–784.

[9] A.W. Snow. The Synthesis, Manufacture, and Characterization of Cyanate Ester Monomers. Chemistry and Technology of Cyanate Ester Resins (I. Hamerton), Blackie Academic and Professional, 1994.

[10] R. Hillermeirer, and J. Seferis. Environmental Effects on Thermoplastic and Elastomer Toughened Cyanate Ester Composite Systems. Journal of Applied Polymer Science, 2000. 77(3): p. 556-567.

[11] S. Black. Are High-Temp Thermosets Ready to go Commercial? High-Performance Composites, Nov. 2004. 12(6): p. 24-29.

[12] J.R. Esslinger, and O.C. Fruchtnicht. Cyanate Ester Matrix Technology for Improved Thermal Performance of Filament Wound Missile Structures, SAMPE Journal, 2004. (40)6: p. 9-15.

[13] K.T. Hsiao, J. Alms, and S.G. Advani. Use of Epoxy/Multiwalled Carbon Nanotubes as Adhesives to Join Graphite Fibre Reinforced Polymer Composites. Nanotechnology, 2003. 14: p. 791-793.

[14] L. Zhai, G. Ling, J. Li, and Y. Wang. The Effect of Nanoparticles on the Adhesion of Epoxy Adhesive. Materials Letters, 2006. 60: p. 3031–3033.

[15] S.A. Meguid, and Y. Sun. On the Tensile and Shear Strength of Nano-Reinforced Composite Interfaces. Materials and Design, 2004. 25: p. 289–296.

[16] S. Tyagi, J.Y. Lee, G.A. Buxton, and A.C. Balazs. Using Nanocomposite Coatings to Heal Surface Defects. Macromolecules, 2004. 37: p. 9160-9168.

[17] G. Tari, M.F. Ferreira, and A.T. Fonseca. Influence of Particle Size and Particle Size Distribution on Drying-Shrinkage Behavior of Alumina Slip Cast Bodies. Ceramics International, 1990. 25: p. 577-580.

[18] G. Tari, M.F. Ferreira, A.T. Fonseca, and O. Lyckfeldt. Influence of Particle Size Distribution on Colloidal Processing of Alumina. Journal of the European Ceramic Society, 1998. 18: p. 249-253.

[19] Z. Guo, T. Pereira, O. Choi, Y. Wang, and H.T. Hahn. Surface Functionalized Alumina Nanoparticle Filled Polymeric Nanocomposites with Enhanced Mechanical Properties. Journal of Materials Chemistry, 2006. 16: p. 2800-2808.

[20] Y. Liu, C. Hsu, and K. Hsu. Poly(methylmethacrylate)-Silica Nanocomposites Films from Surface-Functionalized Silica Nanoparticles. Polymer, 2005. 46: p. 1851-1856.

[21] B.J. Ash, R.W. Siegel, and L.S. Schadler. Glass-Transition Temperature Behavior of Alumina/PMMA Nanocomposites. Journal of Polymer Science Part B: Polymer Physics, 2004. 42: p. 4371-4383.

[22] M. Abboud, M. Turner, E. Duguet, and M. Fontanille. PMMA-Based Composite Materials with Reactive Ceramic Fillers. Part 1.—Chemical Modification and Characterisation of Ceramic Particles. Journal of Materials Chemistry, 1997. 7(8): p. 1527-1532.

[23] W.K. Hall, F.E. Lutinski, and H.R. Gerberich. Hydrogen Held by Solids. VI. The Hydroxyl Groups of Alumina and Silica-Alumina as Catalytic Sites. Journal of Catalysis, 1964. 3(6): p. 512-527.

[24] E. Baumgarten, R. Wagner, and C. Lentes-Wagner. Determination of Hydroxyl Groups on Alumina by IR Spectroscopy. Fresenius' Zeitschrift fuer Analytische Chemie, 1989. 334(3): p. 246-251.

[25] W.K. Goertzen, and M.R. Kessler. Dynamic Mechanical Analysis of Fumed Silica/Cyanate Ester Nanocomposites. Composites Part A: Applied Science and Manufacturing, 2008. 39: p. 761-768.

APPENDIX B.

EFFECT OF ALUMINA NANOPARTICLES ON THE PROPERTIES OF LOW-VISCOSITY CYANATE ESTER ADHESIVES FOR COMPOSITE REPAIR

Published in Proceedings of the 67th Annual Technical Conference for the Society of Plastics Engineers

Wilber Lio, Katherine Lawler, Xia Sheng, Mufit Akinc, and Michael R. Kessler

Department of Materials Science and Engineering, Iowa State University, and Ames Laboratory, Ames, Iowa

Abstract

Polymer matrix composites (PMCs) are susceptible to microcracks and delaminations from impacts and thermal/mechanical loadings that greatly reduce their mechanical integrity. This is especially a problem for high-temperature PMCs because current repair resins have low glass transition temperatures (T_g's) that stem from the low prepolymer viscosities required of injectable resins. Bisphenol E cyanate ester has both a high cured T_g and low prepolymer viscosity, ideal for the injection repair of high-temperature PMCs. Alumina nanoparticles were incorporated to improve adhesive strength and engineer prepolymer viscosity. Lap shear tests were performed to evaluate the effects of alumina nanoparticles on the adhesive strength of the resin.

Introduction

Polymer composites are used in a wide range of applications, from airplanes to bicycle frames, and as the desire for stronger and lighter materials continues to grow, composites will be in ever-increasing demand. Composite materials, however, are susceptible to damage that can greatly

compromise their mechanical properties. Depending on their applications, this can yield disastrous effects.

Defects in composites can be caused by various events that occur throughout a structure's lifetime. They may arise as a result of poor manufacturing techniques, or they may be introduced when a part is damaged while in service [1, 2]. The majority of in-service damage results from some form of impact. Cracks, dents, delaminations, and disbonds caused by impacts can lead to a dramatic decrease in mechanical properties. Low-velocity impacts can be especially troublesome because the presence and amount of damage is often difficult to detect, yet can be greatly detrimental to the integrity of the part [1]—a 70% reduction in compressive strength has been reported in specimens that showed no visible damage [3]. For this reason, it is imperative for the integrity of composites to be properly maintained.

Resin-injection is a non-patch composite repair technique used to repair disbonds and delaminations within a composite. This is usually done by injecting a resin into the delamination zone, applying pressure to allow the resin to fully infiltrate the specimen, and heating the part to cure the resin (Figure 1). As simple as that sounds, there are many things that must be taken into account.

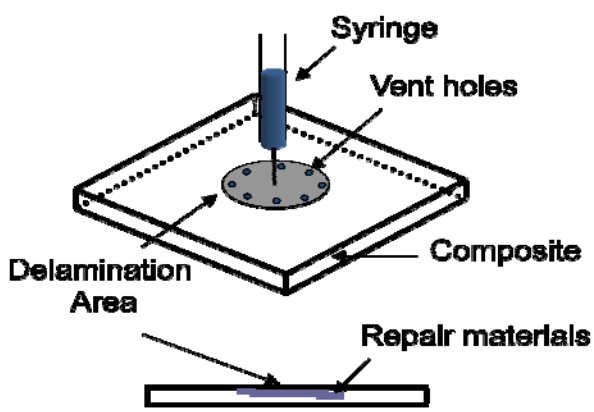

Figure 1. Resin-injection repair of composites.

One of the biggest challenges faced when designing an injection repair system involves resin viscosity. Injection repair is often limited to low-temperature composites because of the general trend for low-viscosity prepolymers to have low cured T_g's [4]. This trend is shown in Figure 2. A current problem in the field of composite repair thus lies in the resin-injection repair of high-temperature composites. High-temperature composite repair requires repair resins with high T_g's; however, because the high T_g's are usually accompanied by high prepolymer viscosities, these resins are very difficult to process, and as one can imagine, difficult to inject.

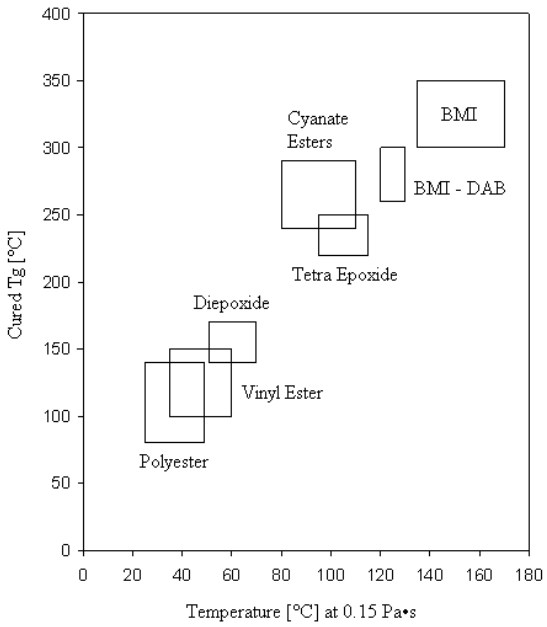

Figure 2. Polymer's T_g vs. temperature at which the monomer's viscosity is 0.15 Pa·s: most high-temperature resins in turn have high viscosities [4, 5].

A unique type of cyanate ester monomer called bisphenol E cyanate ester (BECy, 1,1'-bis(4-cyanatophenyl)ethane) is one exception to this trend. The chemical structure of BECy is shown in Figure 3. BECy monomer has an extremely low viscosity between 0.09 -0.12 Pa·s at room

temperature [4], and yet, cured BECy has a T_g around 260 °C. These characteristics make BECy an excellent candidate for the resin-injection repair of high-temperature polymer composites.

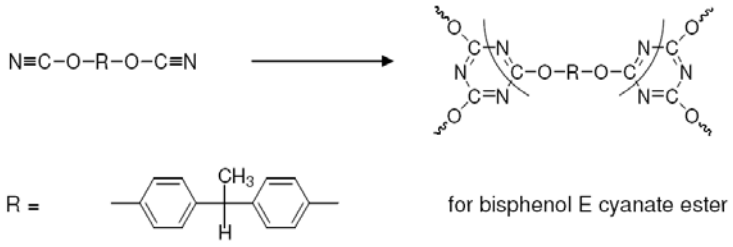

Figure 3. Chemical structure of bisphenol E cyanate ester and polymerization scheme.

Nanomaterials have not only been shown to increase adhesive strength by as much as 45% [6], but they have also been shown to drastically influence rheological properties. The majority of literature on the role of particles on rheology involves microparticle suspensions [7-11]. Aqueous alumina suspensions with sub-micron to micron-sized particles exhibit shear thinning behavior approaching a constant viscosity at high shear rates. The smaller the particle size, the higher the shear rate at which the limiting viscosity is reached. To explain the shear thinning behavior, it has been claimed that as shear rate is increased, floc networks are broken, releasing “entrapped” fluid [7,8]. Extrapolation of this model to nanoparticle suspensions implies that the viscosity of nanoparticle suspensions could result in a gel at zero shear and a low- viscosity liquid at high shear rates, or so-called thixotropic behavior. Rand and Fries [12] reported that as the particle size decreased, thixotropic behavior was much more pronounced due to increased interaction between the particle surfaces and fluid.

This behavior is attractive for resin-injection repair because the repair agents could be tailored to become shear thinning with the addition of nanoparticles. Shear thinning behavior is

expected to allow easy injection into the damaged region and provide the suspension with sufficient integrity after injection until the monomer is cured.

The goal of this work is to evaluate the effect of nanoparticles on viscosity and adhesive strength for bisphenol E cyanate ester, a candidate resin for an optimized resin-injection repair process for composite materials.

Materials

The BECy monomer (EX1510 resin), purchased from Bryte Technologies, Inc. (Morgan Hill, CA), was used as received without further purification. The liquid phase organometallic-based catalyst, EX1510-B, was supplied with the resin.

An epoxy resin, EPON 828, was used as a benchmark comparison to the cyanate ester being investigated. The epoxy along with its curing agent, Epikure™ 3223, was purchased from Miller-Stephenson Chemical Company, Inc. (Morton Grove, IL). Butyl glycidyl ether (BGE) was used as a reactive diluent to lower the viscosity of the benchmark resin, and was purchased from Sigma-Aldrich (Milwaukee, WI).

Spherical alumina nanoparticles were supplied by Nanophase Technologies, Inc. (Romeoville, IL) as NanoTek aluminum oxide, which is γ-phase alumina (density of 3.6 g/cm^3) with an average particle size (diameter) of 48 nm and a specific surface area of 44 m^2/g. Before use, the nanoparticles were dried at 110 °C for 2 hr.

Methods

BECy/alumina nanoparticle suspensions containing 1 to 20 vol.% alumina were prepared. BECy monomer was first weighed into a glass vial. Dried alumina nanoparticles were then weighed and added. The vial was then sealed and suspended in an ultrasonic water bath for 50 min. After ultrasonic treatment, the suspensions were stored in a desiccator for further characterization.

BECy/alumina nanoparticle suspensions were tested for rheological properties using a TA Instruments AR2000ex rheometer with a Peltier temperature control stage, utilizing a cone/plate geometry (45 mm diameter cone with 1° angle). A steady state flow test was conducted for each sample from shear rates of 0.1 to 500 s^{-1} (10 points per decade) at 25 °C. Before samples were loaded, suspensions were ultrasonicated for 5 minutes to ensure the particles were dispersed.

TEM samples were prepared by sectioning the cured BECy/alumina nanocomposites with an ultramicrotome to produce 50-60 nm thick sections which were placed on copper TEM grids. A JEOL 2100 transmission electron microscope (Tokyo, Japan) at an accelerating voltage of 200kV was used.

Aluminum coupons and bismaleimide/carbon fiber (BMI) coupons for lap shear tests were machined to ASTM D 1002-05 and 5868-01 standards, respectively. The aluminum coupons were bead-blasted on the adhesive surfaces, and the BMI coupons sanded, to aid in adhesion. Lap shear specimens were prepared by applying resin onto one coupon, and applying adequate pressure to hold the second coupon in place during the cure cycle.

The resins for lap shear tests were mixed and cured in the following manner. For both BECy and BECy/alumina suspensions (2.5 vol.% alumina), catalyst was added in a 100:3 (resin:catalyst) weight ratio and cured in a convection oven with the following cure schedule: 1) heat from room temperature to 180 °C at a rate of 1 °C/min, 2) isothermally cure at 180 °C for 2 hr, 3) increase temperature to 250 °C at 1 °C/min, 4) isothermally cure at 250 °C for 2 hr, and 5) cool to room temperature in the oven at a rate of 2 °C/min. The benchmark epoxy and curing agent were mixed in a 10:1 weight ratio and cured at 80 °C for 1 hr. The diluent BGE was added to the epoxy (25 wt.% BGE) in order to decrease its viscosity to the same level of that of BECy.

An Instron 5569 tensile testing machine (Norwood, MA) was used to perform lap shear tests. Spacers were used during tests to compensate for the inherent offset of the lap shear samples. Aluminum and BMI substrate samples were pulled at extension rates of 1.3 and 0.5 mm/min,

respectively, until failure. High-temperature tests (conducted at 200 °C) were performed on aluminum substrate lap shear samples using an Instron SFL Heatwave temperature controlled chamber.

Results and Discussion

The dependence of viscosity on nanoparticle loading is shown in Figure 4. The viscosity of neat BECy was found to be 0.068 Pa·s and independent of shear rate. With increased alumina nanoparticle loading, the viscosity of the suspensions increased. In addition, the suspensions exhibit shear thinning behavior. The shear thinning became more pronounced as the volume fraction of particles exceeded 10 %. At 20 vol.% loading, significant shear thinning was observed below 100 s^{-1} but at higher shear rates the material exhibited slight shear thickening behavior.

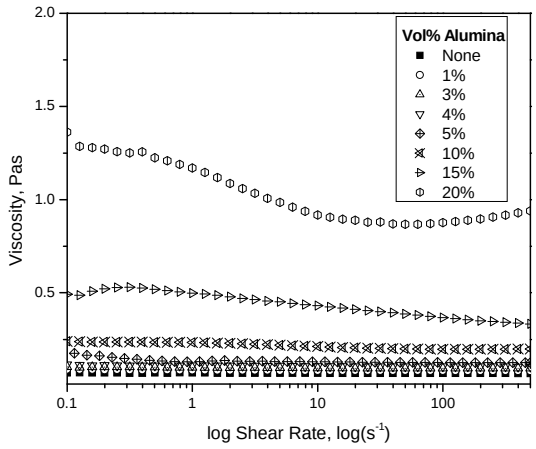

Figure 4. Viscosity vs. shear rate for BECy/alumina nanoparticle suspensions. The viscosity of the suspension increases greatly with particle loadings above 5 vol.%.

The viscosity of the BECy monomer was observed to be Newtonian: the viscosity was independent of shear rate. However, with higher volume fraction of solids, the viscosity increased

and exhibited shear thinning behavior. This may be due to the interaction and flocculation of nanoparticles in the suspension. As the shear rate is increased, flocs are broken up, and the liquid becomes free to flow, resulting in a decrease in viscosity. This shear thinning behavior, seen in suspensions with 15 vol.% nanoparticles or less, is promising for resin-injection applications. The resin is expected to be easy to inject because it has a low viscosity at high shear rates, and to remain in the damage zone (at a shear rate near zero) during cure.

TEM images (for example Figure 5) show that the particles are well dispersed in the matrix. White colored areas are due to particle pull-out during sectioning. The voids are elongated along the cutting direction.

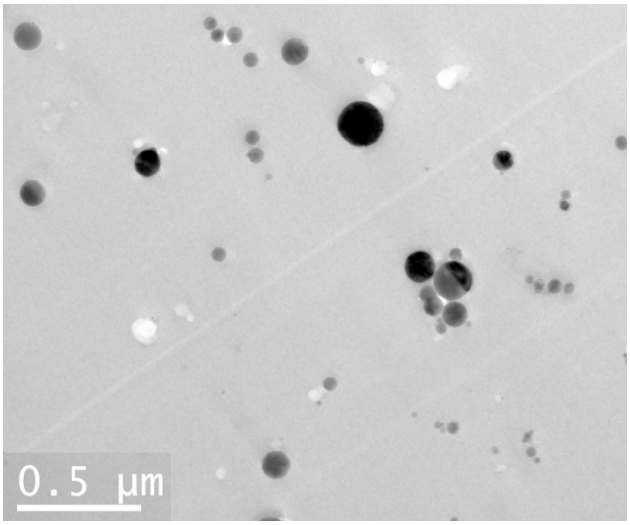

Figure 5. TEM image of cured BECy/2.5 vol.% alumina sample.

The lap shear test results are summarized in Figure 6 and Figure 7. Aluminum substrate samples were tested at room temperature as well as 200 °C. At room temperature, both the neat BECy and BECy/alumina nanocomposite outperformed the benchmark epoxy. The BECy/alumina nanocomposite, however, was weaker than the neat resin. At 200 °C, the failure stress of the neat BECy greatly exceeded that of the epoxy even more so than at room temperature.

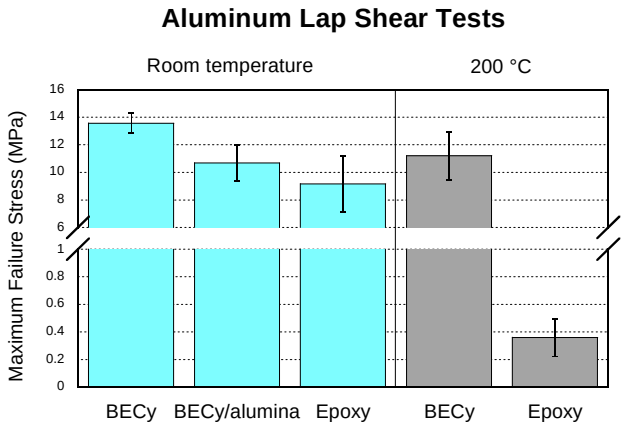

Figure 6. Lap shear test results at room temperature and 200 °C on aluminum substrates.

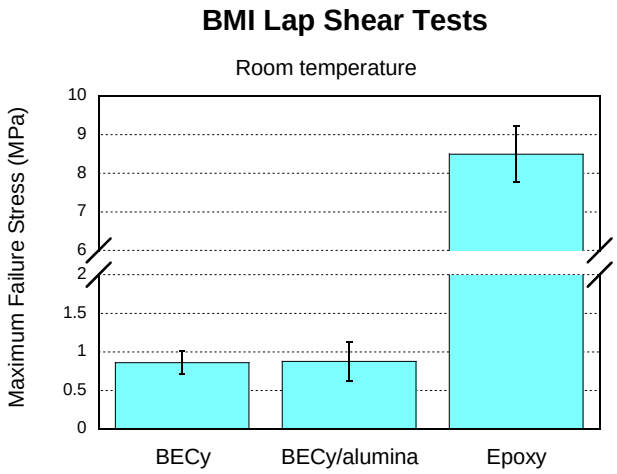

Figure 7. Lap shear test results at room temperature on BMI composite substrates.

On the other hand, the benchmark epoxy drastically outperformed both the neat BECy and nanocomposite at room temperature on BMI substrates. High-temperature tests on BMI substrates have yet to be conducted. The incorpoartion of alumina nanoparticles did not seem to effect the adhesive strength on the composite substrate.

The maximum failure stress of the BECy aluminum lap shear samples was 13.6 MPa. This is nearly 50% greater than the benchmark epoxy resin under the same conditions. At 200 °C, BECy

outperformed the epoxy resin even more so than at room temperature. Oppositely, the maximum failure stress of the epoxy BMI lap shear samples was an order of magnitude greater than that of the neat BECy BMI samples.

The aluminum oxide layer on the surface of the aluminum substrates may be responsible for the exceptionally high adhesion of BECy on aluminum. It is possible that the surface hydroxyl groups promote adhesion by forming covalent bonds with BECy [5, 13].

Possible explanations for the relatively poor adhesion of BECy on BMI include the lack of hydroxyl groups, poor wetting due to the surface energy, or perhaps, similar to grit blasting, as reported by Chin and Wightman [14], sanding of the BMI substrate could be detrimental to lap shear strength. In any case, further tests need to be conducted to fully understand these observations, including the investigation of different surface treatments.

The incorporation of alumina nanoparticles on adhesive strength was not very clear. There seems to be some sort of substrate dependence. The addition of alumina nanoparticles in the lap shear samples on aluminum substrate showed a decrease in adhesive strength, whereas a slight increase in strength was observed in samples on BMI substrate. More tests are being conducted to determine exactly what the effects of alumina nanoparticles are on adhesive strength.

Conclusions

The effect of nanoparticle loading on the viscosity and adhesive strength of bisphenol E cyanate ester was evaluated. The addition of alumina nanoparticles increased the viscosity of resulting BECy/alumina suspensions and also rendered the suspensions shear thinning. This could be beneficial for resin-injection as the viscosity of the resin would be low during injection, and high afterwards, remaining stable within the delaminations.

Adhesive strength of BECy and BECy/alumina nanocomposites were also evaluated against a benchmark epoxy via lap shear tests. BECy was found to perform superior to the epoxy in aluminum

substrate lap shear tests; however, performed inferior on BMI substrates. The effect of alumina nanoparticles requires further investigation.

Acknowledgments

The research described in this article was supported by a grant from the Strategic Environmental Research and Development Program (SERDP), under the "Environmentally Benign Repair of Composites Using High Temperature Cyanate Ester Nanocomposites" project (Project Number WP-1580).

Thanks to Brian Richard for his help in preparing lap shear samples.

References

[1] Baker, A. A, *Composites Materials in Aircraft Structures*, Ed. D. H. Middleton, Addison-Wesley Longman, Limited, 207 (1990).

[2] W. J. Cantwell and J. Morton, *J. Strain Anal.*, **27,** 29 (1992).

[3] S.D. Bartus, *J. Adv. Mater.*, **39,** 3 (2008).

[4] D.A. Shimp and W. M. Craig, Jr., *34th Annual International SAMPE Symposium*, 1336 (1989).

[5] D.A. Shimp, *Chemistry and Technology of Cyanate Ester Resins*, Chapman and Hall, 282 (1994).

[6] K.T. Hsiao, J. Alms, and S.G. Advani, *Nanotechnology*, **14**, 791 (2003).

[7] G. Tari, M.F. Ferreira, and A.T. Fonseca, *Ceram. Int.*, **25**, 577 (1990).

[8] G. Tari, M.F. Ferreira, A.T. Fonseca, and O. Lyckfeldt, *J. Eur. Ceram. Soc.*, **18,** 249 (1998).

[9] M. Schneider, J. Claverie, C. Graillat, and T.F. McKenna, *J. Appl. Polym. Sci.,* **84**, 1878 (2002).

[10] A.A. Zaman, B.M. Moudgil, *J. Rheol.*, **42**, 21 (1998).

[11] A. Zupancic, R. Lapasin, and A. Kristoffersson, *J. Eur. Ceram. Soc.*, **18** 476 (1998).

[12] B. Rand and R. Fries, *CeramicTransactions*, **62**, 165 (1996).

[13] W.K. Goertzen, X. Sheng, M. Akinc, and M.R. Kessler, *Polym. Eng. Sci.,* **48**, 875 (2008).

[14] J.W. Chin and J.P. Wightman, *Compos. Part A-Appl. S.*, **27**, 419 (1996).

APPENDIX C.

TOXICITY OF CYANATE ESTER/NANOCOMPOSITE RESINS FOR COMPOSITE REPAIR

A white paper submitted to SERDP

Michael R. Kessler, Mufit Akinc, Xia Sheng, Katherine Lawler, and Wilber Lio

Department of Materials Science and Engineering, Iowa State University, and Ames Laboratory, Ames, Iowa

1. Introduction

Interlaminar fracture, or delamination, is a common failure mode which often occurs in composites as a result of low energy impact or manufacturing defects. Localized delaminations are repaired by scarf removal of material and subsequent rebuilding (which requires cleaning and paint removal with hazardous VOC containing solvents) or by resin infusion which involves injecting low viscosity resin via an access hole into the failed area. In some cases the repair resin is diluted with volatile organic solvents or reactive diluents to achieve low viscosity. Once the resin solution is infiltrated, volatile solvents evaporate or remain until the resin is cured (typically at elevated temperatures). Additionally, these low viscosity resins usually have lower glass transition temperatures than the matrices in many military grade composites, limiting their application for elevated temperature service. For very high temperature composites, such as bismaleimides (BMIs), field repairs are not even attempted with current repair resins because of the low glass transition temperature of the cured adhesives.

In an ongoing SERDP research project, we are investigating a new class of extremely low viscosity adhesives based on bisphenol E cyanate ester (BECY) which do not require dilution and which result in a cured polymer adhesive with excellent mechanical properties and thermal stability.

We are finding that these polymer systems make excellent candidates for the repair of military composite structures. The use temperature limit for the BECY polymer for the repair of military composites will be high because of the polymer's high T_g of greater than 500°F (260°C) and onset of decomposition above 750°F (400°C). The cyanate ester monomer also has near infinite room temperature stability (shelf life), facilitating reduced wastes due to spoilage compared to traditional thermosets. We are rheologically engineering these repair systems with the incorporation of nanosize alumina and silica particles (average diameter of 40 nm) for optimum crack filling and stability for repairment to withstand high loadings, environmental extremes and service temperatures.

It is believed that these repair resins will reduce the environmental hazards associated with current composite repairs and open up new repair opportunities specifically for high temperature composites, such as BMI matrix composites. In this paper, we review the toxicity of the cyanate ester/nanocomposite repair resin and its environmental impact. We start by discussing the toxicity of the base cyanate ester monomer. Next, we review some of the background and issues related to the synthesis of the relatively benign monomer. Then the toxicity of nanoparticles in general is reviewed. Finally, we report on our experiments using coupled pyrolysis-gas chromatography (GC)/mass spectrometry (MS) and thermogravimetric analysis (TGA)-MS experiments for the BECy monomer. Occasionally, we will refer to a baseline epoxy resin (a bisphenol-A/amine based epoxy, referred to as EPON 828) which is one of the resins we have selected as a benchmark system to which to compare the mechanical, adhesive, and volatility properties of our newly developed resin system.

2. Toxicity and handling precautions of cyanate ester monomers

Cyanate ester monomers are relatively low in toxicity[1]. Table 1 shows the oral, dermal and mutagenic test results of three commercial cyanate ester monomers, demonstrating their relatively low toxicity[2,3]. For comparison, the commonly used benchmark resin, EPON 828, is also listed in Table 1.

Table 1. Toxicity testing of cyanate ester monomers[2,3] and benchmark EPON 828 resin.

Sample	Acute oral LD_{50} (rat) (g/kg)	Acute dermal LD_{50} (rabbit) (g/kg)	Dermal irritation (rabbit)	Eye irritation (rabbit)	Dermal Sensiti-zation	Mutageni-city (Ames)	Inhalation LD_{50} (mg/m^3)
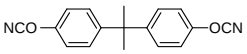 bisphenol A cyanate ester	> 2.5	> 2.5	None	-	Negative	Negative	>440
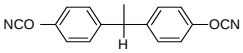 bisphenol E cyanate ester (BECy)	0.5-1.0	> 5.0	None	Mild**	Mild**	Negative	-
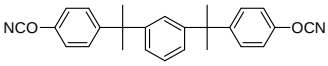 RTX-366	> 5.0	> 2.0	None	None	-	Negative	-
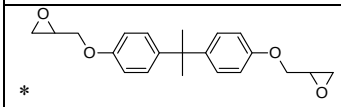 * EPON 828 Epoxy	> 4.0	> 20.0	-	2mg/24h severe	Allergic	-	>2E10

* MSDS, "BISPHENOL A DIGLYCIDYL ETHER", Sigma-Aldrich.
** MSDS, "EX-1510 Liquid Resin", Tencate Ltd.

According to Table 1 and the MSDS data for the resins, the toxicity of BECy is much lower than the benchmark epoxy resin. Under conditions where exposure to vapors or mist is possible, BECy could cause respiratory tract irritation[4]. The long-term exposure may aggravate pre-existing eye, skin and respiratory disorders. However, the experiments of chronic effects on humans and animals are not established; the significance of mutagenic activity to man is still unknown. BECy is not a systemic carcinogen and is not listed as carcinogenic by the International Agency for Research on Cancer (IARC), National Toxicology Program (NTP), or Occupational Safety and Health Administration (OSHA).

The hydrolysis of cyanate ester does not produce hydrogen cyanide. Hydrolysis produces carbamates (or urethanes) which will rapidly liberate volatile decomposition products on heating, so shielding precautions should be taken if significant quantity of carbamate is suspected to be encapsulated in a resin during heating. Most cyanate ester monomers contain multiple aromatic rings and have very low volatility. The single ring cyanate ester monomers, such as hydroquinone

dicyanate, phenyl cyanate and low molecular weight alkyl and fluoroalkyl cyanates have a noticeable, sharp odor. Bisphenol E cyanate ester (BECy) monomer contains two aromatic rings and has very low volatility and no noticeable odor.

The curing reaction of BECy is autocatalytic and highly exothermic (700J/g). Overheating, non-uniform heating and overcatalyzing can cause uncontrollable exothermal reaction and should be avoided. The uncontrollable exothermal reaction may increase temperature locally in excess of 400°C along with smoke and char formation[5].

3. Issues in the synthesis of cyanate ester monomer

Organic synthesis of cyanate ester monomers can be traced back more than 100 years to a reaction of an alkoxide with cyanogen chloride[6]. This procedure and later attempts with aryloxides were not successful because the excess oxide reacted with organic cyanate to yield mixtures of imidocarbonate and cyanurates (Figure 1).

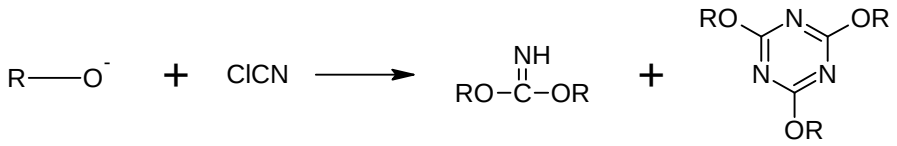

Figure 1. Chemical reaction of alkoxide with cyanogen chloride forming imidocarbonate and cyanurate.

In 1960, an approach was successful when ortho-substituted phenols were used, and the first aryl cyanate was isolated[7]. The steric hindrance of substitution prevents the excess aryloxide from consuming the product under the reaction conditions (Figure 2).

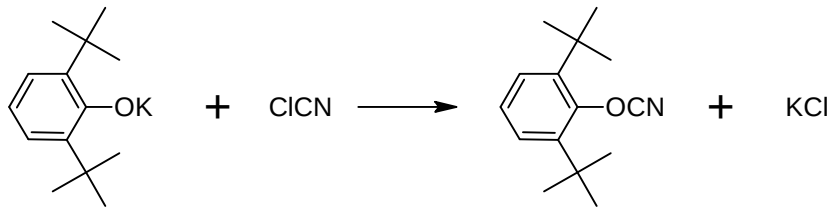

Figure 2. Chemical reaction between aryloxide and cyanogens chloride to yield aryl cyanate.

In 1963, a simple and efficient synthesis was reported when addition of a base to the phenol-cyanogen halide mixture was shown to avoid the excess oxide problem, and this process was easily adaptable to an industrial scale[8,9]. A very large number of aryl and haloalkyl cyanates were readily synthesized in excellent yield and found to be remarkably stable[10]. Since then, most commercial cyanate ester monomers are prepared by the alcohol-cyanogen halide method.

Cyanogen halides, such as ClCN, BrCN, are highly toxic agents. They cause immediate injury upon contact with the eyes or respiratory organs. Symptoms of exposure are loss of consciousness, convulsions, paralysis, and death. ClCN is especially dangerous because it is capable of penetrating the filters in gas masks.

In 1987, Dow Chemical developed a synthesis where the cyanogen chloride is generated *in situ* and a polyfunctional cyanate is formed, based on an addition of phenol and dicyclopentadiene[11]. Even with improvements in techniques and synthesis methods, the starting materials of cyanate ester monomer synthesis are highly toxic, which increases the cost of cyanate ester monomer and may have important impacts on the environment.

4. Toxicity of Nanoparticles

4.1 Introduction

Nanomaterials are defined as materials that possess at least one dimension of 100 nm or less. These materials have significantly different properties compared to their bulk counterparts, making

them unique materials with a wide range of applications (e.g. carbon nanotubes, quantum dots, etc.). However, the same characteristics that lend these materials desirable properties may also impart adverse characteristics such as toxicity.[12] Steps have been taken to understand the adverse effects nanomaterials may inflict on our health and the environment, but there is still not a very extensive literature base on the topic.[13] Additionally, there are many conflicting findings concerning the same materials,[13,14,15,16] which may be partly due to the fact that there is no set standard for testing the toxicity of nanomaterials.[17]

Although logically, nano-sizes may facilitate transport within cells, this does not necessarily make nanomaterials toxic.[13] Because so much is unknown and toxicity behavior of nanomaterials is hard to extrapolate to behavior *in vivo*,[18] it is clear that much is still unknown in the field of nanomaterial toxicology, and there is much work yet to be done to determine the exact toxicity of nanomaterials.

4.2 Mechanisms of exposure

The increased use of nanomaterials in industry will undoubtedly increase the unintentional, and potentially harmful, exposure during manufacturing and processing. It is also likely that nanomaterials will leach into the environment during the entire process from manufacture to disposal of products containing nanomaterials.[18]

The main methods of introducing nanomaterials into the body are through 1) inhalation, 2) ingestion, 3) the skin, and 4) injection.[18]

Inhalation of particles can be highly toxic.[15,16] Small particle sizes oftentimes give rise to higher deposition efficiencies and slower clearance rates. Because they have a very high particle-to-mass ratio, they can easily overload the body's natural mechanisms for clearance. The size of the particles can greatly affect their deposition location and retention within the lungs.[18] The respiratory system can also be a gateway to other body systems, which can be detrimental in the case of toxic

particles. Nanoparticles have been shown to translocate from the lungs into the blood and circulatory system,[12,18] as well as via nerve endings, into the brain and nervous system.[12] Inhalation is a major mechanism by which nanomaterials may be introduced into the body. However, to be inhaled, nanoparticles must be in their solid, dry form, and since nanoparticles are often synthesized in the liquid phase, inhalation may not be as significant a problem as other forms of exposure, such as oral or dermal.[13,18]

When ingested, nanoparticles pass through the GI tract and are eliminated via urine and feces.[12,18] However, as they are able pass from the respiratory tract into the circulatory and nervous systems, it is possible that they may also be able to translocate from the GI tract into other body systems as well.

What happens to nanoparticles when they come in contact with the skin is also not completely understood.[15] Studies have shown healthy skin to be impermeable to nanoparticles,[12,15] however there are also conflicting studies that have found nanoparticles to be able to penetrate skin.[15] Damaged skin is also more susceptible to nanoparticle penetration.[12,18]

It must also be noted that the individual properties of nanomaterials such as size and surface chemistry, can drastically affect their properties *in vivo*.[18]

4.3 Factors that influence toxicity

There are many properties that can influence the toxicity of nanoparticles. The most logical property to consider is size. However, other properties, such as composition, surface properties, and solubility may also play a role;[12,17,19,20] however, it is still unclear which properties have the largest influence.

The smaller the size, the more easily a particle is able to be taken into a cell.[18] Due to their size, nanomaterials also have very high surface areas which may also have a strong influence on toxicity.[12,15,18,20] At the same time, studies have also shown that size does not influence the toxicity of

nanoparticles.[14,16,21,22] It must be noted that in some of these studies, the nanoparticles agglomerated and therefore the actual particle sizes were significantly larger than the reported or advertised primary particle sizes. [14,19,20,22,23]

Literature with conflicting findings on the influence of the chemical composition of nanoparticles also exists. In one study, it was found that cytotoxicity did not depend on the chemical species,[21] whereas another study found cytotoxicity to be chemical composition dependent.[22] Other studies have shown that the shape of nanoparticles can also affect toxicity.[21] Toxicity may also depend on other factors not related to the specific nanomaterials, such as exposure time[14] and the cells involved.[23]

4.4 Mechanisms of toxicity

Mechanisms of nanotoxicity, while still not fully understood,[24] can be grouped into three main categories: 1) chemical, 2) mechanical, and 3) unknown.[17,19] Included in chemical mechanisms are factors such as composition, which may lead to the release of ions, which have been shown to effect cytotoxicity.[20,21] In addition, nanoparticles have been shown to form reactive oxygen species that can impose oxidative stresses on cells,[12,19,24] which can be also prove toxic. In one study with silica nanoparticles, a linear correlation was found between cell viability and reactive oxygen species.[14] Mechanical mechanisms include possible stresses that their nano-sizes, shape, or surface may inflict on cells.[17]

4.5 Silica (SiO_2) and Alumina(Al_2O_3) nanoparticles

Silicon dioxide, or silica, nanoparticles are currently used in a wide variety of industries and applications such as paints and viscosity modifiers.[14] As stated numerous times before, there are many studies that have presented conflicting findings regarding the toxicity of silica nanoparticles. Findings range from those that show silica to be non-toxic,[17] to semi-toxic,[19,23] to toxic.[14]

Although they have been shown to be non-toxic, and less toxic than other nanoparticles, the fact that certain forms of silica (e.g. crystalline) are known to be toxic after long-term accumulation, however, is still disconcerting. In one study,[25] silica nanoparticles were shown to be able to penetrate cells, but not necessarily the nucleus. Their ability to penetrate cells also varied cell to cell. Toxicity has been shown to increase with time and concentration in some studies as well.[14,25] In another study, nanoparticle silica was found to have less of an effect on fibrogenesis than micro-sized particles.[26] It was suggested that this was because the nano-sizes allowed the particles to translocate to different areas of the body and therefore were more diffuse than the microparticles. Studies on alumina nanoparticles have generally shown them to be non-toxic.[20,22,24] However, in one study, alumina nanoparticles were shown to inhibit root growth of several plant species.[16]

4.6 Conclusion

The data gathered thus far on nanomaterial toxicity is insufficient to conclude anything more than nanomaterials may be toxic. Different studies have shown contradicting results that warrant further investigation. Further investigation to determine factors that influence toxicity and mechanisms by which nanomaterials induce toxicity should be conducted to better understand the materials. In addition, before assessing the risk of nanomaterials, other things will need to be considered aside from the toxic effects, or hazard of nanomaterials, such as exposure and dose.[27] The risk of using nanomaterials cannot be fully assessed until conclusive data on all parts are examined.

5. Experimental Characterization of VOCs

5.1 Mass loss due to VOCs by ASTM and TGA

Throughout our SERDP research program we have evaluated the volatile content of various resin candidates and benchmark resins according to ASTM standard 1259-85. The ASTM standard calls for the heating of a certain geometry of material at 105 °C for ½ hour and measuring the mass

loss. Thermogravimetric analysis (TGA) experiments under the same isothermal conditions were also performed as a concomitant measurement of the volatile content. [28] The isothermal TGA results are shown in Table 2. The BECy has just 0.7% volatile content (as defined by the ASTM standard isotherm for 30 min) while the butyl glycidyl ether (BGE) diluted epoxies had a volatile content of 24.8%. While the neat EPON 828 resin did have a lower volatile content than the neat BECy resin (0.4% vs. 0.7%), that system has a much higher viscosity and is not being considered as a suitable benchmark system unless it is diluted with the reactive diluent (BGE) so that the two resins have the same viscosity (for injection requirements). The last two columns in Table 2 are the time (and corresponding temperature) at which the sample is completely volatilized i.e., the entire sample is gone.

Table 2. Comparison of Volatile Content from TGA.

	TGA (105 °C for ½ h)	**TGA (ramp until 100% wt. loss)**	
	Change in wt%	Time (min)	Temperature (°C)
BECy	0.7	36.2	741
EPON	0.4	28.4	584
EPON/BGE	24.8	27.0	556

While the ASTM and TGA testing confirm that there is very little volatile content of the BECy resin at the 105 ° C isotherm (~0.7%), further analysis of the small volatile content was performed to determine the composition of the evolved gases using two different techniques: pyrolysis coupled with GC/MS measurements and TGA coupled with MS measurements.

5.2 Testing Method for pyrolyzer-GC/MS

The sample was analyzed by a CDS 5200 pyrolyzer and Varian 2200 GC/MS instrument. The Varian 2200 consists of a Varian 3800 GC and Varian 2200 Ion Trap MS. The MS has a scan range of 30-650 amu. Scan rate is dependent on scan range.

To obtain GC traces of the volatile gases evolving, 15.5mg sample was placed in the pyrolyzer (py) and heated to 105°C, holding for 30mins (similar to ASTM conditions) in helium atmosphere. During the trapping stage the Tenax TA was held at about 40°C, when the Tenax TA trap was desorbed and the GC trace obtained.

In the GC/MS system, helium was the carrier gas and the capillary column used was DB-5: 30m × 0.25mm × 0.25μm. The split ratio is 1:20, which means that for every 20 parts injected one part goes into the column and the rest travels out the exhaust and is not tested. The temperature of the transfer line was 300°C. The GC oven conditions used were as follows: initial temperature of 35°C for 5 min, ramped to 300°C at 8°C/min, holding for 10min. The transfer line needs to be heated to ensure that the sample travels through the column and is not stuck in the injection port. This high temperature may have caused the trapped gasses to further split into smaller fractions.

5.3 Testing Method for TGA-MS

TG/MS experiments were carried out on a TG/MS system consisting of a TA 2960 SDT interfaced with a Fisons BG Thermolab Mass Spectrometer using a heated capillary transfer line. In this system the sample was ramped very fast to 105°C, held at this temperature for 30 min, and then ramped to 500°C at a rate of 1 °C/min under 100ml/min nitrogen flow. The capillary transfer line was heated to 200 °C, and the inlet port on the mass spectrometer was heated to 150 °C. The MS unit is based on a quadrupole design and the mass scan ranged from 0-300 amu. The sample gas from the SDT was ionized at 70eV. The system was operated at a pressure of 1×10^{-5} torr.

5.4 Py-GC/MS Results

A complete list of all compounds detected by py- GC/MS is presented in Table 5.

The total number of compounds detected by py-GC/MS was 38. Yet, only five compounds made 98% of the total volatiles. These five compounds with most likely composition and relevant characteristics are summarized in Table 3.

Table 3. Volatile components of BECy present in greatest amounts. % volatile is based on the area of the GC peak compared to the total area.

Peak no	RT (min)	Compound	Formula	CAS	MW	% volatile	of total sample
4	7.01	Hexanoic acid, hexyl ester	$C_{12}H_{24}O_2$	6378-65-0	200	16.88	0.068%
8	10.39	3,5-Diamino-1,2,4-triazole	$C_2H_5N_5$	1455-77-2	99	76.28	0.305%
27	19.91	5-hydroxytryptophan	$C_{11}H_{12}N_2O_3$	4350-09-8	220	1.66	64ppm
28	20.29	Acetophenone, 4' - hydroxy	$C_8H_8O_2$	99-93-4	136	1.6	64ppm
35	29.52	4,4' -ethylidenediphenol	$C_{14}H_{14}O_2$	2081-08-5	214	1.65	66ppm
					total :	98.07%	0.4%

Concentration of the remaining 33 compounds were <0.4% each and most <0.1% each may have been fractioned from larger molecules when the volatile gas was injected into the GC at 300°C.

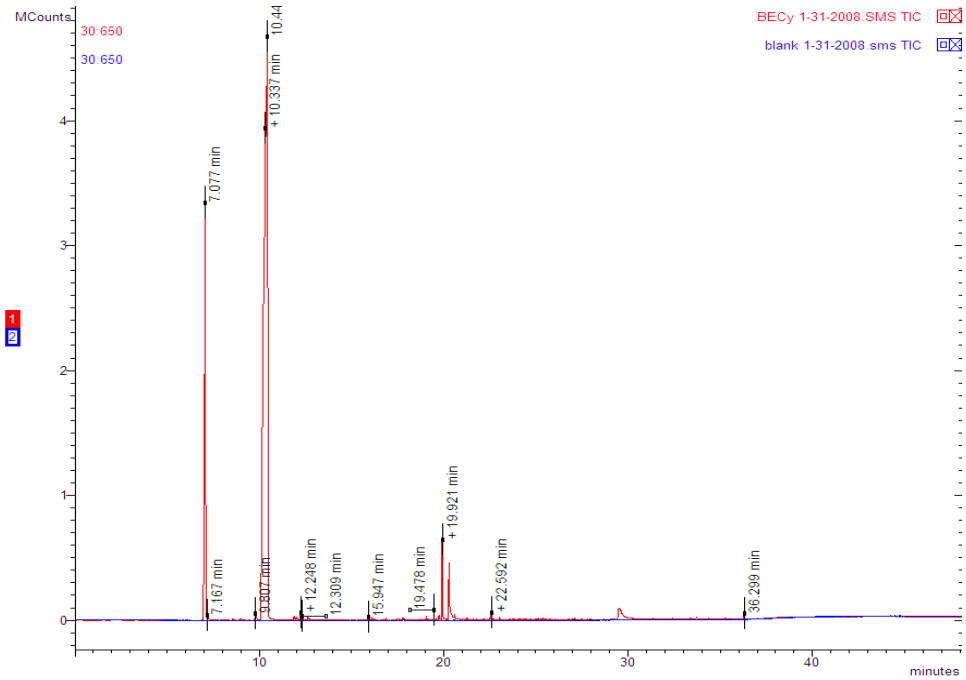

Figure 3. Total Ion Chromatogram for the sample.

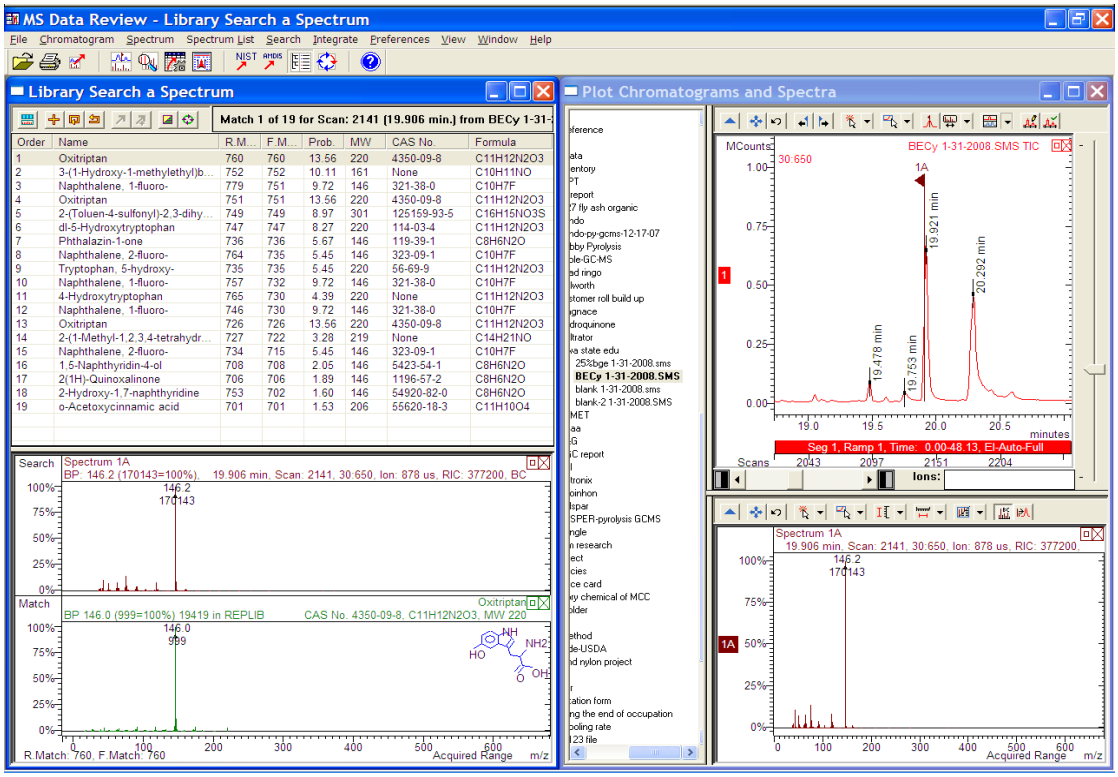

Figure 4. Example compound identification (Peak 27).

5.5 TGA-MS Results

For sample BECy, in the first stage, the mass no 16, 17 and 18 are evolving from the sample. The mass no 16 may be due to NH_2 and 17 and 18 may be due to evolution of water (OH and HOH). In the second and third stage mainly the mass no 16, 17, 18, 44, 50, 51, 52, 55, 61, 62, 63, 65, 66, 77, 78, 91, 92, 94, 107, 108 and 122 are evolving from the sample. Again the first three peaks may be due to NH_2 and H_2O evolution. The mass no 44 most likely represents evolution of carbon dioxide (CO_2, M_{wt} 44). The mass no 50, 51, 52, 77 and 78 may be due to the evolution of benzene and its fragments (C_6H_6, M_{wt} 78) whereas 65, 66 and 94 to that of phenol (C_6H_5OH, M_{wt} 94), and 91 and 92 may be due to evolution of toluene ($C_6H_5CH_3$ M_{wt} 92). The mass no 107, 108 and 122 may be due to the other higher molecular weight hydrocarbons that may have evolved from the resin or formed during the transfer of volatiles to MS at elevated temperature.

The MS data above does not disprove that the compounds listed in Table 1 are incorrect. Also, the NH_2 radical, and H_2O may be added to the list of volatile components at 105°C.

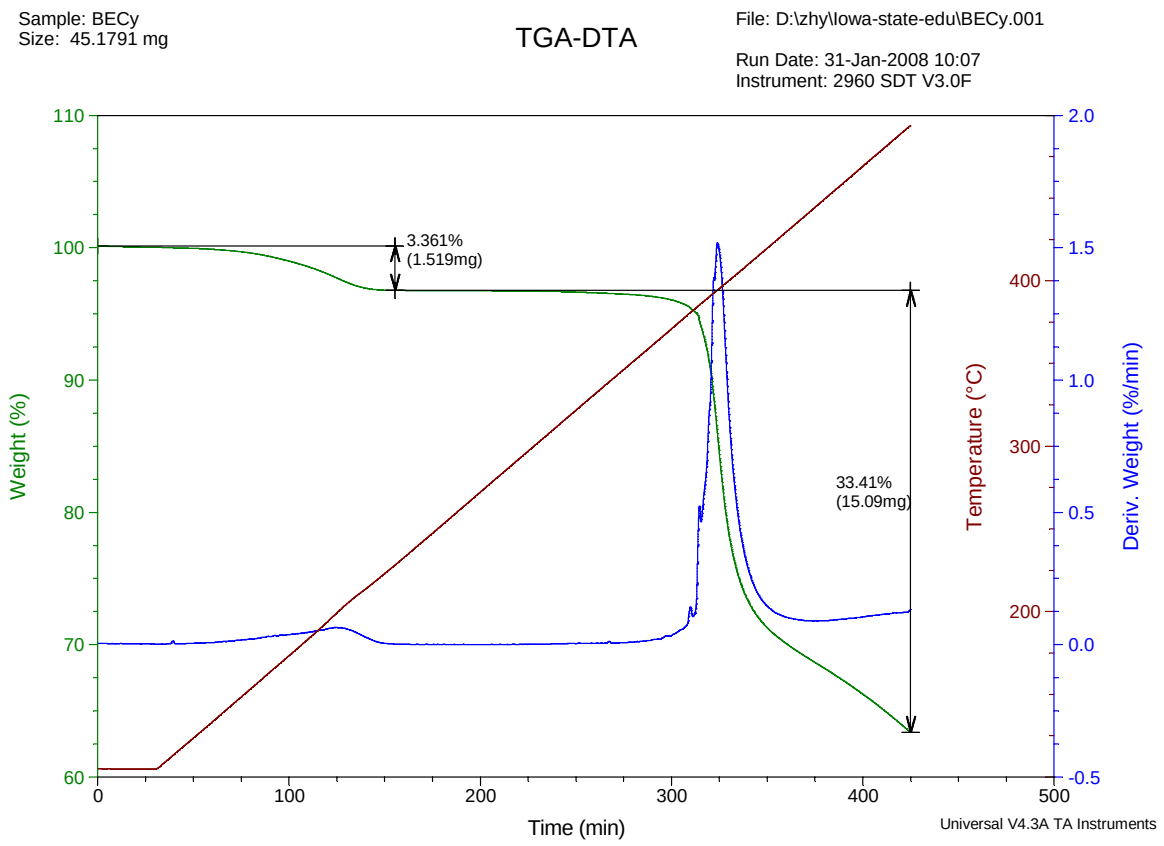

Figure 5. TGA plot of the BECy sample.

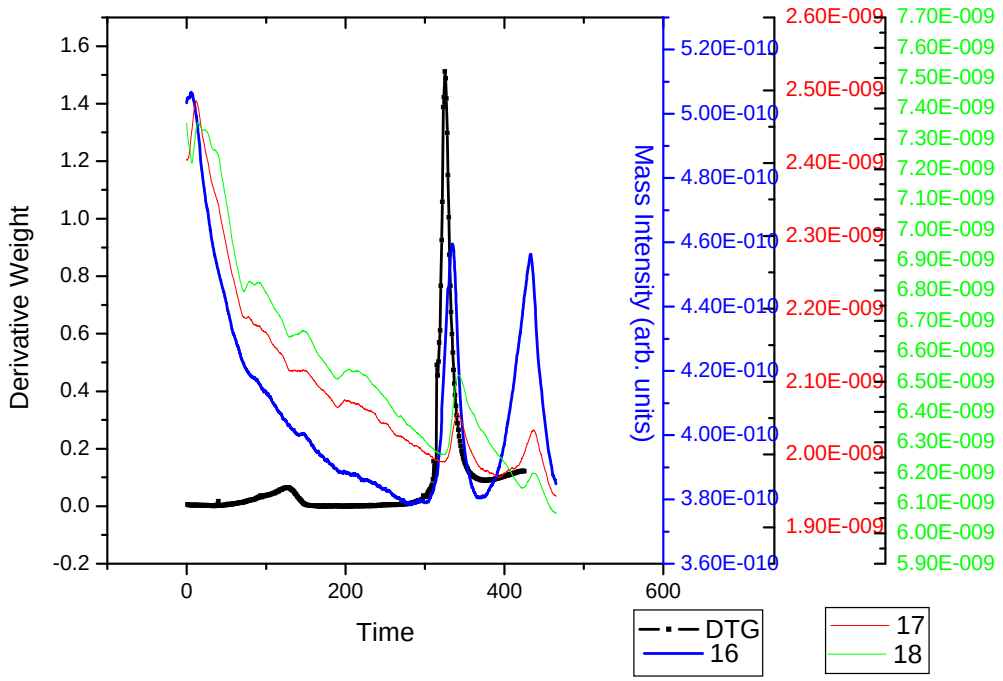

Figure 6. m/z = 16, 17 and 18 MS plot of BECy (Example).

It should be noted that GC and MS chemical assignments are based on the highest probability among possible compounds. Below, the structures of the five compounds with highest concentration in the volatiles are shown (see Table 3). These structures are similar to the monomer:

- Hexanoic acid could be formed by the opening of 6-member carbon ring.
- 3,5-Diamino-1,2,4-triazole and 5-hydroxytryptophan are composed of N, H, C and O all of which are found in the monomer,
- Acetophenone, 4'-hydroxyl is similar to half the monomer with hydroxyl group and carbonyl (C=O) may form from cleavage of cyanate (OCN) group,
- 4,4'-ethylidenediphenol is similar to the Bisphenol E monomer, with cyanate groups replaced by hydroxyl groups.

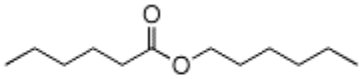

Peak 4 - Hexanoic acid, hexyl ester (hexyl hexanoate)

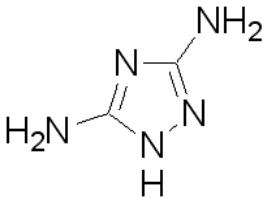

Peak 8 - 3,5-Diamino-1,2,4-triazole

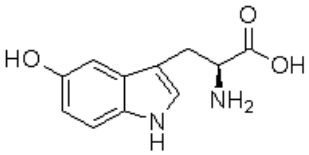

Peak 27 - 5-hydroxytryptophan

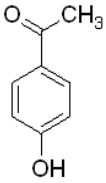

Peak 28 - Acetophenone, 4' – hydroxy

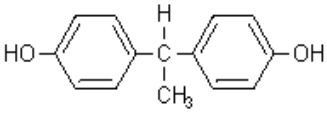

Peak 35 - 4,4' –ethylidenediphenol

5.6 Toxicity

The five compounds in Table 1 were researched for their toxicity. The following paragraphs summarize the information available in the literature with respect to their toxicity:

Hexanoic acid, also called caproic acid, is a fatty acid and a naturally occurring fragrance found in apple, melon, passion fruit, pear, sherry, strawberry, and tomato[29] A study of the toxicity of this acid states: "Conclusions of this criteria document (status December 2002): the acute toxicity of **caproic acid** is low; it is corrosive to the skin and eyes of rabbits; an occlusive patch test with 1% **caproic acid** on **human** volunteers did not show any sensitization; **caproic acid** is not mutagenic in the Salmonella mutagenicity test but is cytotoxic *in vitro*."[30]

3,5-Diamino-1,2,4-triazole. A synonym for this compound is Guanazole. This substance has been used in many clinical trials to treat cancer patients[31]. One study states[32]: "The pharmacokinetics of guanazole, (3,5-diamino-1,2,4-triazole) were evaluated in rats, mice and 3 cancer patients. In humans, IV doses ranging from 3.5-10 g/sq m were used. Half-life in blood was 1-2 hr. The drug was eliminated almost quantitatively in the urine in 24 hr. No metabolites could be detected in the perfusate or bile of the isolated perfused rat liver preparation, suggesting that the drug itself rather than a metabolite is responsible for antitumor activity."

5-hydroxytryptophan, or Oxitriptan, is "An aromatic amino acid with antidepressant activity. In vivo, 5-hydroxytryptophan (5-HTP) is converted into 5-hydroxytryptamine (5-HT or serotonin) as well as other neurotransmitters. 5-HTP may exert its antidepressant activity via conversion to serotonin or directly by binding to serotonin (5-HT) receptors within the central nervous system (CNS). Endogenous 5-HTP is produced from the essential amino acid L-tryptophan. Exogenous therapeutic 5-HTP is isolated from the seeds of the African plant Griffonia simplicifolia"[33].

Acetophenone, 4'-hydroxy is also known as 4'-hydroxyacetophenone, or Piceol. This substance has been found in the leaves of the Chilean plant *Lomatia hirsuta*[34], *and* may reduce inflammation[35]

No toxicity studies were found for 4,4' –ethylidenediphenol.

The MSDS sheets for each of the 5 major constituents were examined to gather more information on the toxicity of these compounds. The MSDS sheets do not provide much information in this regard. However, the type of personal protective equipment necessary to handle each compound is listed and summarized in Table 4.

Table 4. PPE required to work safely with the five compounds by the MSDS sheets.

Compound	Personal Protective Equipment (PPE)
Hexanoic acid, hexyl ester	Respiratory: Not required. Use multi-purpose combination Hand: Protective gloves Eye: Chemical Safety goggles
3,5-Diamino-1,2,4-triazole	Respiratory: Air-purifying respirators or dust mask type N95 or type P1 Hand: Compatible chemical-resistant gloves Eye: Chemical safety goggles
5-hydroxytryptophan	Respiratory: Full-face particle respirator type N99 or type P2 Hand: Compatible chemical-resistant gloves Eye: Chemical safety goggles
Acetophenone, 4' - hydroxy	Respiratory: Air-purifying respirators or dust mask type N95 or type P1 Hand: Compatible chemical-resistant gloves Eye: Chemical safety goggles
4,4' -ethylidenediphenol	Respiratory: Air-purifying respirators or dust mask type N95 or type P1 Hand: Compatible chemical-resistant gloves Eye: Chemical safety goggles

5.7 Regulation

To find out whether the chemicals determined to be present in the sample by py-GC/MS were regulated, the document entitled "The Consolidated List of Chemicals Subject to Emergency Planning and the Community Right to Know Act" was referenced[36]. Only five out of the 38 chemicals listed in the table below were found in the list. All five chemicals found in the list had a concentration of less than 0.1% each in the evolved gas.

Table 5. Complete list of all peak assignments with the CAS number.

Peak No.	Rt (min)	Compound	Molecular weight	CAS #	Conc. %	Regulated
1	3.31	Propane, 2-cyclopropyl-	84	3638-35-5	0.03	
2	5.49	Toluene	92	108-88-3	0.02	Yes
3	5.83	Acetic acid, 2-methylpropyl ester	116	110-19-0	0.01	Yes
4	7.01	Hexanoic acid, hexyl ester	200	6378-65-0	16.88	
5	8.59	o-xylene	106	95-47-6	0.05	Yes
6	9.04	1,1'-bicycloheptyl	194	23183-11-1	0.05	
7	9.79	5-Octen-4-one, 7-methyl-	140	32064-78-1	0.34	
8	10.39	3,5-Diamino-1,2,4-triazole	99	1455-77-2	76.28	
9	11.88	Butanoic acid, butyl ester	144	109-21-7	0.04	
10	11.91	Dipropylene glycol monomethyl ether	148	34590-94-8	0.03	
11	11.99	Dipropylene glycol monomethyl ether	148	34590-94-8	0.06	
12	12.24	2-propanol, 1-(2-methyoxyproxy)-	148	13429-07-7	0.12	
13	12.31	3-Ethyl-3-hexene	112	16789-51-8	0.03	
14	12.63	Butyl carbamate	117	592-35-8	0.08	
15	14.25	2-Nonen-1-ol, (E)-	142	31502-14-4	0.01	
16	15.91	Cyclohexane, (3-methylpentyl)-	168	61142-38-9	0.01	
17	15.94	Cyclopentane, 1-pentyl-2-propyl-	182	62199-51-3	0.04	
18	16.1	Hydroxylamine, O-decyl-	173	298-79-1	0.04	
19	16.2	Cyclohexane, 1,1'-(1,2-dimethyl-ethanediyl)bis-,	222	54889-87-1	0.02	
20	16.24	Cyclodecanol	156	1502-05-2	0.01	
21	16.88	Cyclohexane, (1-methylethyl)-	126	696-29-7	0.04	

22	17.47	Hydroquinone	110	123-31-9	0.07	Yes
23	18.79	Cyclohexane, 1,1'-(1-methylpropylidene)bis-	222	54890-02-7	0.02	
24	19.05	1,7-dimethyl-4-(1-methylethyl)cyclodecane	210	645-10-3	0.05	
25	19.48	Cyclotetradecane	196	295-17-0	0.16	
26	19.73	1-n-Pentyladamntane	206	50782-11-1	0.12	
27	19.91	Oxitriptan	220	4350-09-8	1.66	
28	20.29	Acetophenone, 4'-hydroxy-	136	99-93-4	1.60	
29	21.27	Phenol, 2,4,6-tris(1-methylethyl)-	220	2934-07-8	0.03	
30	22.55	Diethyl phthalate	222	84-66-2	0.06	Yes
31	22.6	10-Heneicosene(c,t)	294	95008-11-0	0.09	
32	25.38	9-Nonadecene	266	31035-07-1	0.03	
33	27.08	Pentadecanoic acid, 14-methyl-, methyl ester	270	5129-60-2	0.04	
34	27.46	1,2-benzenedicarboxylic acid, butyl 2-methylpropyl ester	278	17851-53-5	0.02	
35	29.52	4,4'-ethylidenediphenol	214	2081-08-5	1.65	
36	32.41	Nonadecane	268	629-92-5	0.02	
37	33.71	1,2-benzenedicarboxylic acid, diisooctyl ester	390	27554-26-3	0.05	
38	36.29	2,6,10,14,18,22-tetracosahexaene, 2,6,10,15, 19, 23-hexamethyl-, (all-E)-	410	111-02-4	0.11	

6. Conclusion

As an integral part of developing a novel and environmentally friendly composite repair process, quantity and composition of the gasses evolving from BECy resin were studied. In particular, protocol described in ASTM standard 1259-85 was followed. Total evolved gas was determined by heating the samples with prescribed geometry to 105 °C for 30 minutes and measuring the mass loss. As a benchmark comparison, EPON 828, and EPON 828 diluted with butyl glycidyl ether (BGE), to have the same injectable viscosity, were also tested. The BECy lost 0.7% compared to the butyl glycidyl ether (BGE) diluted EPON 828 which lost 24.8% of its mass. While the neat EPON 828 resin did have a lower volatile content (0.4% vs. 0.7%), it is not being considered as a suitable benchmark without the reactive diluent (BGE).

Chemical composition of the total evolved gases from BECY resin was studied by py-GC/MS and TGA/MS techniques. A total of 38 mass fractions were identified by MS. Of this total, five of them constituted the 98% of the total volatiles. Of the remaining 33 compounds, all but two had concentrations less than 0.1% each. The other two had concentration of 0.34 and 0.16% each. It should be noted that these concentrations represent 24 and 11 ppm of resin. Furthermore, It is certainly possible that the significant number of volatiles detected by the mass spectrometer might have formed during volatile gas transfer to MS at elevated temperature.

Identification of evolved gas fractions by mass spectroscopy is not a trivial task. Using the instruments database and the parent resin BECy's chemical structure, most probable compositions were assigned to each of the five most abundant volatiles. Literature was screened for toxicity assessment of the evolved gases. None of the five significant components was "regulated." Only five of the remaining 33 compounds were on the list of "regulated" compounds. Concentration of each of these compounds is 0.07% of total volatiles (or 5 ppm of resin) or less.

Literature on the toxicity of these "regulated" compounds is rather scarce and not specific. Therefore, accurate assessment of toxicity and permissible exposure levels is difficult if not

impossible. However, it suffices to say that the limited study we have conducted on the amount of volatiles and their toxicity does not raise any immediate concern. Considering the fact that some of the volatile fragments may not even be evolved during heating to 105 °C but formed during the analysis step, may lower the potential toxicity concerns for the use of this resin for composite repair applications.

Toxicity and risks associated with the nanoparticles is a current topic of research. The few reports available in the literature are often inconclusive and conflicting. Although some concerns have been expressed for inhaling air born nanoparticles, toxicity does appear to be more associated with the chemical composition and crystal structure of the particles than their size. The reader is reminded that nano size clay particles have been handled by humans for millennia without an established health hazard. Similarly, colloidal gold has been injected into the human body for improving the condition of joints and other ailments. Toxicity of alumina nanoparticles suspended in liquids has not been properly evaluated but there is no obvious indication that they may pose serious health hazards.

Perhaps, it should be emphasized that the volatiles and toxicity assessment was limited in scope and depth, and was carried out by materials scientists not by an expert toxicologist. It might be prudent to have this report reviewed by toxicologists, and if necessary, additional work should be carried out before this repair technology is reduced to practice.

7. References

[1] I. Hamerton, "Chemistry and technology of cyanate ester resins", First edition, 1994 Chapman & Hall.

[2] Bogan, G. W., Lyssy, M. E., Monnerat, G. A. and Woo, E. P. (1988) *SAMPE J.*, **24**, 19.

[3] Kohn, J. and Langer, R., (1986) *Biomaterials*, **7**, 176.

[4] MSDS, "EX-1510 Liquid Resin", Tencate Ltd.

[5] Shimp, D. A., Christenson, J. R. and Ising, S. J., (1991), *Cyanate ester resins-chemistry, properties and applications, Technical Bulletin*, Ciba, Ardsley, NY.

[6] Crigat E. and Putter R., 1967, *Angew. Chem. Internat. Edit.*, **6**, 206.

[7] Stroh R and Gerber H., 1960, *Angew. Chem.*, **72**, 1000.

[8] Crigat E. and Putter R, 1963, German Patent 1, 195, 764.

[9] Crigat E. and Putter R, 1964, *Chem. Ber.*, **97**, 3012.

[10] "Chemistry and Technology of Cyanate Ester Resins", Hamerton I., Ed., Chapman and Hall, London, 282 (1994).

[11] Bogan G.W., Lyssy M.E., Monnerat G.A. and Woo E.P., 1988, *SAMPE J.*, **24**, 19.

[12] Andre Nel, et al. Toxic potential of materials at the nanolevel. Science. 311 (Feb 2006) 622.

[13] Vicki L. Colvin. The potential environmental impact of engineered nanomaterials. Nature Biotechnology. Vol 21 No 10 (Oct 2003) 1166-1170.

[14] Weisheng Lin, et al. In vitro toxicity of silica nanoparticles in human lung cancer cells. Toxicology and Applied Pharmacology. 217 (2006) 252–259.

[15] Roberta Brayner. The toxicological impact of nanoparticles. Nanotoday. Vol 3 No 1-2 (Feb-Apr 2008).

[16] L. Yang et al. Particle surface characteristics may play an important role in phytotoxicity of alumina nanoparticles. Toxicology Letters. 158 (2005) 122–132.

[17] Tobias J. Brunner et al. In vitro cytotoxicity of oxide nanoparticles: comparison to asbestos, silica, and the effect of particle solubility. Environmental Science and Technology. Vol 40 No 14 (2006) 4374-4381.

[18] Günter Oberdörster et al. Nanotoxicology: an emerging discipline evolving from studies of utlrafine particles. Environmental Health Perspectives. Vol 113 No 7 (July 2005) 823-839.

[19] Laura K. Adams et al. Comparative eco-toxicity of nanoscale TiO_2, SiO_2, and ZnO water suspensions. Water Research. 40 (2006) 3527–3532.

[20] Xiaoshan Zhu et al. Comparative toxicity of several metal oxide nanoparticle aqueous suspensions to zebrafish (Danio rerio) early developmental stage. Journal of Environmental Science and Health Part A. 43 (2008) 278–284.

[21] Akiko Yamamoto et al. Cytotoxicity evaluation of ceramic particles of different sizes and shapes. Journal of Biomedical Materials Research Part A. Vol 68A, Issue 2 (2003) 244–256.

[22] Andrew J. Wagner et al. Cellular Interaction of Different forms of aluminum nanoparticles in rat alveolar macrophages. Journal of Physical Chemistry B. 111 (2007) 7353-7359.

[23] Jenq-Sheng Chang et al. In vitro cytotoxicity of silica nanoparticles at high concentrations strongly depends on the metabolic activity type of the cell line. Environmental Science and Technology. 41 (2007) 2064-2068.

[24] Daohui Lin et al. Phytotoxicity of nanoparticles: Inhibition of seed germination and root growth. Environmental Pollution. 150 (2007) 243-250.

[25] Yuhui Jin. Toxicity of Luminescent Silica Nanoparticles to living cells. Chemical Research in Toxicology. 20 (2007) 1126–1133.

[26] Ying Chen et al. Comparing study of the effects of nanosized silicon dioxide and microsized silicon dioxide on fibrogenesis in rats. Toxicology and Industrial Health. 20 (2004) 21-27.

[27] Possible adverse health, environmental and safety impacts. Nanoscience and Nanotechnologies. (July 2004) 35-50.

[28] Kessler, Michael R., and Akinc, Mufit. Environmentally Benign Repair of Composites Using High Temperature Cyanate Ester Nanocomposites, Project WP-1580 FY07 Annual Report.

[29] http://www.thegoodscentscompany.com/data/rw1028161.html

[30] S. Hirzel Verlag, Birkenwaldstrasse 44, 70191 Stuttgart, Germany, 2005. Xi, 85p. http://toxnet.nlm.nih.gov/cgi-bin/sis/search/f?./temp/~JtglAj:1

[31] Toxnet. Toxicology Data Network. http://toxnet.nlm.nih.gov/cgi-bin/sis/search/r?dbs+toxline:@term+@rn+1455-77-2+@OR+@mh+%22+Guanazole+%22+@OR+@na+%22+Guanazole+%22+@OR+@ab+%22+Guanazole+%22+@OR+@kw+%22+Guanazole+%22

[32] Pharmacokinetics of guanazole in man. Clin. Pharmacol. Ther.; Vol 14 ISS Mar-Apr 1973, P264-270

[33] National Cancer Institute. NCI Drug Dictionary. http://www.cancer.gov/Templates/drugdictionary.aspx?CdrID=459776

[34] Simonsen, Henrik T. Anne Adsersen, et. al. BMC Complementary and Alternative Medicine 2006, 6:29.

[35] Alvarez, Maria Eugenia, Alejandra Ester Rotelli, et al. Il Farmaco 55 (2000) 502-505.

[36] http://www.epa.gov/ceppo/pubs/title3.pdf